REPORT NO. FRA/ORD-79/33 PB

DYNAMIC LOADS ON THE UNDERCARRIAGES OF FREIGHT CARS

JULY 1979

Prepared for

U.S. DEPARTMENT OF TRANSPORTATION
FEDERAL RAILROAD ADMINISTRATION
Office of Research and Development
Washington, D.C. 20590

NOTICE

This document, which is being distributed by the Federal Railroad Administration, was received under the provisions of the bilateral arrangement; US/USSR Agreement for Cooperation in the Field of Transportation, in the hope that it might be of assistance in railway research and operation.

The translation and publication of this document does not constitute approval by the U.S. Department of Transportation of the inferences, findings, or conclusions contained therein. Publication is solely for the exchange and stimulation of ideas.

Technical Report Documentation Page

1. Report No.	2. Government Accession No.	3. Recipient's Catalog No.
FRA/ORD-79/33		

4. Title and Subtitle	5. Report Date
DYNAMIC LOADS ON THE UNDERCARRIAGE OF FREIGHT CARS	July 1979
	6. Performing Organization Code
	8. Performing Organization Report No.
7. Author(s) N. N. Krudryautseu	
9. Performing Organization Name and Address Izdatel'stvo Transport, Moscow, 1977	10. Work Unit No. (TRAIS)
	11. Contract or Grant No.
	13. Type of Report and Period Covered
12. Sponsoring Agency Name and Address U.S. Department of Transportation Federal Railroad Administration 2100 Second Street, S.W. Washington, D.C. 20590	14. Sponsoring Agency Code

15. Supplementary Notes

The report is a translation of a current Russian Compendium on Wheel/Rail Dynamic Interaction.

16. Abstract

A description is presented of the procedure and the equipment used to study the dynamic loads acting on the undercarriages of freight cars. The results are presented from testing the four axle and eight axle gondolas and tank cars on the primary routes of the railroad network as part of operating and experimental freight trains. The generalizing relations are obtained for the vertical and horizontal (lateral) forces and the derailment coefficient . The test data would be useful for further, more precise definition of the calculated norms when designing cars considering the prospective operating conditions. The book is designed for scientific and technical workers connected with the construction, operation, maintenance and repair of freight cars.

17. Key Words	18. Distribution Statement
Wheels, Strain Gages, Rails, Side-Frame, Dynamic Wheel Loads, Vertical Forces, Lateral Forces, Derailment Coefficient	Document is available to the Public from the Sponsoring Agency, RRD-32, while quantities last.

19. Security Classif. (of this report)	20. Security Classif. (of this page)	21. No. of Pages	22. Price
UNCLASSIFIED	UNCLASSIFIED	243	

Form DOT F 1700.7 (8-72) Reproduction of completed page authorized

PREFACE

This translation of a collection of Russian Papers on the subject of "Dynamic Loads on the Undercarriages of Freight Cars" is the most recent Soviet document on the subject, in the possession of the Federal Railroad Administration.

The document is largely self-explanatory; however, some of the literally translated expressions require clarification. Undercarriage then becomes "trucks", tensometric becomes "strain gage bridge", and derailment coefficient is our familiar "L/V ratio". Some of the instrumentation techniques, particularly those involving spoked wheels, are rather unique.

The eight-axle cars studied appear to utilize two two-axle trucks connected by a span bolster.

The authors launch into detailed discussions of the techniques used. Since the methods used are similar to methods used in the U.S., the book should be a good source document for anyone setting up field tests of L/V data.

In the contents section, some comments and titles have been inserted parenthetically to clarify the listing. Double parenthesis (( )) are used to distinguish between these insertions and original insertions from the translation.

Table of Contents

FIGURES

FIGURES

FIGURES

FIGURES

TABLES

UDC 625.245.62.011.1.001.42

DYNAMIC LOADS ON THE UNDERCARRIAGES OF FREIGHT CARS

Moscow DINAMICHESKIYE NAGRUZKI KHODOVYKH CHASTEY GRUZOVYKH VAGONOV in Russian 1977 signed to press 15 Apr 77 pp 1-144

[Book edited by N. N. Krudryavtsev, Doctor of technical sciences, Izdatel'stvo Transport, Moscow, 1977, 1,000 copies, 144 pages]

[Text] Abstract

A description is presented of the procedure and the equipment used to study the dynamic loads acting on the undercarriages of freight cars. The results are presented from testing the four-axle and eight-axle gondolas and tank cars on the primary routes of the railroad network as part of operating and experimental freight trains. The generalizing relations are obtained for the vertical and horizontal (lateral) forces and the derailment coefficients. The test data will be useful for further more precise definition of the calculated norms when designing cars considering the prospective operating conditions. The book is designed for scientific and technical workers connected with the construction, operation, maintenance and repair of freight cars.

There are 64 illustrations, 14 tables and 25 references.

The book was written by the following authors: Chapter I by N. N. Krudryavtsev, doctor of technical sciences, engineers V. M. Saskovets, O. S. Tatrinova, I. N. Stupichev, B. V. Baklanov; Chapters II, IV (items 4 and 5), VIII and IX by engineer V. M. Saskovets; Chapters III, IV, X (item 10.2) by N. N. Krudryavtsev, doctor of technical sciences; Chapters V, VI and VII by L. I. Barteneva, candidate of technical sciences, engineers V. A. Sychev, L. A. Kurasova; Chapter IV (item 4.6) by Yu. M. Cherkashin, candidate of technical sciences; Chapter IV (item 4.7) by engineer V. V. Frants; Chapter X (items 10.1 and 10.2) by A. B. Survillo, candidate of technical sciences.

Foreword

The 10th Five-Year Plan poses the problem of further significant increase in carrying and hauling capacity of the railroads for railroad transportation. This problem can be solved on the basis of increasing the carrying capacity and speeds of the freight trains with more intense use of the car fleet.

The creation of new heavy cars and modernization of the existing ones are impossible without obtaining reliable data on the operating conditions of the bearing elements of the structure in operation. The basis of these data must be the statistical laws of the forces acting on the undercarriages of the cars which determine the operating conditions of all of the basic elements of the trucks and body of the car.

The different types of structural designs of the cars and their undercarriages and the differences in their technical condition require large-scale studies to obtain reliable generalized laws of the force interaction of the cars and the track.

This problem was solved by plan by the Railroad Car Division of the Central Scientific Research Institute of the Ministry of Railways beginning in 1968. This paper is the result of the studies.

Comments should be addressed as follows: Moscow, 129851, 3-ya Mytishchinskaya ul., 10. Editing and Publishing Division of the Central Scientific Research Institute of the Ministry of Railways.

Deputy Director of the Institute, Doctor of Technical Sciences, Professor N. A. Fufryanskiy

Head of the Railroad Car Division, Candidate of Technical Sciences, A. A. Dolmatov

Chapter I. Measurement of Vertical and Horizontal Forces Acting on a Pair of Railroad Car Wheels

1.1. State of the Art With Respect to the Question

The basis for developing methods of measuring the dynamic forces acting on a pair of railroad car wheels is the principle of measuring the mechanical deformations of the surfaces of the individual elements of the car-track system or special dynamometers. The mandatory condition here is proportionality of the deformations to the operating forces.

Strain resistance for measuring the forces can be placed on the elements of the track, the trucks and directly on the wheel pair itself. The choice of the measurement technique depends on the purpose of the investigation.

The method of measuring the forces by the deformations of the track elements in which the strain gauges are applied to one or several cross sections of the rails is the simplest method (in the sense of the measuring system). Inasmuch as this method does not permit measurement of the dynamic forces acting on the wheel pair over a long extent of the track, it has limited application. The complexity of ensuring sufficiently high insulation of

the measuring circuits, especially during their prolonged use in segments of operating railroad lines is an essential deficiency of the method. However, in recent years this method has been improved. The possibility has arisen for continuous measurement of the vertical forces acting on the rail, at the end of a segment of the track. It has been successfully used to discover defects on the rolling surface of the wheels which cause increased effect of the dynamic forces on the track and the axle box assemblies of passenger cars [1] under the moving trains.

The use of dynamometers for measuring the forces acting on the wheel pairs in certain cases gives positive results, but it is also limited by the fact that the dynamometers and other force-measuring devices, which serve as intermediate elements in the assemblies, picking up the measured forces, interfere with the kinematics of the truck to one degree or another. The method of measuring the vertical and horizontal forces with respect to deformations of the side frames of the trucks is the best known and most widely used both in our country [2] and abroad [3]. The strain resistors are applied to the outsides and insides of the lateral frames and they are assembled into systems having, as a rule, good sensitivity with sufficient compensation of the thermal deformations. At the same time, they have little sensitivity to the deformations of other directions. This method will permit continuous measurement of the horizontal (frame) and vertical forces during movement along a section of track of any length. A deficiency of the method is the high precision of measuring the forces acting on the wheel pair.

As has been established [4-6], the horizontal forces acting on the truck frame and the wheel pair can differ both with respect to phase and with respect to amplitude. In individual cases these divergences are quite significant [5]. This is explained by the possibility of clamping the truck frame in the axle box openings, significant removal of the points of applying the strain resistors from the points of application of the forces and other factors.

With constant increase in the intensity of motion and a tendency toward an increase in the speeds of passenger and freight trains, the experimental estimation of the force regimes of operation of the elements of the wheel pairs and the relations of the vertical and lateral forces at the points of contact of the wheels with the rails which determine the stability with respect to rolling of a wheel onto the rail head--one of the basic conditions of safety of motion--is becoming more and more necessary.

The method developed at the Railroad Car Division of the All-Union Scientific Research Institute of Railroad Transportation (the Central Scientific Research Institute of the Ministry of Railways) for measuring forces with respect to deformations of the axle of a pair of wheels in four cross sections [7] ensures more exact determination of them, but as a result of complexity of the calculations it has not found broad application.

The first experiments in the use of the wheel pair webs as elements for measuring the horizontal forces at the point of contact of the wheel with the rail were performed in 1960. A system was developed and checked out

for continuous measurement of horizontal forces, and a theoretical basis was provided for the first time for the possibility of the application of several strain resistors uniformly distributed around the periphery of the web for this purpose.

This experiment had great practical significance, for it made it possible to discover many theoretical difficulties in the use of the elements of the turning wheel pair in complex force and stressed states, as the converter sensors for measuring the dynamic forces at the contact of a wheel with the rail. In particular, it was demonstrated that the angular velocity of the wheel pair has a significant effect on the readings of the horizontal force continuous measurement system. When looking for places to apply the strain resistors the researchers encountered difficulties in excluding the effect of vertical forces on the readings of the measuring circuit. It was recommended that the strain resistors be placed both on the inside and on the outside surface of the web. As a result, in addition to increasing the sensitivity of the system (by 30 percent) the effect of centrifugal forces was eliminated, and the compensation for thermal deformations was improved.

An attempt to create a system for continuous measurement of vertical forces acting on a wheel of an electric locomotive was made in 1964 at the Division of Electrification of the Central Scientific Research Institute of the Ministry of Railways [8]. A pair of spoked wheels with an odd number of spokes (11) was used here. The inconstancy of the scale of measurement of the vertical forces and the low sensitivity of the system did not permit its use in practice. In [8] the possibility of increasing the sensitivity of the system

for measuring vertical forces by including groups of strain resistors in the different arms of the bridge is demonstrated. A piecewise-continuous recording with variable scale is obtained in this case, which also makes deciphering of the recordings very complicated.

In 1965 [9] was published in which a detailed discussion was presented of the procedure for equipping the wheel pair of a passenger car with systems for continuous measurement of the horizontal and vertical forces acting on the wheel webs. The experiments were performed with a wheel pair having wheels 1,050 mm in diameter. In order to achieve greater measurement precision, the webs were turned on a lathe. During the experiment it was demonstrated that when finding the places to apply the strain resistors and calibrating the systems on a bench for testing wheel pairs it is necessary to consider the effect of the displacement of the points of application of the loads on the readings of the force-measuring circuit. The conditions of support of the wheel on the rail (the eccentricity of the contact with respect to the web) had no effect on the readings of the system for measuring the horizontal forces. At the same time, the change in position of the contact point of the wheel with the rail with respect to the web is essentially felt in the deformations recorded by the system for measuring the vertical forces. As was demonstrated in [9], the displacement of the contact point with respect to the rolling surface by 20 mm causes a change in readings of this system by almost 20 percent. It was discovered that when using a web wheel for continuous measurements of the vertical forces, it is in practice impossible to exclude the effect of the horizontal forces

on the readings of the measuring system in spite of the exceptionally high requirements on the precision of marking (to 0.2 mm) the position of the strain resistors. This is promoted by the significantly lower level of deformation of the webs under the effect of the vertical forces than under the effect of the horizontal forces. They are distributed over the webs in such a way that when joining the strain resistors into one arm of the bridge circuit the mean values of the deformations (the null harmonics) are close to zero. In addition, as has already been noted in previous papers, on trips when the speed is varied a characteristic shift of the zero line on the oscillogram was observed which is caused by the effect of the centrifugal forces.

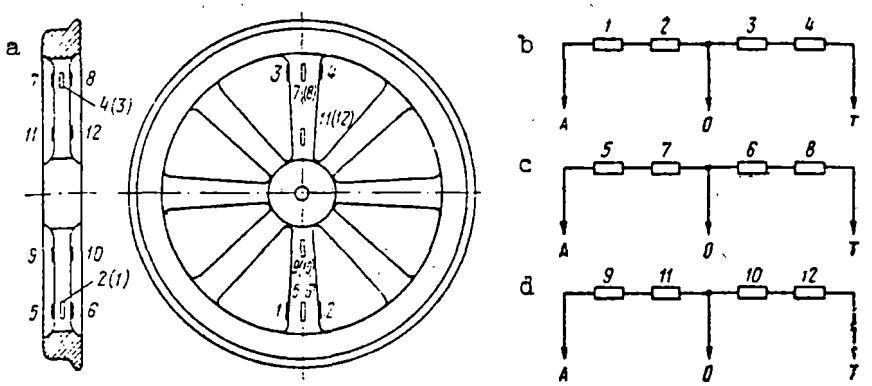

Figure 1.1. Spoked wheel dynamometer and circuit diagram for the strain resistors: a--wheel dynamometer; b--for measuring the vertical forces (strain resistors are located inside the openings); c, d--for measuring the vertical and horizontal forces (the strain resistors are located on the lateral surfaces of the spokes).

The author of [10], considering the deficiencies of this system, arrives at the conclusion of inexpediency of developing a system for continuous recording of vertical forces. The system for precision recording of vertical forces (one measurement per revolution of the wheel) assembled from strain resistors glued on both sides of the web had, according to the bench test data, a maximum error of about 1 percent under the same conditions.

The forces of interaction of the wheels with the rails have also been measured with the help of the tensometric wheel pairs abroad, in particular, on the railroads of Japan [11, 12]. Here a pair of spoked wheels with rectangular sections on the spokes machined on a machine tool were equipped with measuring circuits. The use of the spoked wheel to measure the loads on the wheel, in particular the vertical loads, is exceptionally expedient.

A spoked wheel with the strain resistors placed on the spokes is shown in Figure 1.1.

The high precision of measuring the vertical forces is achieved here as a result of applying the strain resistors to the inside (openings) surfaces of the spokes. The strain resistors measure only the compressive deformations caused only by vertical loads. The effect of the bending deformations of the spokes in the longitudinal direction from the effect of the braking forces is picked up by including two strain resistors that measure the deformations of different signs in the same arm (Figure 1.1a). The inconvenience of this method is that it is possible to take only two measurements per revolution of the wheel. In addition, a comparatively weak

signal is picked up from the measuring bridge. However, according to the Japanese specialists this method, which offers good precision when measuring vertical forces, is entirely free of the effect of the lateral forces (especially on the curved sections of track) and the pressure of the brake shoes. When necessary it is possible to place several of the circuits on the spokes. The point system for measuring the lateral forces is presented in Figure 1.1c.

Without refuting the possibility of continuous measurement of vertical and horizontal forces, the authors of [11, 12] indicate the essential deficiencies of such systems.

Current collectors with working contacts are used on the Japanese railways to pick up signals from the turning pair of wheels. The rings of the collector are made of silver-copper-cadmium alloy and the brushes are made of silver and graphite. In order to improve the reliability of the contact, three brushes are supported on each ring of the collector. In [11, 12] it is pointed out that the collector can remain in operating condition without cleaning the surfaces of the contacts for 1,000 km.

In England the first tensometric wheel pair was manufactured in 1972 [3]. The strain resistors for measuring the vertical and lateral forces were placed on the spokes of a 12-spoke wheel pair. In contrast to the Japanese wheel pair the strain resistors making up the vertical force-measuring circuit (Figure 1.1b) were placed on the lateral surfaces of the spokes.

In the Railroad Car Division of the Central Scientific Research Institute of the Ministry of Railways, the measurement of the forces of interaction of the wheel with the rail by the web deformations began, as was indicated above, in 1960. In contrast to the foreign railroads using special spoked wheels, the studies were aimed at achieving the possibility of using standard web wheel pairs which could be used on all types of cars in operation for the measurements. In addition, in view of the complexity of creating the circuits for continuous recording of the forces and their significant deficiencies primary attention was given to the point measurement circuits with two operating (active) arms made up of strain resistors placed along the diameter of the wheel pair web.

The first efforts to create systems for point measurement of vertical and lateral forces demonstrated that it is complicated to exclude the effect of vertical forces on the readings of the lateral force-measurement circuits and vice versa when using an ordinary web wheel. This is especially true of the vertical force-measuring circuit. Therefore in 1969 the Electronic Tensometric Laboratory of the Division of Railroad Cars of the Central Scientific Research Institute of the Ministry of Railways proposed the manufacture of a wheel pair having radial slits on the webs forming four spokes. Thus, it became possible to place the strain resistors both on the lateral surface of the webs and inside the slits. The tests run on the first pair of wheels of this type in 1970 on a bench and on the road using an experimental ring demonstrated the possibility of using the tensometric wheel pairs with slits on the webs for measuring vertical and lateral forces

with sufficient precision.

In the following years the problems facing the laboratory where development of a detailed, available procedure for determining the places to locate the strain resistors for measuring vertical and horizontal forces with the required precision, a procedure for preparing the tensometric wheel pair for dynamic testing of freight cars and a procedure for manufacture, installation and use of current collectors.

1.2. Structural Design of a Tensometric Wheel Pair

A wheel pair is assembled from standard elements: the RU1-type axle and seamless rolled wheels 950 mm in diameter. First it was proposed that the surfaces of the wheel webs be subjected to machining. However, it turned out that it is quite complicated to do the turning with the required precision. Therefore the wheels were only checked in advance for absence of difference in thickness of the webs.

In order to improve the precision of measurement of primarily the vertical forces, eight through slits were made in the web, forming four spokes.

Drawing No DKV-68-01 of a wheel dynamometer is shown in Figure 1.2a. After making the spokes (slits) the wheels were pressed on the axle by the usual process. Holes 20 mm in diameter were drilled in the assembled wheel pair through which to run the measurement circuit wires going to the current collectors placed on the ends of the axle in the axle box assemblies. The drawing of the assembled wheel pair No DKV-68-00 with the holes is shown

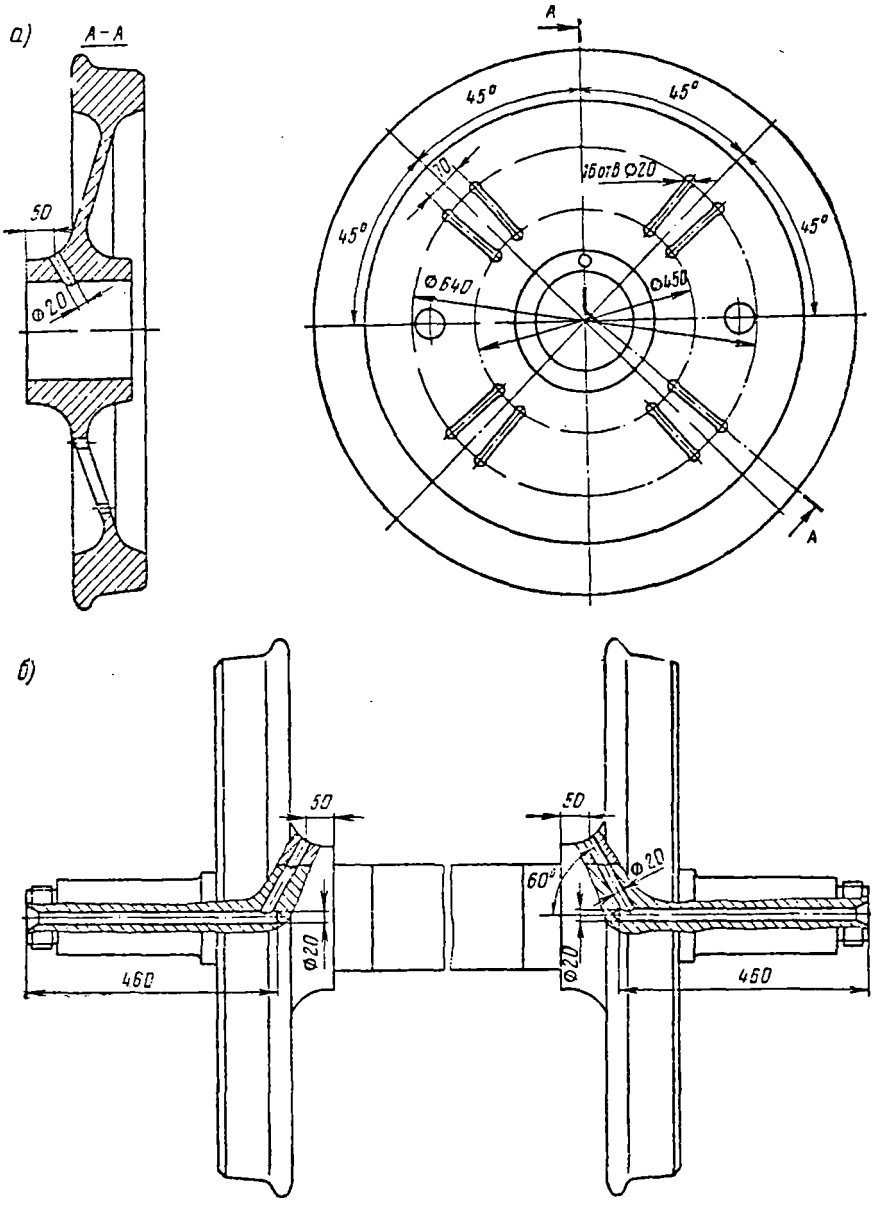

Figure 1.2. Tensometric wheel pair designed by the Railroad Car Division of the Central Scientific Research Institute of the Ministry of Railways: a--wheel dynamometer with slits in the web; b--general view of the wheel pair.

in Figure 1.2b.

It must be noted that the holes were drilled so as to weaken the wheel pair to the least degree. The longitudinal hole in the axle runs along its geometric axis of symmetry and in practice does not decrease the moment of resistance to bending. The inclined hole in the hub connected to the longitudinal hole runs through the middle of the part of the axle under the hub. As the measurements indicate, the bending stresses here are small, and cracks, as a rule, do not form.

Strain resistors were placed on the webs of the first wheel pair, after which it was subjected to static strength testing. It was established that the strength of the wheel was in practice no lower than that of the standard wheel. Accordingly, the drawings were agreed on with the TsV of the Ministry of Railways, and permission was obtained to install the wheel pairs on the railroad cars under the condition that the wheel pair is designed for running on the freight cars and passenger cars during the test period, and the admissible run for a pair of wheels is 50,000 km.

The wheel pair is equipped with axle box assemblies with roller bearings 250 mm in diameter.

1.3. Selection of the Places to Put the Strain Resistors and the Circuitry for Them. Calibration of the Wheel Pairs

The places to put the strain resistors on the web of the wheel pair and the methods of including them in the measuring circuit must be such that the

effect on the circuit of the force of another direction will be excluded with sufficient sensitivity of the circuit to the measured force.

Four groups of 11 strain resistors each were applied to the web of one of the wheels of a wheel pair (Figure 1.3): in the middle of the spoke on the outside surface of the wheel (I), in the middle of a spoke on the inside surface of the wheel (II), midway between spokes on the outside surface of the wheel (III), midway between spokes on the inside surface of the wheel (IV). The distance between the middles of the adjacent strain resistors is 20 mm.

The strain resistors manufactured at the plant for experimental structural elements, products and equipment of the Central Scientific Research Institute of Structural Parts of the USSR Gosstroy have the following parameters: base 10 mm; resistance 200.5 ± 0.2 ohms; strain sensitivity coefficient 2.07.

The radial deformations occurring at the points of applying the strain resistors were determined on the bench for testing the wheel pairs for four positions of the wheel pair: A--group I (II) at the bottom; B--group I (II) at the top; C--group III (IV) at the bottom; D--group III (IV) at the top.

The values of the deformations (in relative units) were calculated as the difference in readings of the TA-1000 device obtained for some value of the load and for no load (the zero regime). Three load regimes were realized: vertical 10 tons-force; horizontal 5 tons-force, pulling the wheels together; horizontal 5 tons-force, pushing the wheels apart. Each load regime was alternated with the null regime.

As a result, relative values of the deformations from the applied forces at the points of applying the strain resistors were calculated (Figure 1.4, 1.5, 1.6). The strain resistors which are sensitive to one type of load were selected by these data. Their sensitivity is presented in Table 1.1 (in relative units of deformation). From Table 1.1 it is obvious that the strain resistors 2 of groups II and IV have the greatest sensitivity to the vertical load, and the strain resistor located between the strain resistors 4 and 5 of group II or between the strain resistors 6, 7 of group IV has the greatest sensitivity to the horizontal load. The sensitivity of the corresponding strain resistors to the measured forces is in practice identical. It is inexpedient to use strain resistors of groups I and III for separate measurement of the forces, for they have less sensitivity to the measured force than the strain resistors of groups II and IV.

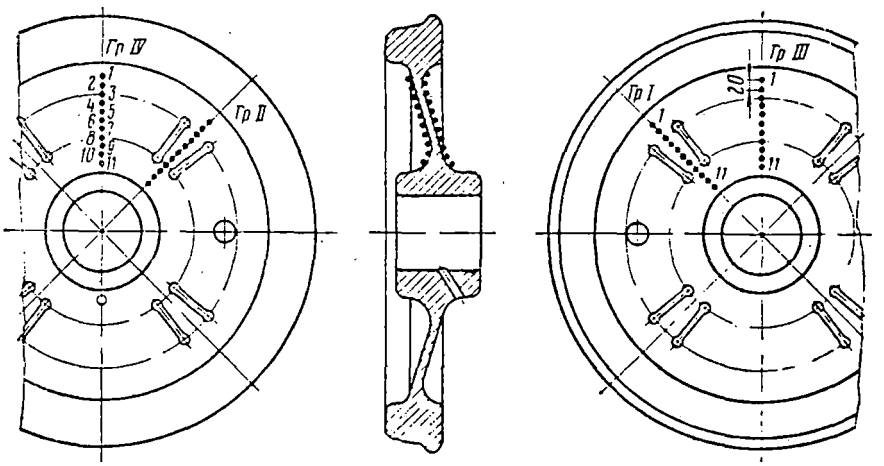

Figure 1.3. Schematic of the arrangement of strain resistors on the wheel dynamometer during calibrations.

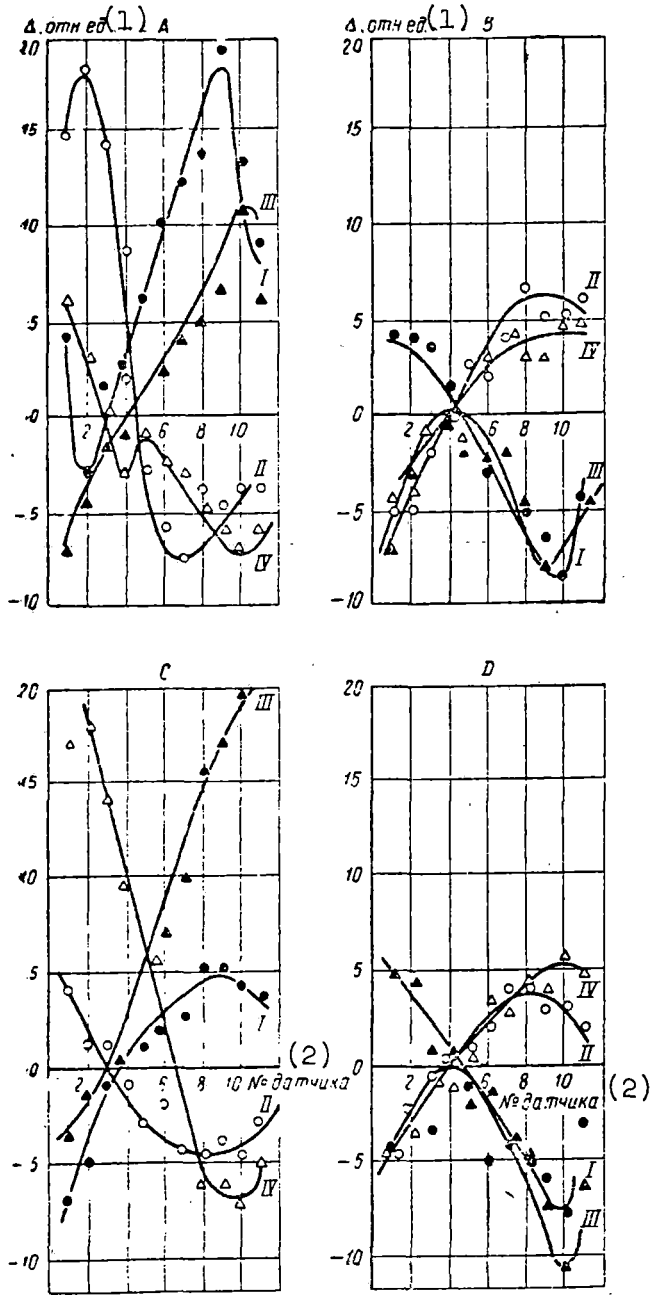

Key: 1. Relative units

2. Sensor number

Figure 1.4. Value of the deformations (in relative units) at the points of applying the strain resistors from the vertical load P = 10 tons applied to the axle boxes for four positions of the wheel pair (A, B, C, D).

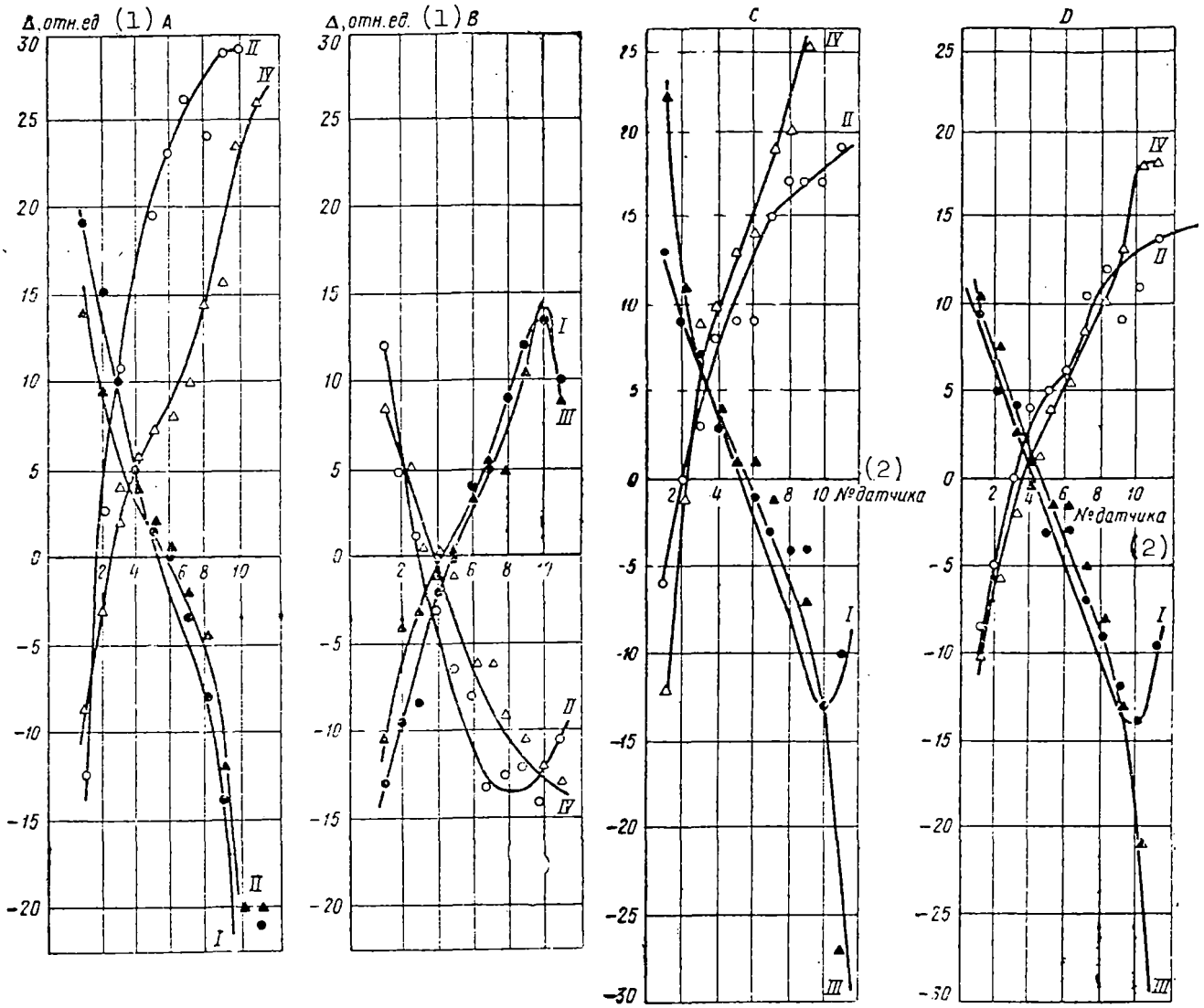

Figure 1.5. Value of the deformations (in relative units) at the points of application of the strain resistors from the horizontal load of 5 tons pulling the wheels in for four positions of the wheel pair (A, B, C, D).

Key: 1. Relative units

2. Sensor number

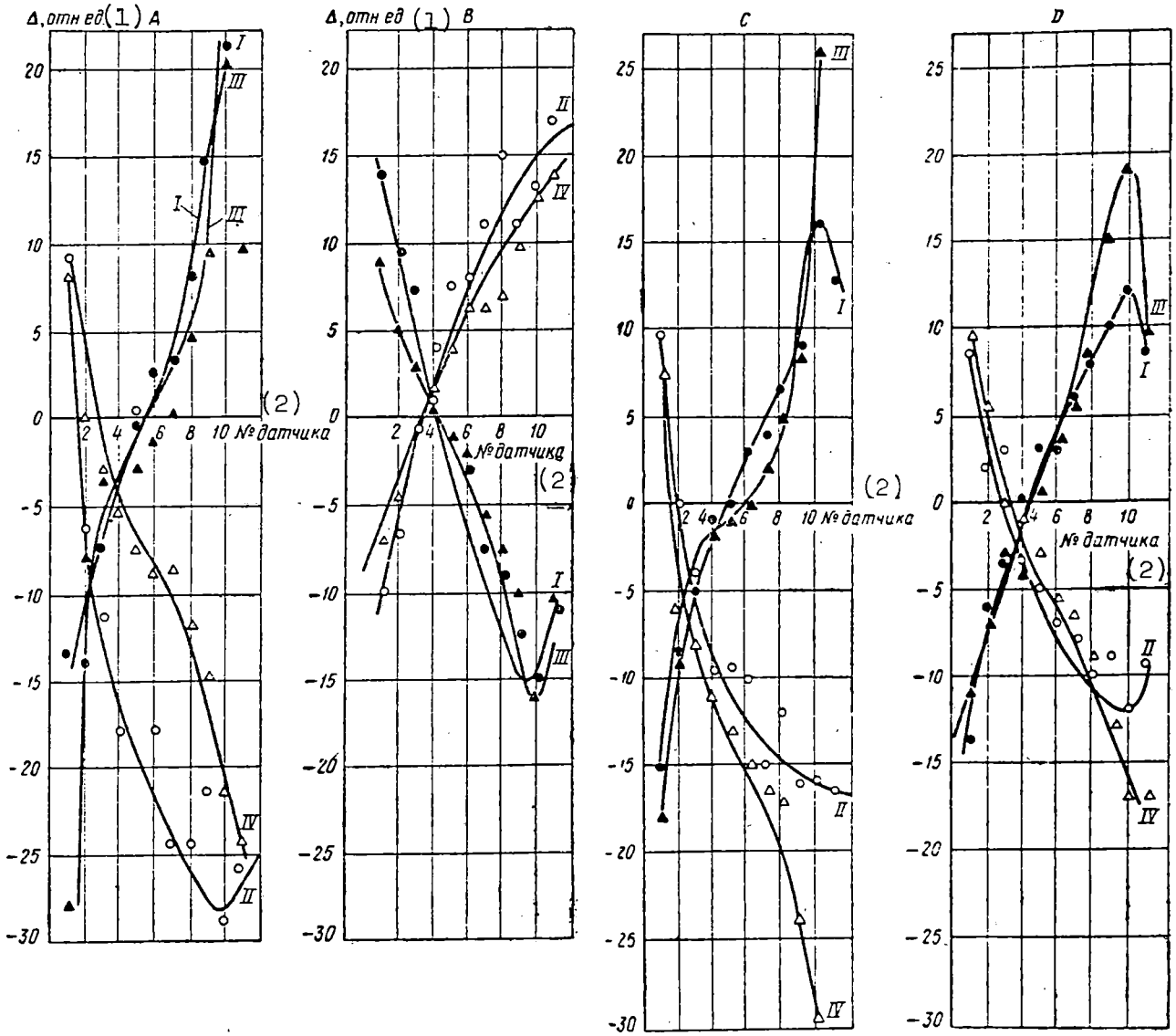

Figure 1.6. Values of the deformations (in relative units) at the points of application of strain resistors from the horizontal load of 5 tons directed outside the wheels with four positions of the wheel pair (A, B, C, D).

Key: 1. Relative units

2. Sensor number

Table 1.1

Положение колесной пары (1)	Группа тензорезисторов (2)	(3) Тензорезисторы, имеющие Δ = 0 при горизонтальной нагрузке		(6) Тензорезисторы, имеющие Δ = 0 при вертикальной нагрузке 5 тс		
		(4) Номер тензорезистора	10 тс (5)	(4) Номер тензорезистора	Стягивание (7)	Распор (8)
A	I	5—6	8,0	3	— 7,5	10,0
	II	2	18,0	4—5	—19,0	19,0
	III	5—6	2,0	3	— 4,0	6,0
	IV	2	3,0	4—5	— 6,0	5,0
B	I	5	1,0	4	— 2,0	3,0
	II	2	1,0	3	— 3,0	3,0
	III	6	8,0	3	— 3,0	7,0
	IV	2	18,0	6—7	—16,0	17,0
C	I	5	0	5	0	0
	II	3	— 2,0	4	6,0	— 7,0
	III	4—5	— 0,5	4	0,5	— 1,0
	IV	4	0	4	1,0	0
D	I	4	0	4	1,0	0
	II	3	— 0,5	4	4,0	— 3,5
	III	4—5	0	4	0	— 1,5
	IV	3	— 1,0	4	1,0	— 1,0

Key: 1. Position of the wheel pair

2. Strain resistor group

3. Strain resistors having Δ = 0 for horizontal load

4. Strain resistor number

5. 10 tons

6. Strain resistors having Δ = 0 for a vertical load of 5 tons

7. Pulling together

8. Pushing apart

The position of the strain resistors must be selected quite precisely. The spacing between the group II strain resistors, sensitive only to the horizontal or only to the vertical forces, is approximately 55 mm; for group IV it is more (about 90 mm). For group II, the mark for the placement of the strain resistors can be made with respect to the slits in the wheel web forming the spokes. It is more complicated to find the exact position of the group IV-type strain resistors than for group II.

Thus, for a separate recording of the forces acting on the pair of wheels, it is possible to apply two strain resistors each to the wheel web of which each is sensitive only to a force acting in one direction. However, it is more expedient to apply two strain resistors each to the diametrically opposite spokes of the wheels symmetrically to the first two with respect to the axle of the wheel pair and to assemble two measuring half-bridges from the symmetric strain resistors. There is then no necessity for the compensation strain resistor, and the repetition frequency of the measurements as the wheel rolls along the rail is doubled.

In order to decrease the measurement error connected with a shift of the contact point of the wheel with the rail relative to the rolling surface, it is possible to make up the measuring circuit from strain resistors applied to the inside and outside of the web. For this purpose, on the outside of the web it is necessary to select the strain resistors (from groups I and III) sensitive only to the vertical and horizontal loads and to combine them into circuits with the corresponding strain resistors on the inside of the web. In Figure 1.7 the procedures are shown for inclusion of the strain

resistors in the half-bridge circuits for measuring the vertical D_v (Figure 1.7b) and horizontal D_h (Figure 1.7c) forces using strain resistors placed on the inside of the web; the same using strain resistors placed on both sides of the web (Figure 1.7d and 1.7e); bending deformations in the overhanging σ_{III} and middle sections σ_{34} of the axle (Figure 1.7e and 1.7f).

With automatic processing of the recordings of the forces acting on the tensometric wheel pair, it is not necessary to select the combination of strain resistance which has zero sensitivity to the force in one direction and sufficient sensitivity to the force in the other direction. It is possible to take any pair of strain resistors which have sufficient sensitivity to one force or another. If the sensitivity of each circuit to the horizontal and vertical forces and the results of measuring the forces obtained using these circuits are known, then by solving two equations with two unknowns on a computer, it is easy to determine the values of the horizontal and vertical forces acting on the wheel pair. The data of such circuits must be processed on the computer at the same time as the readings of the strain resistor circuits which are sensitive to forces in only one direction can be used directly. Therefore the latter circuits are preferable.

During the tests the wheel pairs were equipped with the simplest circuits (see Figure 1.7b, e, f, g); each was made up of two strain resistors. The dynamometric wheel pairs were calibrated on a special bench permitting application of vertical loads to the journals (or to the axle boxes), and horizontal loads to the rims of the wheels. The results of the calibrations

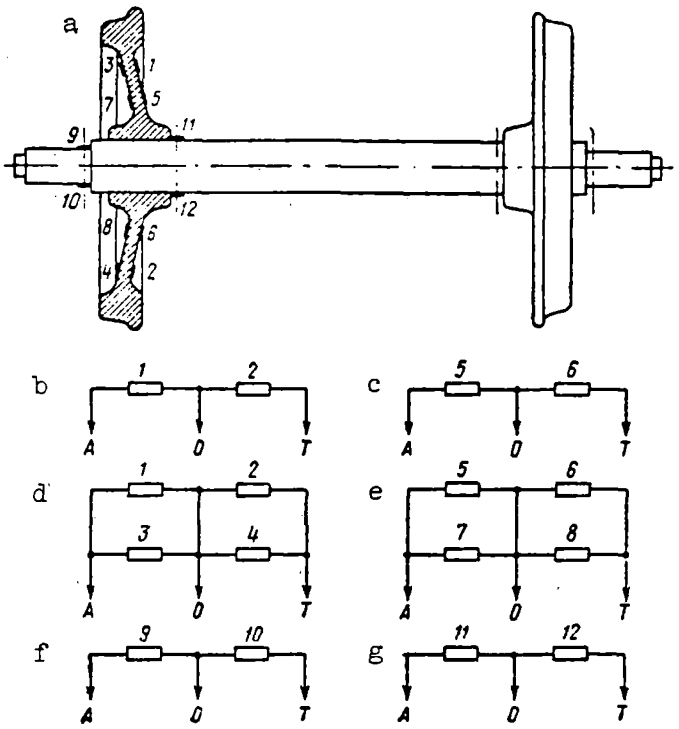

Figure 1.7. Tensometric wheel pair with strain resistors and their circuit diagrams for the measurements: a--wheel pair; b, c--for vertical D_v and horizontal D_h forces (the strain resistors are placed on the inside of the web); d, e--the same (the strain resistors are placed on both sides of the web); f--bending deformations in the overhanging σ_{III} parts of the shaft; g--the same in the middle σ_{34} parts of the shaft.

are presented in Table 1.2. For example, according to the calibration data for the wheel pair No 1 (the right wheel) the sensitivity of the circuit D_v assembled from the strain resistors 1 and 2 to the vertical force equal to 10 tons and horizontal force of 5 tons, respectively, is equal to 3 and 36.5 relative units. This means that the vertical load of 1 ton gives

interference equivalent to 0.04 ton of horizontal force. The analogous satisfactory results were obtained also for other wheel pairs.

Table 1.2

Номер колесной пары (1)	Сторона (2)	Схема (3)	(4) Колесная пара в положении A: (5) Вертикальная сила 10 тс	(6) Горизонтальная сила 5 тс: (7) Стягивание	(8) Распор	(9) Колесная пара в положении B: (5) Вертикальная сила 10 тс	(6) Горизонтальная сила 5 тс: (7) Стягивание	(8) Распор
1	Right	(10) $Д_в$	—29	0	1.5	25.5	2	— 2
		$Д_г$	— 3	—36.5	37.5	3	40.5	—35
	Left	$Д_в$	—24.5	2.5	0	31	— 4	— 1.5
		$Д_г$	2.5	35.5	38.5	0	39.0	—36.5
2	Right	$Д_в$	—19	1	1	21	0	— 1
		$Д_г$	— 3	32	32	3	32	—35
	Left	$Д_в$	—20	— 1	0	24	0	— 2
		$Д_г$	0	—32	30	— 2	31	—32
3	Right	$Д_в$	23	1	0	—24	1	1
		$Д_г$	4	35	—32	— 4	—30	31
	Left	$Д_в$	23	— 1	0	—18	1	— 1
		$Д_г$	1	26	—32	2	—29	31
4	Right	$Д_в$	23	0	0	—24	2	0
		$Д_г$	2	—41	38	— 3	41	—36
	Left	$Д_в$	18	1	0	—24	— 1	1
		$Д_г$	2	—31	33	— 2	35.5	—36

Note: Calibration data are presented in relative units of the device. The scale division is 18.1 kg/cm^2.

Key: 1. Number of wheel pair
2. Side
3. Circuit
4. Wheel pair in position A

Key to Table 1.2 (continued)

5. Vertical force 10 tons
6. Horizontal force 5 tons
7. Inward
8. Outward
9. Wheel pair in position B
10. $Д_в = D_V$; $Д_г = D_h$

1.4. Procedure for the Manufacture of a Tensometric Wheel Pair for Measurements During Dynamic Testing of Cars

A wheel pair is installed on a special bench or rail 45 meters long before the installation of the measuring circuits. The points of application of the strain resistors and laying of the mounting wires to the entrance to the opening in the hub are marked. Holes are drilled at the places marked by the chalk, and they are threaded for attachment of the wires by screws. For installation of the half-bridge measuring circuits, which are put on the hub, the MGShV-0.12 type wire is used. The leads from the ends of the measuring circuits to the ends of the axle are made of wire no less than 0.20 mm in diameter. The mounting wires are wound with cotton tape, and they are fastened in the form of strands to the wheel pair by screws using rigid clamps and inserts made of cotton fabric. In order to exclude the damage to the wires, dense insulation tubes are fitted on the sections of the strands passing inside the hub.

The tensometric wheel pair operates under the conditions of a wide range of dynamic loads, increased moisture and significant temperature fluctuations. In order to ensure reliable operation of the measuring circuits, a special process is used to protect against water, oil and strong vibrations. First

a layer of surgical tape was applied to the strain resistors and its edges were fastened to the surface of the wheel by Mokol glue. After drying, the surgical tape and the connecting wires are impregnated with 12-01 lacquer. Then the layer of surgical tape is again applied over the top, and it is coated with lacquer. The operation is repeated several times. On completion of drying a megohmmeter with 500-volt voltage was used to measure the resistance of the circuit insulation which must be no less than 100 megohms. Then the strain resistors and the installation wires are covered with a layer of moistureproof mastic (wax, resin, lubricant and colophony). The exit opening of the hood is fitted with cotton tape and is filled with mastic.

The operation of the current collector is first checked out (Figure 1.8) in the laboratory. Its contacts are connected alternately to one of the arms of the measuring circuit. With respect to the possibility of balancing and "drift" of the beam on the oscillograph screen on rotation of the head of the collector in both directions (simulation of the operation of the collector) the fitness of 10 of its channels (rings) is determined. The scheme of the oscillograph beam is selected so that on shunting one of the arms of the half-bridge by a calibrated resistor using a 1 megohm resistance the beam recoil was 40-50 mm. For the channels in working order, absence of "jerking" and sharp recoils of the beam on turning the collector head is characteristic. The smooth displacements of the beam within the limits of ±1 mm are admissible.

Before installing the selector on the wheel pair, 10 segments of multistrand wire 0.20-0.35 mm in diameter and 6-8 cm long were soldered to the rotor contacts. The soldering points were insulated from each other and from the housing of the collector. An insulation bushing with 10 two-way clamps is fitted on the head of the rotor. The ends of the wires from the rotor contacts are soldered to these clamps on one side. Ten wires 0.6-0.7 meter long and no less than 0.35 mm in diameter were soldered to the output terminals of the stator. Then all 10 channels of the collectors are named, marked and their insulation with respect to the housing is checked using the megohmmeter.

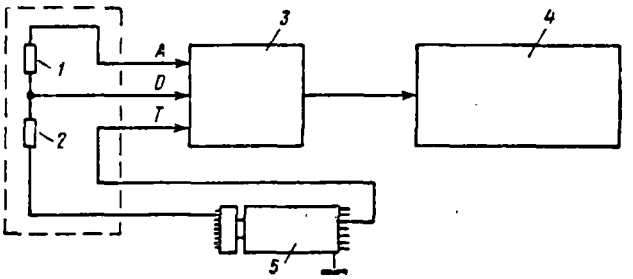

Figure 1.8. Electric circuit for testing the current collectors: 1, 2--active and thermal strain resistors; 3--tensometric amplifier; 4--light beam oscillograph; 5--current collector.

The schematic of the device and the basic elements for attachment of the collector to the axle box of the wheel pair are illustrated in Figure 1.9. It is attached to the bed on shock absorbers and it is aligned with the axis of the fastening cleat on the wheel pair axle. The shafts of the current collector and the fastening cleat for transmitting the moment of rotation are connected by a steel spring. The leads of the measuring circuits

on the end of the shaft are connected to the head of the current collector by thin steel wires with insulation tubes fitted on them. The ends of the wires are soldered to the end shoe so that they are directed not to the current collector but to the end of the shaft (see Figure 1.9). The wires are attached by special clamping-down devices between the soldering point and the end shoe. Then they are smoothly bent in loops and are soldered to the terminals of the insulation bushing of the current collector. The length of the connecting wires must be optimal: they should not contact the pins of the fastener on rotation of the current collector rotor, but they must permit the rotor to turn with respect to the end of the shaft approximately a half turn in both directions after reliable fastening of the wires to the insulation bushing.

This method of connection permits maximum unloading of the measuring circuits from the transmission of the moment of rotation to the current collector and a significant increase in the time of their stable operation during powerful vibrations and shocks. The spring connecting the rotor of the current collector to the shaft of the fastening cleat compensates for small eccentricities which can occur in the case of inexact installation of the fastening cleat to the end of the shaft and the current collector itself.

After testing the measuring circuits, including the transient contacts of the current collector, the shaft box is closed by a special hood which prevents moisture and dirt from getting into it.

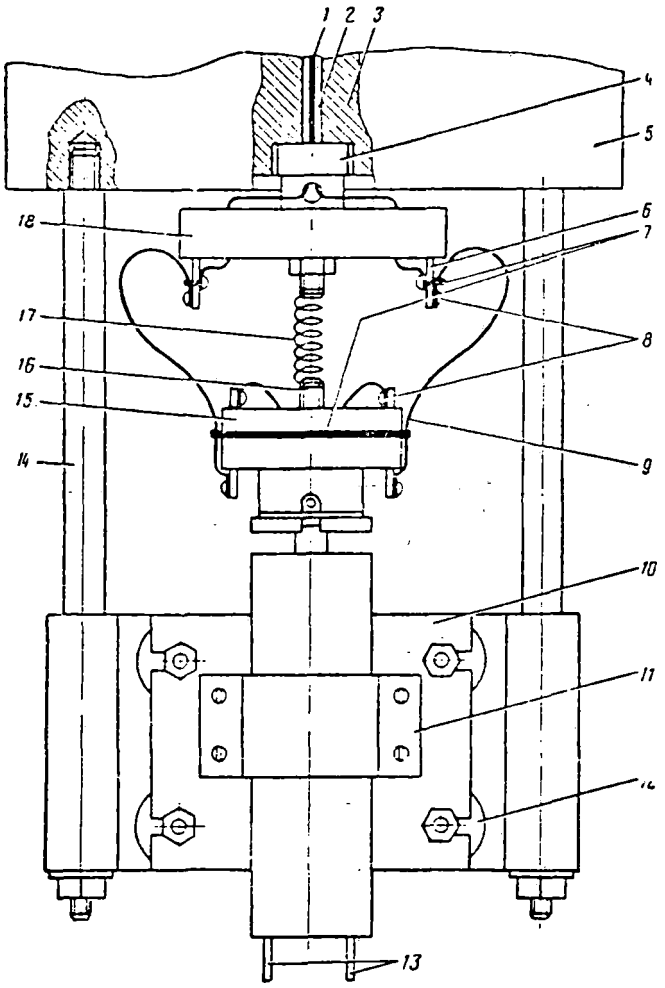

Figure 1.9. Installation of a current collector on the axle box of a tensometric wheel pair (top view): 1--cord; 2--hole in the end of the axle; 3--axle of the wheel pair; 4--fastening cleat with bushing; 5--axle box housing; 6--block contact; 7--clamping-down device; 8--soldering points; 9--connecting line; 10--bed of the collector; 11--clamping-down cleat; 12--rubber shock absorber; 13--output terminals of the current collector; 14--fastening pin; 15--insulating bushing of the current collector; 16--bushing; 17--spring; 18--contact box.

In view of the fact that the collector designed by the VNITI has 10 rings, it can be used for signal transmission only from three measuring circuits (each circuit is made up of half-bridges with three leads). On combining the midpoints of the two circuits five rings are sufficient. Therefore for a simultaneous recording of the signals of all four measuring circuits which have leads going out to the end of the axle from one side, the midpoints are connected in pairs. With good insulation of the current collector rings and the measuring circuits themselves, this connection has no effect on the measurement precision or the measurement reliability. If necessary joining of the common points of all four circuits and transmission of the signals using nine rings are permitted.

It is recommended that the signals from the measuring circuits of the tensometric wheel pair be recorded on magnetic tape with subsequent computer processing. In order to monitor the operation of the tensometric wheel pair and for the possibility of express analysis of the data some number of experiments, as a rule, are recorded on light beam oscillographs. With a speed of the experimental object from 60 km/hr and higher the speed of the photographic paper of the oscillograph must be no less than 100 mm/sec. This gives a smooth, high-quality recording of the process convenient for processing.

Before the experimental trips it is necessary to check the calibration of the measuring circuits of the tensometric wheel pair. The circuits for measuring the horizontal pairs directly under the train car are calibrated using the thrust dynamometer with special clamps made in the shape of the

wheel flange and tread. The clamps permit horizontal forces of 5-6 tons to be applied to the wheels, pulling them out or pushing them out.

If the static loads on each wheel are known, the circuits for measuring the vertical forces and stresses in the axle can be calibrated, unloading the webs of the wheels by two portable hydraulic jacks installed under the axle boxes of the tensometric wheel pair.

Rolling over a smooth section of track at low speed can also be used to determine the scales of the recording. However, in this case it is necessary to consider that the presence of friction of the wheels across the rails can cause the appearance of spreading orces which, in addition to bending the webs, cause variation of the stresses also in the parts of the axle beyond the hubs. Therefore by the rolling results it is possible to determine the scales only of the circuits for measuring the vertical forces and stresses in the overhanging parts of the axle. A correction considering the spreading frictional forces is required for the circuit for measuring the stresses in the part of the axle beyond the hub.

Inasmuch as the tensometric wheel pair is an element of the undercarriage of the railroad car that does not have spring suspension, the measuring circuits record the forces of interaction of the wheels with the rails in a wide frequency range. The preliminary studies performed by the Railroad Car Division demonstrated that the amplifying and recording equipment used for measuring these forces must transmit signals in the range of 0-300 Hz without distortion.

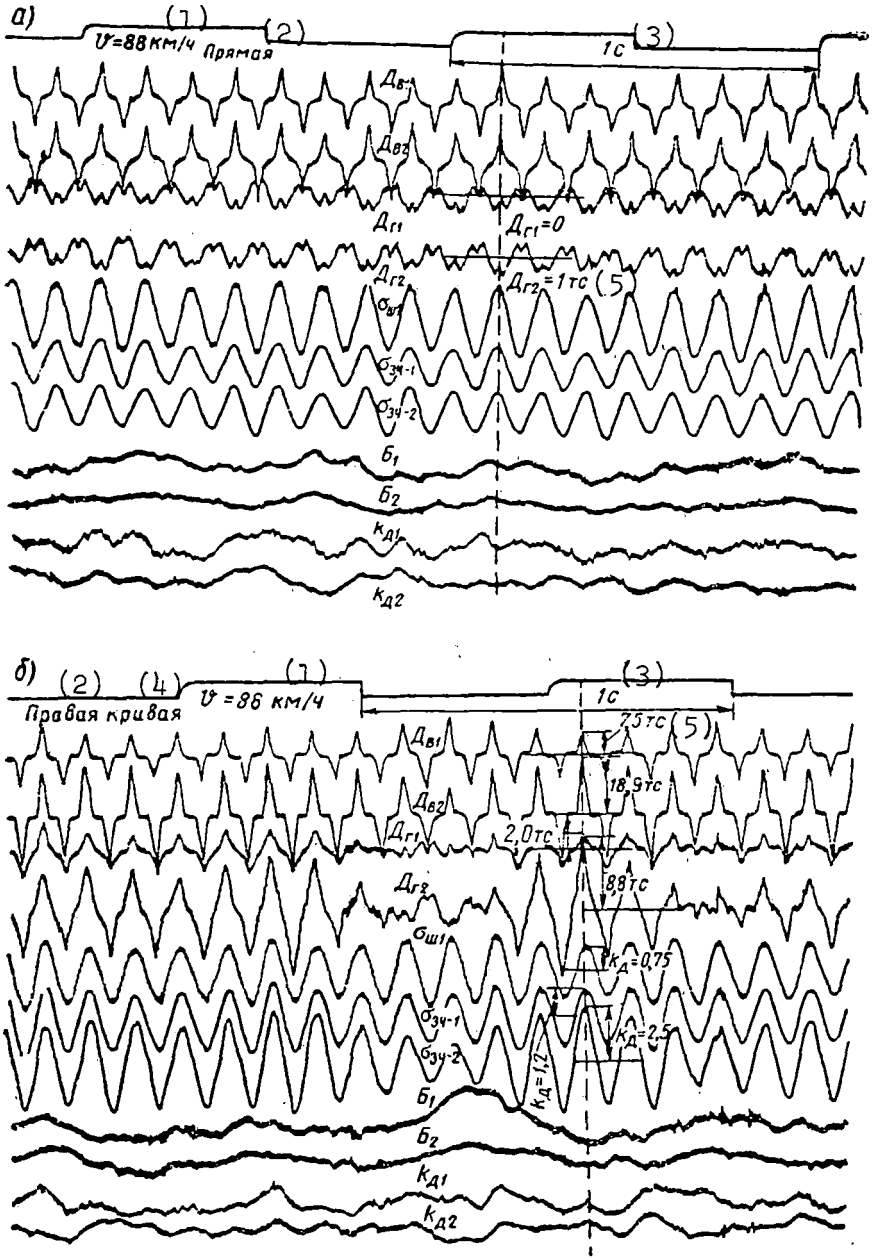

Figure 1.10. Example of recording process when a railroad car is moving: a--on a straight section of track without the wheels running against the rails; b--in a curved section of track.

Key: 1. ... km/hr 3. 1 sec 5. TC = ton-force

2. Straight 4. Curved

In order to estimate the measurement precision, the problems of picking up the high-frequency loads on interaction of the wheels of the tensometric wheel pair with the rails having different unevennesses under actual conditions, including short unevennesses on the rolling surface, require additional study.

1.5. Some Results and Prospects of the Application of Tensometric Wheel Pairs

The recording of the forces operating on the webs at the contact points with the rails and the stresses in the axle of the tensometric wheel pair is presented in Figure 1.10.

A distinguishing feature of the systems with point measurement of the values used in the tensometric wheel pair is the sign-variable recording of the forces and stresses not actually changing its sign (for example, the recordings of the vertical forces D_v and stresses σ_{shch}). This form of recording is explained by inclusion of two active strain resistors in the different arms of the half-bridge. The advantage of this recording consists in the simplicity of finding the null line (the reading line). In the continuous recording circuits, the determination of the null line is complicated with possible drift of the nulls of the amplifying and recording equipment, especially on appearance of a constant component of the signal on the curves of the sections of the track.

The recordings of the horizontal forces D_h have a more complex form (see Figure 1.10). This is explained by their sign-variable nature. The actual

direction of their horizontal force is established as follows. If the recording of D_h is in the same phase with the recording of the vertical force D_v, the horizontal force is directed inside the track; in the case of noncoincidence of the phases, this force is directed outside the track.

The application of the tensometric wheel pair for measuring vertical and horizontal forces permitted a significant degree of expansion of the ideas of the processes occurring on interaction of the wheel with the rail.

The qualitative analysis of the recordings of D_h demonstrated that on movement without running of the flange against the rail (Figure 1.10a) the spreading frictional forces directed outside the track act on the webs. They appear as a result of bending of the axle under the effect of the vertical forces. The frame force in this case is within the limits of the values of the frictional forces of the wheels across the rails, and it is determined by the difference of them. A similar picture is observed, as a rule, on moving along the straight sections of the track. The schematic of the effect of the forces taken by the wheel at the point of contact with the rail in this case is shown in Figure 1.11a.

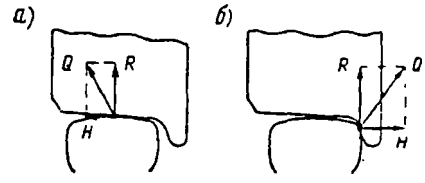

Figure 1.11. Schematic of the forces acting on the wheel from the rail: a--in the case of free rolling of the wheel; b--if the flange runs against the head of the rail with contact at one point.

The measurement of the horizontal forces with respect to deformations of the webs of a tensometric wheel pair made it possible to establish that the frictional forces in this direction in operation usually do not exceed the value of $H_{friction} = 2.6$ times.

When one of the wheels runs its flange against the rail the tensometric measurement circuit on the web records a force acting toward the inside of the track (Figure 1.10b). These events determine the stability of the wheel with respect to running up on the rail head.

The schematic of the forces acting on the web of the oncoming wheel in the case of single-point contact with the rail is presented in Figure 1.11b. The horizontal (transverse) H and vertical R forces acting on the wheel from the rail are the resultants of the forces at the point of contact considering the frictional forces. A more complex picture of the force interaction when the flange runs against the rail head occurs in the case of a two-point contact of the wheel with the rail [13, 14]. However, even in this case the deformations of the oncoming wheel web are proportional to the resultant forces in the vertical and horizontal (transverse) planes.

The horizontal transverse forces acting on the web of the oncoming wheel can reach significant values. In experiments with freight cars when testing a tensometric wheel pair in 1974 forces of 10-12 times were recorded.

When the flange of the wheel runs against the rail head, the web of the opposite wheel running without colliding against the rail records a horizontal force at this time also acting toward the inside of the track (see

Figure 1.10b). The appearance of forces of this direction is caused by friction between the surfaces of the wheel that does not collide with the rail head and the rail.

The friction forces directed inside the track can be appreciably greater than the spreading friction. In the experiments on an experimental wheel going around curves at low speeds (45-50 km/hr) frictional forces were noted equal to 5-5.5 tons. If the horizontal and vertical forces acting on the noncolliding wheel are recorded simultaneously, it is possible to estimate the frictional coefficient of the noncolliding wheel across the rail.

The development of a tensometric wheel pair and an improved procedure for preparing it and performing measurements made it possible to begin the systematic application of the tensometric wheel pairs during dynamic tests. In particular, they were widely used for accumulating data on the loads acting on the wheels and the axle, when performing the studies with respect to estimating the load regimes of the undercarriages of the freight cars of different types under the existing and prospective operating conditions.

Chapter II. Determination of the Coefficient γ--The Ratio of the Horizontal and Vertical Forces Acting on the Wheel When It Collides With the Rail

2.1. Determination of the Coefficient γ by Deformations of the Truck Frame

One of the basic factors influencing the stability of the wheel with respect to running onto the rail head is the ratio of the horizontal and vertical forces acting on the wheel at the point of contact with the rail when it hits.

Determination of the forces at the contact is a highly complex problem, for in particular, the contact zone shifts constantly along the rolling surface of the wheel and the rail. In addition, in order to estimate the stability of the wheel with respect to running onto the rail head it is necessary to calculate the ratios of the forces over a long extent of the track continuously, inasmuch as even the individual cases of exceeding admissible values of the ratios can be the cause of safety violations of the movement.

It is natural that the methods of manual processing and calculation of the stability previously used are not appropriate for estimating the

safety of movement with continuous growth of traffic intensity and increased speeds of the trains. Therefore in recent years the studies have been aimed at the development and improvement of methods of measuring the forces operating at the point of contact of the wheel with the rail and the development of methods of automatic determination of the stability based on the application of modern means of recording and processing the data: magnetic tape and computers.

In 1969 the Railroad Car Divison of the Central Scientific Research Institute of the Ministry of Railways developed and successfully used a method of automatic calculation of the ratios of the horizontal and vertical forces of interaction of a wheel with a rail determined by the deformations of the lateral frames of the track for estimating the derailment coefficient of the cars [15].

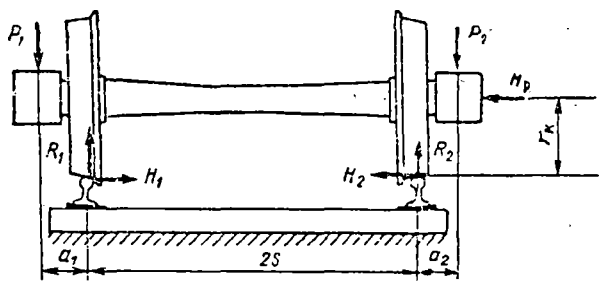

Figure 2.1. Schematic of the forces acting on a wheel pair (the wheel runs its flange against the rail).

In Figure 2.1 a wheel pair is shown in the position where one of the wheels (the left wheel) runs its flange into the rail. The problem is stated to determine the horizontal H_1 and H_2 and vertical R_1 and R_2 components of the forces of interaction of the wheels with the rails.

The initial values which are recorded during movement of the car are the frame force H_p (the force of interaction of the wheel pair with the frame of the truck) and the coefficients of vertical dynamic loading of the lateral frame k_{d1} and k_{d2}. In addition, by the results of wheel-by-wheel weighing of the loaded railroad car, the static vertical loads on both wheels from the rails R_{1st} and R_{2st} and also the static components P_{1st} and P_{2st} of the vertical load from the body on the axle boxes of the investigated wheel pair P_1 and P_2 are determined.

In the case where the mass of the loaded body on the wheel pair is uniformly distributed between the axle boxes, inequalities occur:

$$R_{1st} = R_{2st} = R_0; \tag{2.1}$$

$$P_{1st} = P_{2st} = P_0. \tag{2.2}$$

Taking this into account, the vertical loads on the axle boxes will be:

$$P_1 = P_0 + P_0 k_{d_1}; \tag{2.3}$$

$$P_2 = P_0 + P_0 k_{d_2}. \tag{2.4}$$

In order to determine the forces H_1, H_2, R_1 and R_2, the equations of statics are used. The horizontal force H_1 acting from the rail on the collidng wheel is

$$H_1 = H_p + H_2. \tag{2.5}$$

The horizontal force H_2 acting on the other wheel is determined by the vertical force and the frictional coefficient of the wheel across the rail μ:

$$H_2 = \mu R_2. \tag{2.6}$$

In this case

$$H_1 = H_p + \mu R_2. \tag{2.7}$$

The vertical forces R_1 and R_2 at the contacts of the wheels with the rails are determined from the equations of moments with respect to these points:

$$R_1 = \frac{2s+a_1}{2s} P_1 + \frac{r_к}{2s} H_p - \frac{a_2}{2s} P_2 + q_к; \tag{2.8}$$

$$R_2 = \frac{2s+a_2}{2s} P_2 - \frac{r_к}{2s} H_p - \frac{a_1}{2s} P_1 + q_к, \tag{2.9}$$

where q_k is the mass of the parts of the truck for one wheel not spring suspended.

After the substitution of the values of P_1 and P_2 in expressions (2.8) and (2.9) and transformations we obtain:

$$R_1 = \frac{2s+a_1}{2s} P_0 k_{д1} + \frac{r_к}{2s} H_p - \frac{a_2}{2s} P_0 k_{д2} + P_0 + q_к; \tag{2.10}$$

$$R_2 = \frac{2s+a_2}{2s} P_0 k_{д2} - \frac{r_к}{2s} H_p - \frac{a_1}{2s} P_0 k_{д1} + P_0 + q_к. \tag{2.11}$$

In view of the small difference between a_1 and a_2 by comparison with the distance between the points of contact of the wheels with the rails, we set $a_1 \approx a_2 = a$.

Let us note, in addition, that

$$P_0 + q_k = R_0. \tag{2.12}$$

Taking this into account, we obtain:

$$R_1 = \frac{a+2s}{2s} P_0 k_{д1} + \frac{r_к}{2s} H_p - \frac{a}{2s} P_0 k_{д2} + R_0; \quad (2.13)$$

$$R_2 = \frac{a+2s}{2s} P_0 k_{д2} - \frac{r_к}{2s} H_p - \frac{a}{2s} P_0 k_{д1} + R_0. \quad (2.14)$$

Equations (2.13) and (2.14) are easily realized on an analog computer.

It is known that the coefficient γ is equal to the ratio of the horizontal and vertical components of the forces acting on the wheel colliding with the rail head by its flange:

$$\gamma = H_{coll}/R_{coll}. \quad (2.15)$$

Here, the horizontal force acting on this wheel is

$$H_{coll} = H_p + \mu R_{n.coll}, \quad (2.16)$$

where $R_{n.coll}$ is the vertical force acting from the rail on the wheel rolling without running into the rail with its flange.

The vertical force acting from the rail on the colliding wheel is determined by expressions (2.13) or (2.14) depending on which wheel has contact with the rail on the flange surface at the given point in time.

The block diagram of determination of the coefficient γ with respect to the deformations of the lateral frames of the truck on an analog computer is presented in Figure 2.2.

The control signal in the system is the frame force signal H_p. The connections in the system are made so that a defined sign of the frame force signal corresponds to hitting the rail by the flange of one of the wheels of the wheel pair; on variation of the signal H_p the other wheel becomes the colliding wheel. Thus, for a sign-variable signal H_p formulas (2.13) and (2.14) become universal.

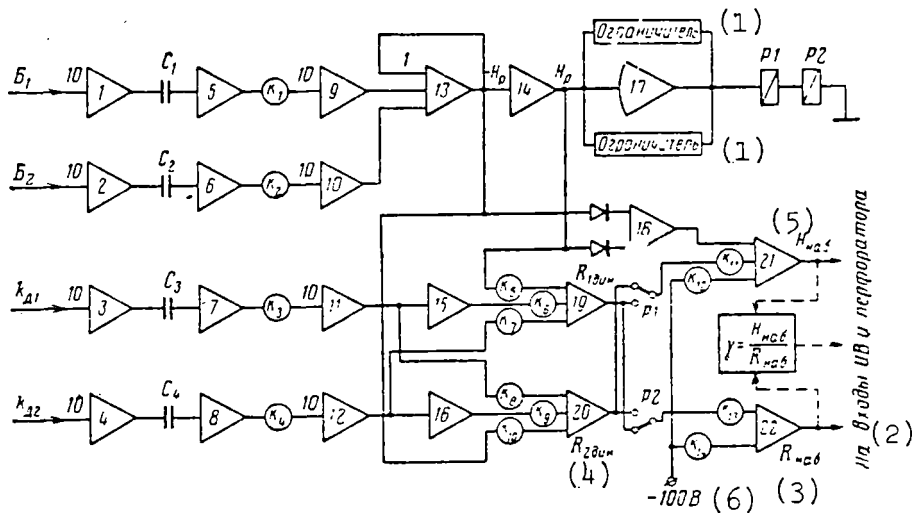

Figure 2.2. Block diagram for calculation of the coefficient γ on an analog computer by the deformations of the side frames of the truck.

Key: 1. Limiter

2. To the inputs of the digital computer and punch

3. R_{coll}

4. $R_{...dyn}$

5. H_{coll}

6. - 100 volts

In accordance with the sign of the frame force, the corresponding switches are made in the circuit using the contacts of relays P1 and P2 permitting

realization of expressions (2.16), (2.13) and (2.14). The control circuit is assembled from an amplifier 17, to the input of which the windings of the P1 and P2 relays are connected.

The frame force signal H_p is formed on the amplifier 13 which sums the components B_1 and B_2 on the required scale. The amplifier 14 serves for variation of the sign of the signal H_p. The signals of the dynamic components of the vertical forces R_{1dyn} and R_{2dyn} on the required scale are formed respectively on the amplifiers 19 and 20. The signal of the modulus of the frame force required for proper addition with the frictional force of the noncolliding wheel is formed on the amplifier 18.

The signals of H_{coll} and R_{coll} are formed on the amplifiers 21 and 22. Here:

a) if wheel 1 is the colliding wheel, as is shown in Figure 2.1, the signal R_{1dyn} is fed through the contacts of the relay P2 to the input of the amplifier 22, where it is summed with the static component of the vertical load and forms the signal R_{coll}. At the same time the signal R_{2dyn} is fed through the contacts of the relay P1 to the input of the amplifier 21, where it is summed with the static component. It is multiplied by the friction coefficient μ and together with H_p forms the horizontal force signal acting from the rail on the colliding wheel, that is,

$$H_{coll} = H_p + \mu(R_{2dyn} + R_0);$$

b) if wheel 2 becomes the colliding wheel, switching of the P1 and P2 relay contacts takes place automatically. In this case the signal of the vertical

force is formed by R_{2dyn} and R_0, and the signal of the horizontal force is equal to the sum of the frame force and the frictional force of wheel 1 across the rail, that is,

$$H_{coll} = H_p + \mu(R_{1dyn} + R_0).$$

The static component of the vertical loads is formed on the amplifiers 21 and 22 with feeding of a reference voltage of -100 volts to their inputs with the corresponding coefficients.

The scaling coefficients k_1-k_4 are calculated by the formula

$$k_i = \frac{U}{100\, m\, u_т}, \tag{2.17}$$

where U is the value of the shunt by which the electric calibration of the measurement circuit, the unit measured value, is carried out; m is the scale of representation of the measured value on the analog computer; u_t is the calibrated recoil from shunting of the operating arm of the measuring circuit, volts.

The scale is selected beginning with the proposed (or known) maximum values

$$m = \frac{y_{max}}{100}, \tag{2.18}$$

where Y_{max} is the maximum measured value.

The remaining coefficients in the circuit, in accordance with expressions (2.13), (2.14) and (2.16) are defined by the formulas:

$$k_5 = k_{10} = \frac{r_к}{2s} \frac{m_{Hр}}{m_{R_{дин}}} ; \quad (2.19)$$

$$k_6 = k_9 = \frac{a+2s}{2s} P_0 \frac{m_{кд}}{m_{R_{дин}}} ; \quad (2.20)$$

$$k_7 = k_8 = \frac{a}{2s} P_0 \frac{m_{кд}}{m_{R_{дин}}} ; \quad (2.21)$$

$$k_{11} = \mu \frac{m_{R_{дин}}}{m_H} ; \quad (2.22)$$

$$k_{12} = \frac{\mu R_0}{100 m_H} ; \quad (2.23)$$

$$k_{13} = \frac{m_{R_{дин}}}{m_{R_{наб}}} ; \quad (2.24)$$

$$k_{14} = \frac{R_0}{100 m_{R_{наб}}} . \quad (2.25)$$

The signals H_{coll} and R_{coll} obtained in this way were fed to the division circuit of the analog computer, the values of γ from the output of which were measured by a digital voltmeter and were punched on the punch tape (the circuit diagram is depicted in Figure 2.2 by the dotted line). The distribution parameters of the coefficients of γ were calculated on the Nairi-S digital computer.

The experience in determining the ratio of the horizontal and vertical forces for estimating the derailment coefficient of freight cars in operation by the investigated circuit demonstrated that the operation of division on the analog elements is performed with errors which can distort the results of determining the ratios, especially for small values of the dividend and the divisor.

The development of the two-channel device for coupling the digital voltmeters to the punch made it possible to punch the values of H_{coll} and R_{coll} measured at one time on the punch tape, and to calculate the coefficients

of γ on a digital computer. This greatly increased the precision of determining the relations for estimating the derailment coefficient of the cars. The improved processing program made it possible to obtain, in addition to the distribution of the coefficient γ and its parameters, analogous data for the values of the horizontal and vertical forces acting on the wheel which hits the rail head with its flange. For large unloading of the colliding wheel the values of H_{coll} and R_{coll} are printed out.

Data on the ratios of the horizontal and vertical forces acting on the wheel colliding with the rail by its flange obtained using this method by the improved program were used for estimating the derailment coefficient of various types of freight cars in operation and at increased speeds. The results are presented below.

It must be noted that the method of determining the dynamic forces acting on the wheels at the points of contact with the rails do not have high precision with respect to the deformations of the side frames of the truck on the basis of a number of assumptions. In particular, the use of the frame force signal as the control signal presupposes constant running of the wheel pair against the rail first with one wheel and then the other. In reality, the presence of the frame force still does not mean mandatory collision of one of the wheels with the rail by its flange. As the experiments with the tensometric wheel pair indicate, the frame force can occur with the difference of the horizontal forces acting on both wheels at the points of contact with the rails directed outside the rail, and not inside as occurs for the actual running of one of the wheels against the rail head by its flange.

The friction coefficient μ is assumed constant and equal to 0.25 when determining the frictional force of the wheel not colliding against the rail. Indeed, this value is a variable which depends on many factors, including random ones. In addition, the additional errors are caused by the exclusion of the inertial component when determining the forces acting at the points of contact of the wheels with the rails by the forces measured in the truck frame.

However, as the analysis of a large number of recordings indicates, the precision of the method for large values of the active forces increases. Therefore, considering the simplicity of the measuring circuit and the possibility of continuous recording of the forces on any extent of the path, the method of determining the coefficient γ by the deformations of the side frames of the truck for estimating the derailment coefficient of the cars is recommended for use in the case where high measurement precision is not required.

In all remaining cases it is necessary to use the more improved method of measuring the forces acting on the wheels at the points of contact with the rails--by the deformations of the webs of the tensometric wheel pair.

2.2. Determination of the Coefficient γ by the Deformations of the Wheel Webs

Above (see the first chapter) a detailed study was made of the problems of the preparation and application of tensometric wheel pairs for measuring horizontal and vertical forces acting on the wheels at the points of contact

with the rails. The recordings of these forces obtained using a tensometric wheel pair permit exact establishment of the times of collision of the wheel against the rail by its flange and calculation of the ratios of the forces determining the stability of the wheel with respect to running up on the rail head.

For express analysis of the signals from the tensometric wheel pair during the trips with experimental objects, it is possible to use recordings on photographic paper obtained using the light beam oscillograph.

However, the basic means of recording and processing the data must be the magnetic recording equipment and modern analog and digital computers. Work on the automation of the calculation of the ratios γ of the horizontal and vertical forces determined by the deformations of the wheel web has been done at the Railroad Car Division since 1970. In that year the flow charts and the procedure for the automatic calculation of the coefficient γ and the basic parameters of its distribution using an analog-to-digital automatic data processing complex were developed. In Figure 2.3 the block diagram is presented for calculating the coefficient γ by the deformations of the wheel web on an analog computer. The diagram was constructed so that the coefficient γ is defined only at the time when the horizontal force directed inside the track acts on the wheel, which usually occurs when the wheel runs against the rail head with its flange (Figure 2.4).

The signals of the vertical D_v and horizontal D_h forces acting on the wheel are reproduced simultaneously from the tape recorder 1, and they are fed to

the aligning and scale-setting modules 2 and 4. Then the signal D_V is fed to the module for generating the maximum vertical force 9, from the output of which it goes to the input X of the division circuit of the analog computer 10.

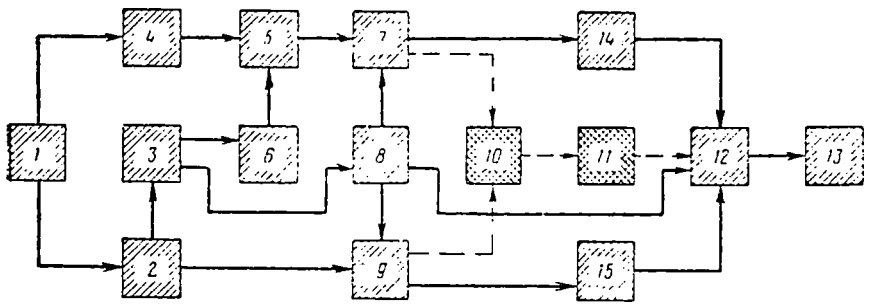

Figure 2.3. Block diagram for calculation of the coefficient γ on an analog computer by the deformations of the wheel webs.

In order to generate the signal for the horizontal force H acting inside the track corresponding to the case of the wheel running against the rail, in the circuit use is made of the property of the signal of the horizontal force D_h on changing direction of effect to change the phase with respect to the signal of the vertical force D_V by 180°. For this purpose the logical comparison circuit 5 is used. One of its inputs is fed the signal D_h, and the other, the signal from the resolving pulse source 6, which is controlled by the signature module D_V 3. At the output of the circuit 5 the signal H appears only when the phases of D_h and D_V coincide. Then the signal H is fed through the module for generating the maximum 7 to the input Y of the division circuit 10 in which the coefficient γ equal to the ratio H/R is calculated.

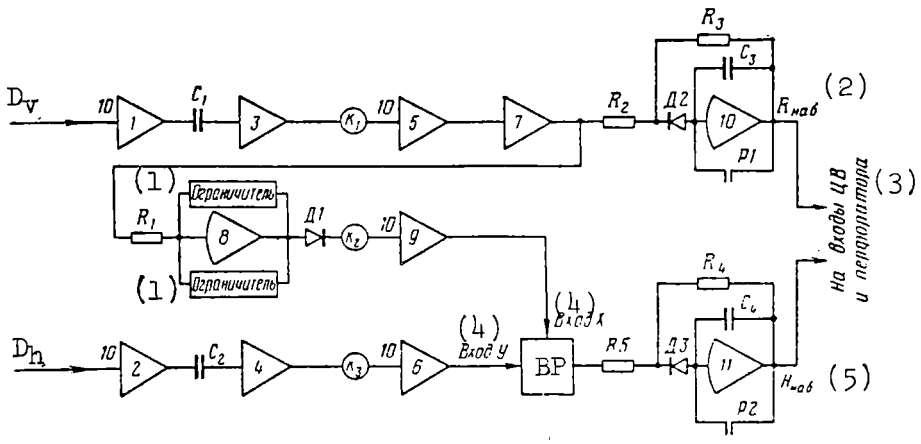

Figure 2.4. Circuitry for generating the horizontal and vertical force signals corresponding to the times that the wheel hits the rail on an analog computer.

Key: 1. Limiter

2. R_{coll}

3. To the inputs of the digital computer and the punch

4. Input ...

5. H_{coll}

The values of γ measured by the digital voltmeter 11 are fed through the coupler 12 to the punch 13. The reading of the values of γ and punching them on the punch tape are accomplished by signals from the control circuit 8 with the repetition rate of the amplitudes D_V (twice per wheel revolution).

With the development of the two-channel coupler with the punch and the improved data processing program for the Nairi-S digital computer, there was no longer any necessity for calculating the coefficient γ on the analog

computer. The two-channel coupler made it possible to punch the pairs of values of H and R successively on the punch tape. As a result of the calculations on the Nairi-S digital computer, after reading the data from the punch tape, the distributions of the coefficient γ, the lateral forces H and vertical forces R and the basic distribution parameters are printed out. In addition, for large unloadings of the colliding wheel, the corresponding pairs of numbers H and R are printed out.

Chapter III. Experimental Determination of the Trajectories of Motion of the Axle Box of the Wheel Pairs of Freight Cars

3.1. State of the Art With Respect to the Problem

The wheel pairs of a moving car, in addition to the translational motion along the track, have displacements in the vertical and horizontal (across the track) planes. In the case of cylindrical wheels, the displacements in the vertical plane are caused by the vertical unevenness of the rail. The horizontal displacements take place as a result of the twisting movement of the wheel pair on the track and various unevennesses in the track in the plan view. Thus, the determination of the trajectories of motion of the axle box of the wheel pairs is a means of studying the unevennesses of the rail.

At the same time the disturbances acting from the track on the railroad car are transferred through the wheel pairs, and more precisely, through their axle boxes. Therefore the trajectories of motion of the axle boxes, being time functions, can be considered as the forcing functions in the differential equations describing the vibrations of the car.

The trajectory of motion of the axle box can be determined experimentally by two methods: the method of indirect leveling or using measuring devices installed on the moving car.

The second method offers the possibility of determining the trajectories in a section of any length; therefore it should be given preference.

The method of measuring the vertical trajectories of the wheels of the railroad rolling stock was developed for the first time in the Railroad Car Division of the Central Scientific Research Institute of the Ministry of Railways in 1962. Authors' certificates on the invention were issued [16, 17]. The method is based on calculating the difference between the absolute displacements of the body of the car and the displacement of the body with respect to the axle box. The absolute displacement of the body is determined either by the low-frequency vibrometer or double integration of the signal coming from the accelerometer installed in the body above the axle box.

The results of measuring the trajectories of the axle boxes of passenger cars were published in [7, 18], where a classification of the unevenness of the joined rail is presented; it is demonstrated there that for a track with rails 12.5 meters long, group I unevennesses in the form of an "arch" or a sine curve are typical. For a track with rails 25 meters long, group II unevennesses in the form of a double-humped curve are typical. The mean and mean square deviations of the amplitudes of the unevennesses were determined for a section of the track of the Moscow railroad 200 km long. Then the systems for measuring the trajectories of the wheels were improved, and

this made it possible to perform analogous measurements on the unjoined track [19]. The results of the measurements demonstrated that on the equalizing links, group I unevenness is typical. On the unjoined track the amplitudes of the unevennesses, as a rule, are less than on the joined track. The amplitudes of the unevennesses fluctuate within large limits, but on the average they correspond to the length of the rails forming the standard length.

As experience has demonstrated, the application of the procedure developed at the Railroad Car Division of the Central Scientific Research Institute of the Ministry of Railways for measuring the trajectory for freight car wheels is connected with large difficulties. The accelerometer fastened to the body of the freight car is subjected to the effect of significant high-frequency accelerations. This lowers the precision with which the absolute displacement of the body and, consequently, the movement of the axle box is measured. Therefore, in order to determine the trajectory of the axle boxes of freight cars, it was decided to use the method which is used on the railroads in Canada [20] in which the accelerometer is attached either to the axle box or to the lateral frame of the truck of the freight car, and its signal is integrated twice. This method was tested at the Railroad Car Division of the Central Scientific Research Institute of the Ministry of Railways in 1962, but it did not become widespread as a result of the increased measurement errors. The high-frequency components of the accelerations of the axle box were the source of these errors, the level of which is many times greater than the useful signal. For example, the

accelerations from the group I and II unevennesses of a rail element do not exceed ±1 g, and the level of the high-frequency components in the joints can exceed 25-30 g. In order to reduce the level of high-frequency accelerations, it is necessary to protect the axle box accelerometer by a special vibration-protective insert which was done on the Canadian railroads [20].

Along with the protection of the accelerometer with the vibration insert, in order to lower the error in determining the trajectories of the axle box, it is necessary correctly to select the parameters of the double integration circuit for the acceleration signal.

3.2. Selection of the Double Integration Circuits of the Acceleration Signal

The double integration circuit of the accelerometer signal installed on the axle box must correspond to designed requirements of which the most important are the following:

a) the amplification coefficient of the entire channel must be such that the operation amplifiers of each element operate with sufficiently high signal level, but they are not overloaded;

b) the frequency-amplitude characteristic of the system in the operating frequency range must correspond as precisely as possible to the frequency-amplitude characteristic of the ideal double integrator;

c) the amplification coefficient of the entire channel on the "null" frequency must be equal to zero. This permits exclusion of the effect of brakes in the track profile and shift of the zeros of the measuring channel

on the measurement results;

d) the transition processes occurring in the system must damp quite quickly;

e) in order to perform the operations of integration and multiplication by a constant coefficient, the series analog computer must be used, for example, the MN-10M type which is convenient for placement in the laboratory car.

Figure 3.1 shows the schematic diagram for double integration executed from the MN-10M type analog computer elements which can be used for our studies.

The operation amplifier Y1 is a scaling amplifier. Its amplification coefficient $k_1 = R_2^I/R_1^I$ is selected in such a way that the signal u = 10 volts will correspond to an acceleration of j = 10 g at the output. The capacitance C_2^I is used to lower the level of the high-frequency components of the acceleration signal. Figure 3.2 shows the frequency-amplitude characteristic of the amplifier Y1 which plays the role of the low-frequency filter for different values of $T_1 = R_2^{II}$, C_2^I. When studying the unevennesses of great length corresponding, for example, to the length of the rail element, the optimal value of T_1 is found within the limits of $0.001 \leq T \leq 0.005$. Here, at the upper boundary of the operating frequencies f = 10 Hz, the distortions with respect to amplitude do not exceed 5 percent, and the phase shift $\phi \approx 10°$. The amplifiers Y2 and Y4 perform the integration operation by the inertial element system. Along with the capacitance of $C_2^{II} = C_2^{IV} =$ 1.0 microfarads, the negative feedback includes the resistors R_2^{II} and R_2^{IV}. The capacitors C_1^{II} and C_1^{IV} which perform the role of the upper frequency filters are included at their input along with the resistors R_1^{II} and R_1^{IV}.

As a result of these capacitors, item c of the above-indicated requirements is satisfied. The amplifier Y3 is the scaling amplifier. Its amplification coefficient $k_3 = 10$. In order that the signal u = 10 volts at the output of the amplifier Y4 correspond to the displacement of the accelerometer h = 10 cm, the conditions $R_1^{II} = R_1^{IV} = 0.1$ meter is necessary.

In order to satisfy the requirements discussed in items b and d, several versions of the calculations were performed for selecting the values of C_1^{II}, C_1^{IV} (see Figure 3.1).

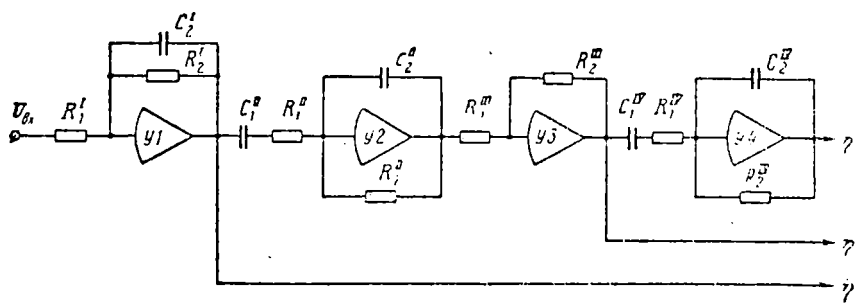

Figure 3.1. Circuit for Double Integration of the Acceleration Signal on the MN-10M Analog Computer: u_{inp}--signal reaching the system input from the accelerometer located on the axle box; η--acceleration signal after the low-frequency filter; η and η --speed and displacement signals of the axle box.

The transfer function of this system in operator form is:

$$H(p) = \frac{k_1 k_2 T_2 T_5 p^2}{(T_1 p+1)(T_3 p+1)(T_4 p+1)(T_6 p+1)(T_7 p+1)},$$

where

$$k_1=\frac{R_2^{\mathrm{I}}}{R_1^{\mathrm{I}}};\ k_2=\frac{R_2^{\mathrm{III}}}{R_1^{\mathrm{III}}};\ T_1=R_2^{\mathrm{I}}C_2^{\mathrm{I}};\ T_2=R_2^{\mathrm{II}}C_1^{\mathrm{II}};$$
$$T_3=R_2^{\mathrm{II}}C_2^{\mathrm{II}};\ T_4=R_1^{\mathrm{II}}C_1^{\mathrm{II}};\ T_5=R_2^{\mathrm{IV}}C_1^{\mathrm{IV}};\ T_6=R_2^{\mathrm{IV}}C_2^{\mathrm{IV}};\quad (3.1)$$
$$T_7=R_1^{\mathrm{IV}}C_1^{\mathrm{IV}}.$$

Expanding the denominator of expression (3.1), we obtain

$$H(p)=\frac{k_1k_2T_2T_5p^2}{ap^5+bp^4+cp^3+dp^2+ep+1},$$
$$a=T_1T_3T_4T_6T_7;$$
$$b=T_1T_3T_4T_7+T_1T_3T_6T_7+T_1T_4T_6T_7+T_1T_3T_4T_6+T_3T_4T_6T_7;\quad (3.2)$$
$$c=T_1T_3T_7+T_1T_4T_7+T_1T_6T_7+T_3T_4T_7+T_3T_6T_7+$$
$$+T_1T_3T_4+T_1T_3T_6+T_1T_4T_6+T_3T_4T_6;$$
$$d=T_1T_7+T_1T_3+T_1T_4+T_1T_6+T_3T_7+T_3T_4+T_3T_6;$$
$$e=T_1+T_3+T_7.$$

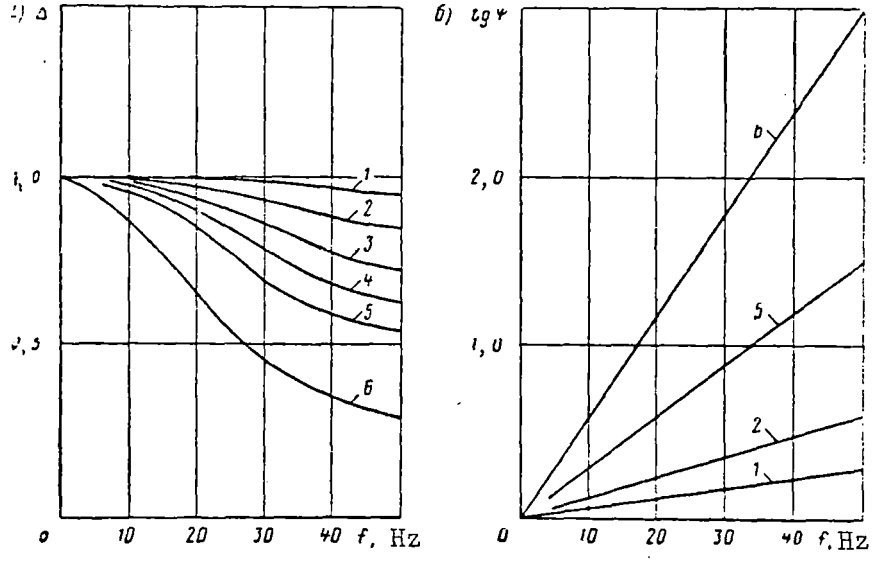

Figure 3.2. Characteristics of the low-frequency filter on the operation amplifier of the MN-10M analog computer: a--frequency-amplitude characteristics; b--phase characteristics; 1-6--for values of C_2^{I}, 0.001, 0.002, 0.003, 0.004, 0.005 and 0.01 microfarads, respectively.

The integration error Δ is defined as the quotient from dividing the transfer function of this system (3.2) by the transfer function of the ideal double integrator with the coefficient $k = 10^4$:

$$\Delta = \frac{k_1 k_2 T_2 T_5 p^4}{10^4 (ap^5 + bp^4 + cp^3 + dp^2 + ep + 1)} . \tag{3.3}$$

Proceeding to the angular frequency by substituting $p = i\omega$, we obtain an integration error with respect to amplitude and phase shift:

$$\Delta_a = \frac{10^4 \sqrt{(b\omega^4 - d\omega^2 + 1)^2 + (a\omega^5 - c\omega^3 + e\omega)^2}}{k_1 k_2 T_2 T_5 \omega^4} ; \tag{3.4}$$

$$\operatorname{tg}\varphi = \frac{a\omega^5 - c\omega^3 + e\omega}{b\omega^4 - d\omega^2 + 1} . \tag{3.5}$$

When performing the calculations, the values of the capacitances C_1^{II}, C_1^{IV} varied within the limits from 5 to 20 microfarads, and the resistors R_2^{II} and R_2^{IV} varied from 0.5 to 2 megohms. The determination of the roots of the characteristic equation to the fifth power of the corresponding differential equation demonstrated that the system (see Figure 3.1) is stable. It has all five natural values of the negative roots. Among the roots there is one complex conjugate $\alpha \pm i\beta$. Therefore when selecting the parameters of the specific circuit (see Figure 3.1), in addition to the requirements presented above, the requirement has appeared which consists in the fact that the natural frequency β determined by the imaginary part of the complex root is removed from the operating frequency band, and the oscillatory nature of the system (the ratio of the imaginary part of the root to the real root) is relatively small.

Figure 3.3 shows the curves for the variation of the integration error as a function of the angular frequency for various values of the calculation parameters. The analysis of Figure 3.3 and the roots of the characteristic equation made it possible to establish that the most optimal is the system in which $C_1^{II} = C_1^{IV} = 5.0$ microfarads, $R_1^{II} = R_1^{IV} = 1.0$ megohms and also the circuit with the parameters $C_1^{III} = 10.0$ microfarads; $C_1^{IV} = 20.0$ microfarads; $R_1^{II} = 1.0$ megohms; $R_1^{IV} = 0.50$ megohms.

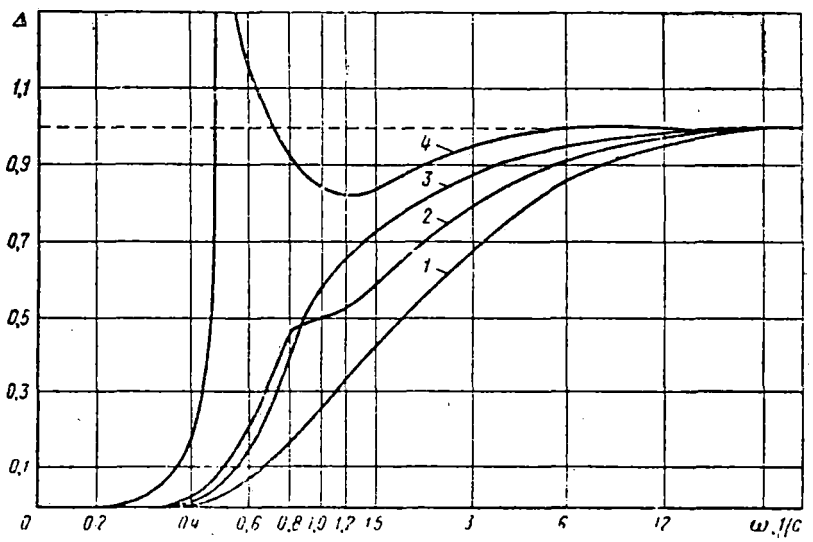

Figure 3.3. Amplitude errors of the double integration circuits for various values of the parameters: 1--$C_1^{II} = C_1^{IV} = 5.0$ microfarads; $R_1^{II} = R_1^{IV} = 0.5$ megohms; 2--$C_1^{II} = C_1^{IV} = 5.0$ microfarads; $R_1^{II} = R_1^{IV} = 1.0$ megohms; 3--$C_1^{I} = 10.0$ microfarads; $C_1^{IV} = 20$ microfarads; $R_1^{II} = 10$ megohms; $R_1^{IV} = 0.5$ megohms; 4--$C_1^{I} = 20.0$ microfarads; $R_1^{II} = R_1^{IV} = 0.25$ megohms.

The first of the indicated systems was tested. Initially, the TUV-67 type tensometric accelerometer was fastened to the elastic overhanging plate

about 1 meter long. It was connected to one channel of the 12-channel TUP-12-71 tensometric unit. The signal was fed from the output of the channel to the input of the scaling amplifier Y1 (see Figure 3.1). A strain resistor was attached to the elastic pipe; it was connected to the other channel of the TUP-12-71 device. The signal at the channel output is proportional to the deflection of the elastic plate, that is, the absolute displacement of the accelerometer fastened to it. Then, setting the elastic plate into oscillatory motion with different frequency, the absolute displacement of the accelerometer (that is, the plate deflection) was compared with the signal received at the input of the double integration circuit. A comparison of the data demonstrated the good correspondence of the experiment and the calculation.

3.3. Procedure for Experimental Determination of the Trajectory of Motion of the Axle Boxes and Analysis of the Recordings Obtained

The trajectories of motion of the axle boxes were determined on the four-axle and eight-axle gondolas. During the trips, the following were recorded: the displacements of both axle boxes of the first (with respect to the direction of motion) wheel pairs of both gondolas, the vertical displacements of the axle boxes from the left side of the first truck, the middle of the lateral frame of the four-axle gondola; the horizontal displacement (in the transverse direction of the track) of the left axle box of the first wheel pair of the same car. The TUV-67 type devices built by the Railroad Car Division of the Central Scientific Research Institute of the Ministry of Railways was used as the accelerometer. They were connected

to the DRM-Ye type strain amplifier built by the Kiova Company. After the amplifier the acceleration signals passed through a low-frequency filter with a trimming frequency of 40 Hz and then went to the MN-10M type analog computer. The scaling of the signals and double integration with respect to the systems presented in Figure 3.1 were carried out on the analog computer. The acceleration, velocity and axle box displacement signals coming from the analog computer were recorded on the magnetic tape of the RTP-20Ye tape recorder built by the same company. A total of 130 realizations from 30 to 160 seconds long were recorded on the random sections of track including straight and curved sections and switches at speeds from 40 to 120 km/hr.

The experimental trips in the majority of cases took place on joined track. Therefore part of our interest was in the problem of the standard types of unevennesses of the joined track. The analysis of the recordings obtained on magnetic tape confirmed the data obtained in [7] that for a track with 12.5-meter rails the group I unevennesses are the most typical, and for the track with 25-meter rails, group II.

Figure 3.4a shows an oscillogram of the unevennesses on the track with the 12.5-meter rails where the group I unevennesses with an amplitude of 6-8 mm are shown. These unevennesses correspond to the characteristic form of vertical velocity of the wheel [7]. In the joint zone (abbreviated Ct on the figure) a sharp change in sign takes place. The amplitude of the velocity is about 10 cm/sec.

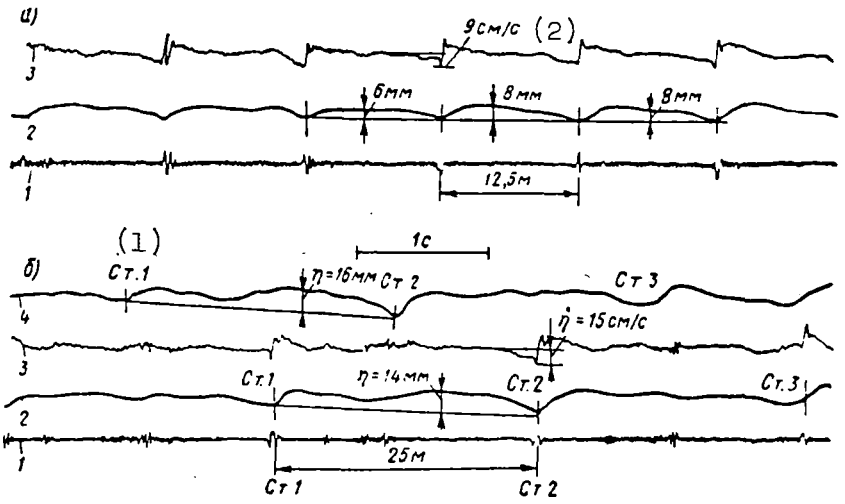

Figure 3.4. Examples of the oscillograms of the displacements of the axle boxes of freight cars during movement of an eight-axle car over a track with 12.5-meter rails (a) and during movement of the four-axle and eight-axle cars over a track with 25-meter rails (b): 1, 2, 3--the vertical accelerations, displacements and velocity of the axle box of the eight-axle cars; 4--vertical displacements of the axle box of the four-axle car.

Key: 1. Joint ...

2. ... cm/sec

In Figure 3.4b, an example is presented of vertical unevennesses under the wheels of the four-axle and eight-axle cars reported on a single string (2 and 4) on the track with 25-meter rails. The element between the joints 1 and 2 is a typical example of a group II unevenness.

Along with the typical unevennesses there are also more complex forms. In a number of cases the unevennesses are very small (the amplitude is less

than 5 mm), and their repetition period does not correspond to the length of the rail elements. The effect of the structural design of the car on the dimensions and the shape of the unevennesses was investigated by comparing the unevennesses obtained for one and the same (the left) rail on the four-axle and eight-axle cars. An example of this type of oscillogram is presented in Figure 3.4b. An analysis of numerous magnetic recordings and oscillograms shows that the unevennesses under the wheels of both cars in practice coincide both with respect to shape and with respect to size. For convenience of comparison in Figure 3.4b three rail joints are numbered. The wheel of the four-axle car passed over the joint before the wheel of the eight-axle car which was behind the four-axle car in the train makeup. Therefore the wheel trajectories turned out to be shifted in time.

During theoretical studies of the dynamics of freight cars having trucks with central spring suspension, the forcing function is assumed in the form of the half-sum of the unevennesses of the first and second truck wheels. Inasmuch as the side frame of the truck is not spring loaded, the forcing function for the railroad car must correspond to the trajectory of the middle of the side frame of the truck. In order to check this in the first version of the experiment, the trajectories of the first and second axle boxes and the trajectory of the middle of the side frame of the left side of the truck of the four-axle gondola were determined. During the process of reproduction of the recordings of the vertical displacements of the axle boxes on magnetic tape and the middle of the side frame of the truck on photographic paper of the oscillograph, the half-sum of the displacements

of the first and second axle boxes was also recorded. In Figure 3.5 we have an example of this type of oscillogram. A comparison of curves 4 and 6 indicates their complete comparison. Thus, the measurement data demonstrated that as the forcing functions when investigating the dynamics of freight cars having single-stage central spring suspension, it is possible to use both the displacement of the middles of the side frames of the trucks and the half-sum of the displacements of the first and second wheels.

As was noted, in the experiments a study was made for the first time of the displacement of a wheel in the horizontal plane (across the track). The analysis of the recordings demonstrated that the procedure used to measure the vertical displacements can be also successfully used to record the horizontal displacements of the wheel pair.

The study of the car vibrations in the horizontal plane at high speeds is of the greatest interest. Therefore these displacements were investigated in the Sverdlovsk-Bogdanovich section where the trips were made with increased speeds. The oscillogram obtained in this section is presented in Figure 3.6. An analysis of the oscillograms indicates the following:

a) the movement of the four-axle car along a straight section of the track at speeds to 90 km/hr as a rule was accompanied by individual vibrations of the wheel pair across the track which quickly damped;

b) the increase in the speed of the car to 110 km/hr caused the appearance of periodic vibrations lasting 3-4 periods with a frequency of about 1.6 Hz;

c) the increase in speed of the car to 120 km/hr caused the appearance of longer vibrations which also damped with time;

d) the movement of the car on the right curves beginning at a speed of 70 km/hr caused the appearance of stable vibrations with the same frequency of 1.6 Hz and double amplitude to 17 mm. On the left curves these vibrations were not observed. The reason for this was not established; therefore it is necessary to make a detailed study of the movement of the cars on the curves with respect to the occurrence of such vibrations.

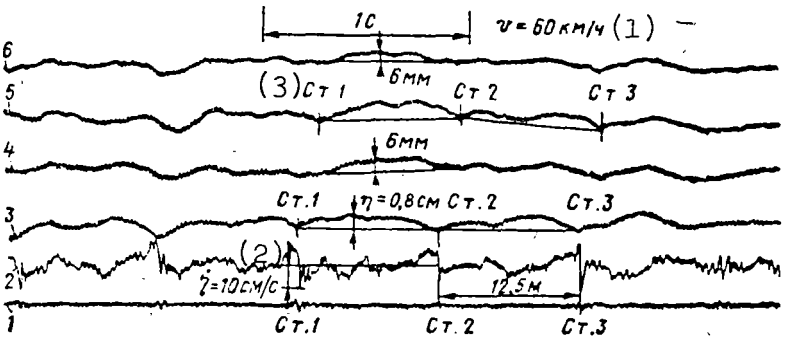

Figure 3.5. Example of oscillograms of vertical displacements of the axle boxes and the side frame of the four-axle car: 1, 2, 3--vertical accelerations, velocity and displacements of the first left axle box of the first truck, respectively; 4--vertical displacements of the middle of the side frame; 5--the same of the second left axle box; 6--half-sum of the displacements of the first and second axle boxes.

Key: 1. ... km/hr

2. ... cm/sec

3. Joint ...

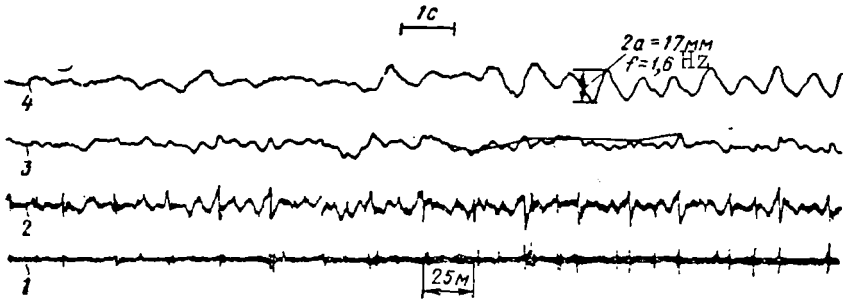

Figure 3.6. Example of the oscillogram of vertical and horizontal displacements of the axle boxes of a four-axle car: 1, 2, 3--the vertical accelerations, velocity and displacements of the axle box, respectively; 4--horizontal displacements of the axle box.

3.4. Spectral Analysis of the Recording of the Axle Box Displacements

The algorithm for calculating the spectral density function of the signal in the 1/3 octave frequency bands was developed by Yu. M. Cherkashin, candidate of technical sciences [21]. The spectral density functions were obtained for the displacements of the axle boxes on the M-6000 type medium computer. For this purpose the realizations recorded on magnetic tape lasting 10.24 seconds were input to the computer through the analog-to-digital converter. The quantization frequency f = 100 Hz.*

In Figure 3.7a, b, c, d examples are presented of the spectral density functions for vertical displacements of the axle boxes, and in Figure 3.7e, for horizontal displacements of the axle boxes. The graphs obtained indicate

* The coupling of the analog-to-digital converter to the M-6000 computer was performed by engineer V. V. Frants. The program for obtaining the spectra was developed by engineer Ye. B. Didova.

that on movement of a car at a speed of v = 47 km/hr (see Figure 3.7a) along a track having rails 12.5 meters long, peaks appear in the frequency bands of f = 0.98-1.24 and f = 1.96-2.48 Hz which correspond to the frequencies of the first and second harmonics, the I type unevennesses [7], equal to f = 1.04 and 2.08 Hz. From Figure 3.7b it is obvious that on movement of the car at a velocity v = 60 km/hr along the track with rails 25 meters long, analogous peaks occur on frequencies of about 0.62 and 1.24-1.56 Hz. This will also correspond to the first and second harmonic frequencies of the II type unevenness [7] which for the given velocity are f = 0.67 and 1.34 Hz, respectively.

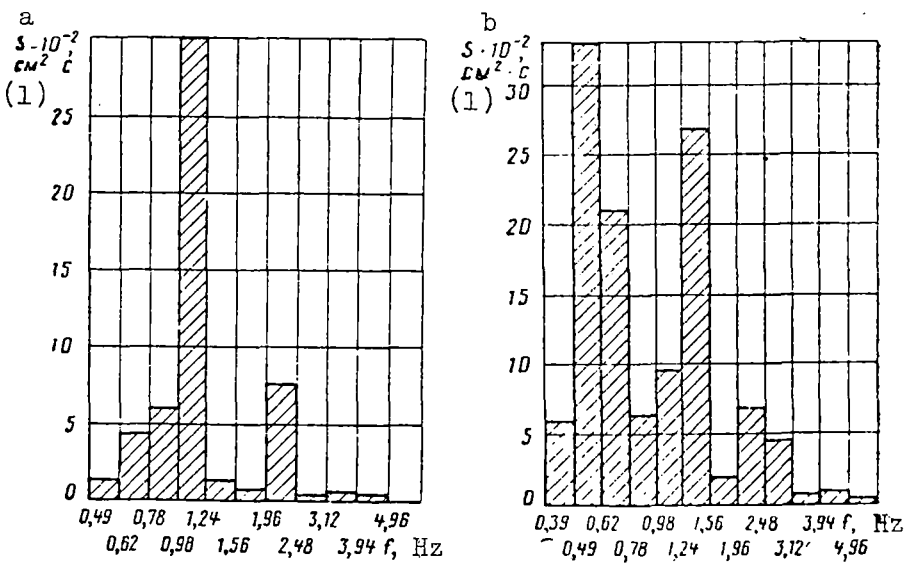

Figure 3.7. Examples of the spectral density functions of the axle boxes: a--vertical displacements of the eight-axle car on the track with rails 12.5 meters long at a velocity v = 47 km/hr; b--the same on a track with rails 25 meters long and a velocity v = 60 km/hr; c--the same for v = 57 km/hr; d--vertical

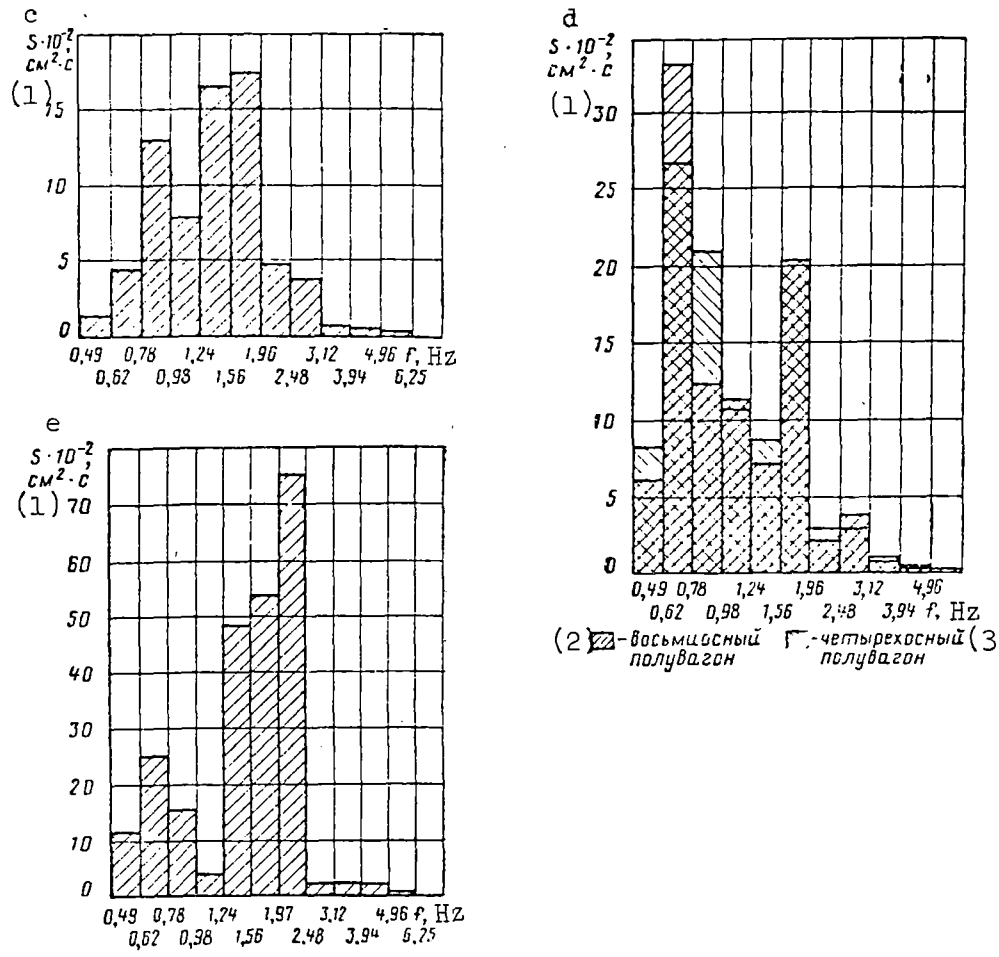

Figure 3.7. (continued) displacements of the axle boxes of the eight-axle and four-axle car with movement over the same section of the track at a speed of v = 63 km/hr; e--horizontal displacement of the axle box of the four-axle car at v = 90 km/hr.

Key: 1. ... cm^2/sec

2. Eight-axle gondola

3. Four-axle gondola

It must be noted that in a number of cases the spectral density functions of the vertical displacements do not have clearly expressed surges. They

have the shape of limited "white noise." An example of this graph is presented in Figure 3.7c. In Figure 3.7d the examples of two spectra of the vertical unevennesses of the first axle boxes in the direction of motion of the train (on the left side) of the eight-axle and four-axle cars obtained simultaneously on the same section of track at a velocity v = 63 km/hr are illustrated.

Both spectra are in practice identical. This confirms the above-drawn conclusion that the vertical unevennesses of the track for the wheels of both types of cars are in practice identical.

In Figure 3.7e, a graph is presented of the spectral density function of the horizontal displacements of the axle boxes of the four-axle gondola obtained by processing of the realization in the Sverdlovsk-Bogdanovich section at a velocity v = 90 km/hr. The stable horizontal oscillations are visible on the recordings. The spectrum had a sharp surge in the frequency range of f = 1.5-2.5 Hz. This corresponds to the oscillation frequency visible in the recordings (see Figure 3.6). The processing of the realizations on which the stable horizontal oscillations were absent demonstrated that in these cases the power of the spectrum is appreciably less, and it approaches the form of limited "white noise."

Chapter IV. Measured Variables, Recording of Them and Processing of the Data Obtained

4.1. Variables Investigated When Setting Dynamic Loads Acting on the Under-Carriages of Freight Cars

The primary intention in the investigation was given to measurements of the vertical and lateral forces acting on the undercarriages of the cars. The dynamic deflections of the spring complexes, deformations and stresses in the truck elements, including the wheel pair axles, vibration accelerations of the sprung and unsprung parts of the cars and in operation, also the speed of the train with determination of the statistical distributions of it in time by measure. Table 4.1 contains the values recorded during the tests and the measuring instruments.

Table 4.1

Measured Variable	Measuring Instrument	Comments
Vertical force acting on the frame of the truck	Strain resistors on lateral frame of the truck	--

Table 4.1 (continued)

Measured Variable	Measuring Instrument	Comments
Horizontal (frame) force	Same	--
Vertical force acting on the wheel	Strain resistors on wheel web	Tensometric wheel pair
Horizontal force acting on the wheel	Same	Same
Deflection of the spring complexes	Elastic plate with strain resistors	--
Stresses in the elements of the undercarriages	Strain resistors	--
Accelerations of the axle	TU-2-67 accelerometer	--
Accelerations of the car body	Accelerometer, Usov design	--
Distribution of the velocities	RRS-2 velocity distribution recorder	

All of the mechanical variables were measured by electrical units based on the application of strain resistors and strain amplifiers. The procedure for measuring the majority of the variables is quite well known, and in many cases it was not subjected to alterations.

The measurement of the vertical and horizontal forces by the deformations of the webs of the tensometric wheel pair, the description of which was presented earlier (see Chapter I), was new.

Some changes were made in the strain resistor circuits, and large changes were made in the procedure for recording the data: oscillograph recording was replaced by magnetic recording of the process.

4.2. Tensometric Amplifier

During the studies, along with investigating the operating conditions of the undercarriages of the freight cars in operation, the procedure for gathering and processing the experimental data was continuously improved. As a result, it became possible to recommend measuring and recording equipment, the procedure for obtaining the required values and processing the data for modern dynamic tests of the railroad cars.

The tensometric equipment designed for operation under the conditions of the laboratory car must satisfy the following requirements: a) have small dimensions and mass, a sufficiently large number of simultaneous recording channels; b) consume the required power from the storage battery; c) ensure a frequency range of the recorded processes from 0 to 200-300 Hz; d) have high stability of the bridge balancing (null stability) and scale balancing; e) have high resistance to interference from the contact network and other sources.

Experience shows that for satisfaction of items d and e the equipment must be constructed on the basis of applying the carrier frequency. In order to satisfy items a and b, it is necessary to apply semiconductor devices instead of the radio tubes.

All of the laboratory cars of the Central Scientific Research Institute of the Ministry of Railways are equipped with multichannel semiconducting tensometric equipment type TUP-12-65 developed by the Electron Tensometric Laboratory of the Railroad Car Division [19]. It has been produced since 1965 by the experimental plant of the Central Scientific Research Institute of the Ministry of Railways. This equipment satisfies the indicated requirements. For recording the processes on the magnetic tape, the output part of the amplifying channels was reworked. Instead of the current output (which is required for light beam oscillographs) the new channels provide voltage output. This device is called the TUP-12-71N.

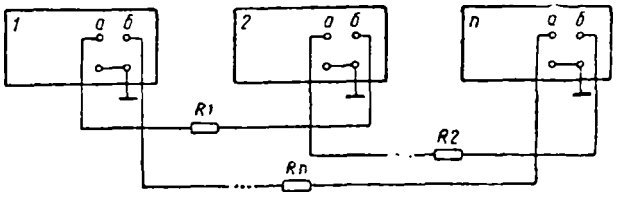

Figure 4.1. Synchronization circuit of several TUP-12 type devices for their joint operation: 1, 2, ..., n--numbers of the devices; a--terminals of the carrier frequency output generator (3 volts, 3,000 Hz); b--terminals for connecting the external generator; R_1, R_2--resistors.

Characteristics of the TUP-12-71N device:

Number of recording channels	12
Maximum voltage at the channel output (load resistance 3 kilohms), volts	±3
Range of recorded frequencies, Hz	0-200

Power supplies:	
Voltage, volts	-24
Current, amps	1.2
Overall dimensions	520 x 320 x 350
Mass, kg	24

Usually several devices operate simultaneously in the laboratory car. In this case their generators must be synchronized. Figure 4.1 shows the recommended synchronization circuit for several TUP-12 devices.

The studies performed in 1972 demonstrated that during long-term tests the stability of the nulls and scales of these devices is insufficient. Therefore the stabilization circuit for the carrier frequency master oscillator was altered. The application of the devices with the altered circuit demonstrated that they satisfy the modern requirements and can be recommended for laboratory cars performing dynamic and strength tests of the cars.

4.3. Precision Magnetic Recording Devices

The study of the dynamic loading regimes of the undercarriages of the cars in operation is possible only on the basis of the application of a magnetic recording and automatic processing of the experimental data. Thus, the magnetic recording is the basis for the research.

For the laboratory cars, the devices for precision magnetic recording must satisfy the following requirements: a) have small dimensions and mass; b) consume the required power from the storage batteries; c) have a quite

large number of recording channels (tracks); d) provide for recording the processes in the frequency band from 0 to 300-600 Hz; e) have good resistance to mechanical vibrations and shocks; f) ensure stability of the nulls and scales of the recorded processes over a long period of time; g) ensure control of the recorded signals during the recording process itself.

At the present time the instruments with analog recording of the signals have become most widespread. Their theoretical characteristics are determined by the international IRIG norms. The instruments executed by these norms are suitable for recording the processes during dynamic testing of the car.

The tape recorder developed and manufactured by the VNIIE was used in the first tests at the Central Scientific Research Institute of the Ministry of Railways. It consumed a great deal of power, it did not have recording control, and so on. In subsequent tests, the YeMM-140 type tape recorders of the TESLA Company (Czechoslovakia) were used which satisfy the modern requirements. They are adaptable for operation in a moving car, which is very important.

Basic technical specifications of the YeMM-140 type tape recorder:

Number of recording tracks (channels)	14
Magnetic tape width, mm	25.4
Recording technique	PFM
Number of signal recording amplifiers	13
Number of sound recording amplifiers	1

Number of signal reproduction amplifiers	13
Number of sound reproduction amplifiers	1
Power supply:	
Voltage, volts	+24
Current, amps	8
Overall dimensions, mm	730 x 490 x 300
Mass, kg	60

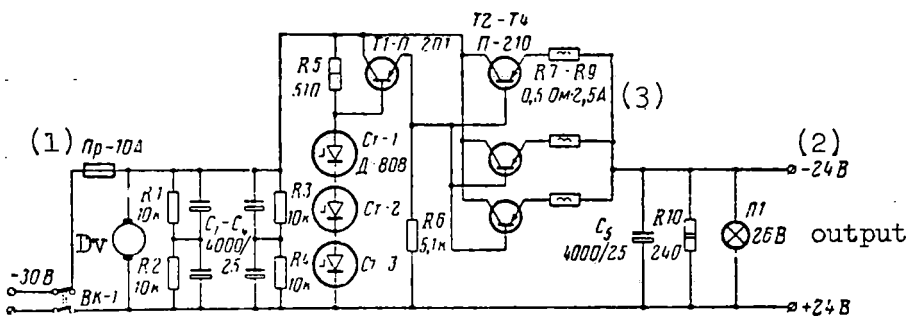

Figure 4.2. Circuit diagram of the 24-volt stabilizer for supplying power to the YeMM-140 tape recorder. Dv--fan motor.

Key: 1. Pr-10A

2. ... volts

3. ... ohms ... amps

The operation of these devices demonstrated that they can be recommended by the laboratory cars, in spite of the fact that they require regular adjustment, they have low reliability of a number of the electron circuits and the main motor. In order to increase their reliability, the following is needed: a) realization of the power supply from the 24-volt voltage stabilizer. Its circuit diagram (Figure 4.2) and structural design were developed at the Railroad Car Division of the Central Scientific Research

Institute of the Ministry of Railways. When using one power supply unit without a stabilizer the tape recorder operates unstably (special cases of failure of the electronic units were noted); b) constant quality control of the recording during the recording process. For this purpose, it is necessary to use the twin-beam oscillograph to monitor and compare the signals fed to the inputs with the signals obtained after reproduction from the tape; c) regularly to adjust the recording and reproduction amplifiers in accordance with the existing instructions.

4.4. Equipment for Monitoring the Operation of the Tape Recorders and Strain Amplifiers

The device for connecting and monitoring the operation of the tape recorders (the panel) was developed as applied to the YeMM-140 type tape recorders. On the basis of the tests, beginning with the requirements of obtaining information in the required volume and the possibility of qualified servicing of the equipment, the basic requirements on the indicated device were formulated. It must have the following: a) two serviced tape recorders; b) three groups of devices recorded by each tape recorder; c) the monitoring of the voltage level and the shape of the signal with respect to the input and output of each track must be ensured along with automatic detection of the track to which the signal is fed with biased null or high-frequency noise; d) the possibility of connecting to one of the tracks of the tape recorder. The power supply of the unit must come from the 24-volt battery.

The schematic diagram of the device by which an experimental model was manufactured and installed in the laboratory car is shown in Figure 4.3.

The signals from the strain amplifier go through the plugs Sh_1-Sh_3 (for the M-1 tape recorder) and Sh_4-Sh_6 (for the M-2). The switches P1 and P2 select the group of devices subject to recording. The switches P3 and P4 permit selection of any track of the tape recorders for visual monitoring. Switch P5 makes it possible to select the tape recorder for monitoring, by the flip-flop switch VK-1 to feed the inputs or outputs of the tracks to the control voltmeter and terminals K9-K10. The twin-beam oscillograph must be connected to the terminals K1-K3 (the track inputs) and K5-K7 (the track outputs). With the cycle generator T-Gen on, the ShI-25/4 step-by-step switch interrogates all of the tracks of both tape recorders alternately. The time for one interrogation is 3 seconds. The first field (the top of the circuit) provides for indication of the number of the controlled tape recorder, in the second, the track number. The third and fourth fields provide for monitoring of the interference and the null bias with respect to each track. On the appearance on any track of high-frequency interference or the constant component (the null bias) the signal tubes L17 and L18 flash respectively. A signal goes to the sound accompaniment track from the plate of the noise amplifier, to the input of which the microphone and the K13, K14 terminals are connected. Voice-frequency signals are fed to them from the tape recorder automatic switch.

The F-204/2 type digital voltmeter (scale 10-0-10 volts) permits measurement of the DC voltages at the inputs and outputs of the tape recorder tracks

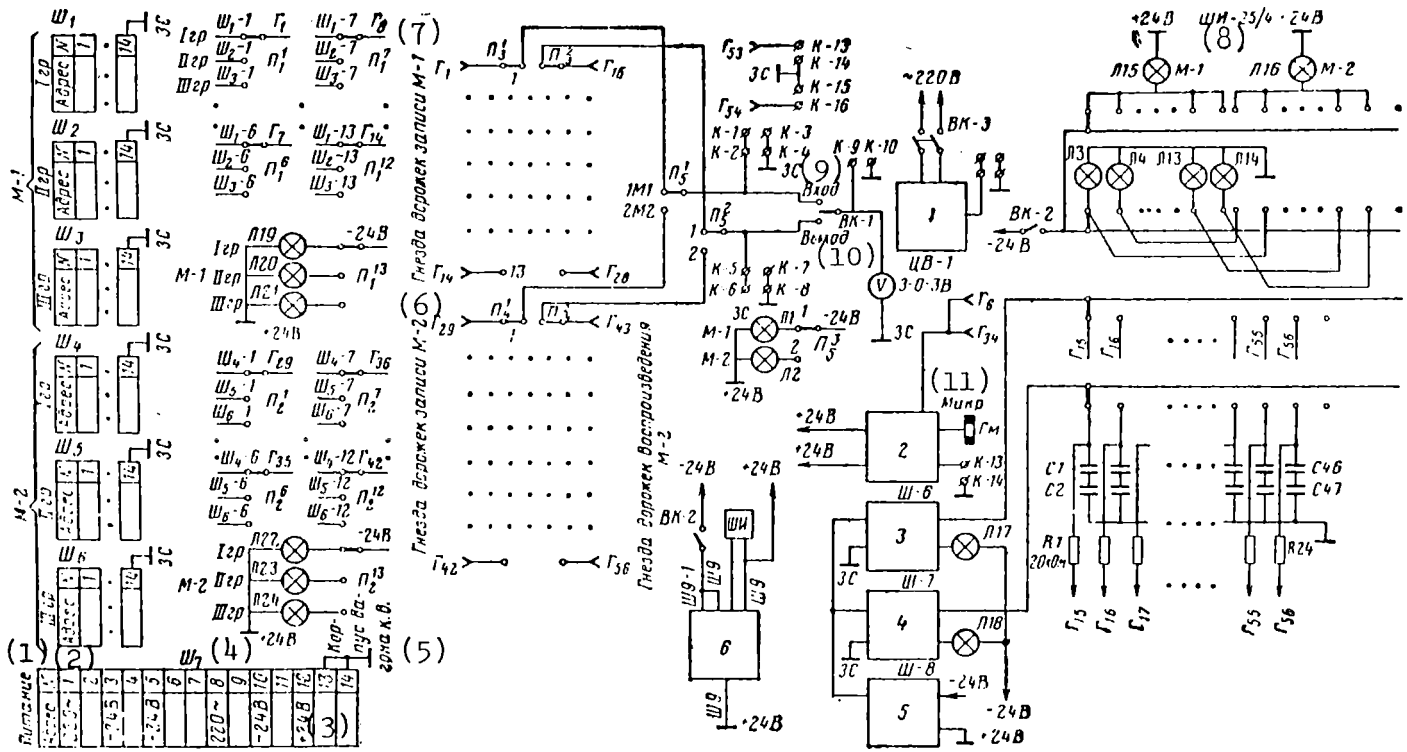

Figure 4.3. Schematic diagram of the device for monitoring the operation of the tape recorders and the strain amplifiers: 1--digital voltmeter; 2--microphone amplifier plate; 3--plate for monitoring the high-frequency interference; 4--null signal monitoring plate; 5-- -24-volt voltage stabilizer; 6--plate for the cycle generator of the motion of the ShI-25/4 step-by-step switch.

Key: 1. Power supply
2. Address
3. ... volts
4. Sh7
5. Car housing
6. M-2 recording track jacks

which is necessary first of all when adjusting them and determining the calibration data.

Key to Figure 4.3 (continued)

7. M-1 recording track jacks
8. ShI-25/4
9. Input
10. Output
11. Microphone

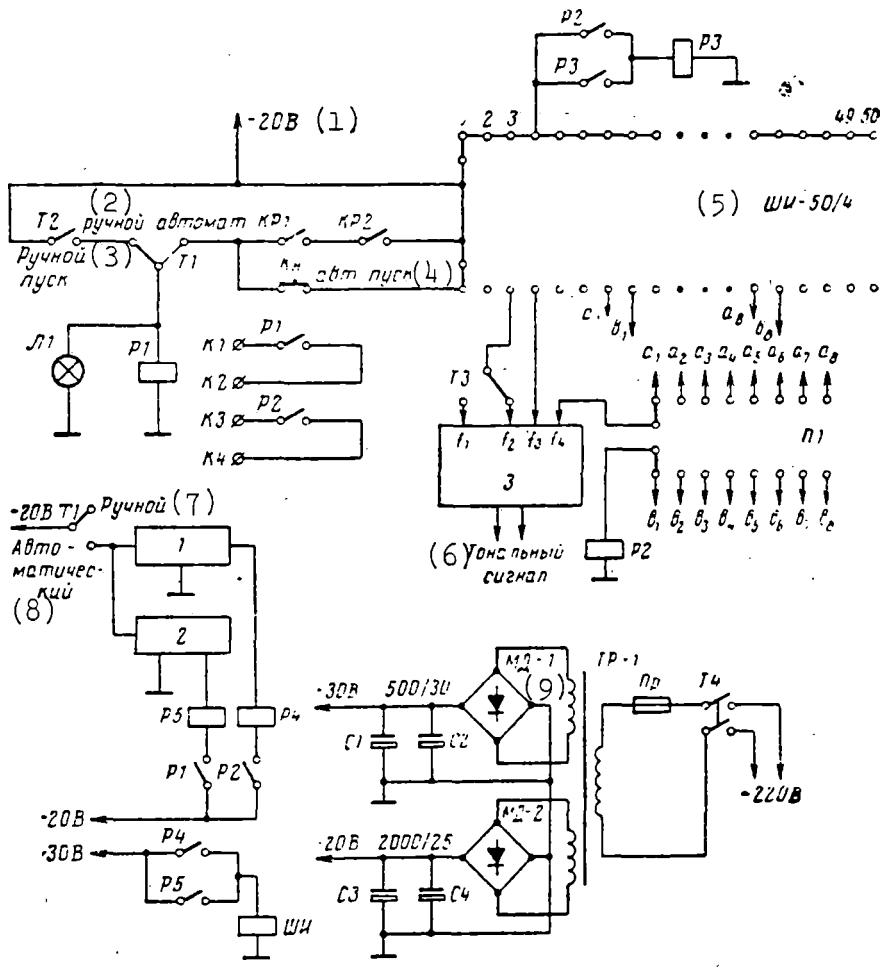

Figure 4.4. Schematic diagram of the automatic switches for the recording instruments: 1, 2--cycle generators of motion of the ShI-25/2 step-by-step switch with a frequency of 1 and 5 Hz, respectively; 3--voice-frequency generator plate.

Key to Figure 4.4:

1. ... volts
2. KR1 automatic switch
3. Manual start
4. Automatic start
5. ShI-50/4
6. Voice-frequency signal
7. Manual
8. Automatic
9. MD-1

Automatic switch for connecting the recording devices. The schematic diagram of the automatic device is shown in Figure 4.4. It provides for switching the tape recorders and other recording instruments on for a given time (from the Kn button) which is selected by the P1 switch. The minimum recording time is 7 seconds and the maximum 47 seconds. The time controller is a Kipp relay with a frequency of 1 Hz and the ShI-50 step-by-step switch. On pressing the automatic start button the R1 relay responds. Its contacts switch on the tape recorder (the K1 and K2 terminals) and they block the Kn button circuit. The brushes of the step-by-step switch will begin to move with a step of 1 second. On expiration of 2 seconds after switching on the automatic device, a signal for the sign of the experiment with frequency f_1 or f_2 (selected by the T3 toggle switch) is fed from the voice-frequency generator to K13 and K14 terminals. The signal of the beginning of the experiment with frequency f_3 is also fed after 1 second. When the

brush reaches the lamela a_1, a_2, ..., a_8 a signal is sent (the end of experiment). Then after 1 second the brush reaches the lamela b_1, b_2, ..., b_8 and includes the R2 relay, the normally closed contacts of which open the circuit of the R1 relay, and the tape recorder is switched off. Simultaneously the contacts R2 include the relay R3 which ensures fast return of the step-by-step switch to the initial position. The manual control of the tape recorder is possible. For this purpose it is necessary to set the toggle switch T1 to the manual position. The toggle switch T2 provides for switching the R1 relay on and off and consequently, connecting and disconnecting the tape recorder. The power supply for the device comes from the AC network. For a simultaneous connection of two or more devices, for example, YeMM-140 type tape recorders, it has turned out to be necessary to develop an additional device.

4.5. Device for Electrical Calibration of Tensometric Circuits

During the process of performing the experiments it is necessary regularly to perform an electrical calibration of the channels of the strain amplifiers. For this purpose usually there are standard resistors (shunts) in the laboratory cars by which the active and compensation arms of the strain resistor bridges are shunted alternately manually.

Let us note that the bridge imbalance occurring here (and, consequently, the signal at the output of the strain amplifier) corresponds to deformation of the material to which the strain resistor is applied:

$$\varepsilon_T = R_d/R_{sh}\rho, \qquad (4.1)$$

where ε_T is the deformation of the material;

R_d is the resistance of the active strain resistors;

R_{sh} is the resistance of the standard resistor (shunt);

ρ is the sensitivity factor of the strain resistor.

For the materials subordinate to Hook's law, the indicated signal corresponds to the stress in the material.

$$\sigma_T = ER_d/R_{sh}\rho, \tag{4.2}$$

where σ_T is the stress of the material;

E is the modulus of elasticity of the material.

For steel having $E = 2.1 \cdot 10^6$ kg-force/cm and strain resistors having $\rho = 2.1$, formula (4.2) assumes the form

$$\sigma_T = R_d/R_{sh}, \tag{4.3}$$

where R_d is the resistance of the strain resistor, ohms;

R_{sh} is the shunt resistance, megohms.

Thus, electric calibration permits determination and monitoring of the recording scales.

When using several tape recorders which record two or three groups each, the total number of measured parameters (and, consequently, the number of strain amplifier channels) exceeds 50. In this case the manual calibration is labor-consuming and does not exclude errors. Therefore for multichannel magnetic recording of the dynamic processes, centralized (preferably

automatic) calibration of all of the channels is possible. This device was developed and used in a number of tests. Its schematic diagram for one strain unit is presented in Figure 4.5. The device provides for the calibration of the channels by a shunt of 1 megohm or that is 100 kilohms. The selection is made by the VK1-VK12 toggle switches. The RES-22 type relays having odd numbers connect the shunts to the active arms of the bridges, and the even ones to the compensation arms.

The relays R1-R5 are connected through the relay R7 using the button Tar. A located on the panel of the tape recorder control unit. The relays R2-R6 are connected through the relay R8 using the Tar. T button. The device is connected to the terminal panel for connecting the strain resistors by a shielded cable using a hose connection.

The calibration is done in the following way: the tape recorders are connected for recording the first group of processes, and first the Tar. A button is pressed, and then the Tar. T button. Then this procedure is repeated also for the other groups of processes.

For monitoring the constancy of the recording scales, periodically the results of the electrical calibrations for each process from the output of the tape recorder are measured by a digital voltmeter and they are recorded in a special table. This process is labor-consuming; therefore it should be automated on the basis of applying a digital printer.

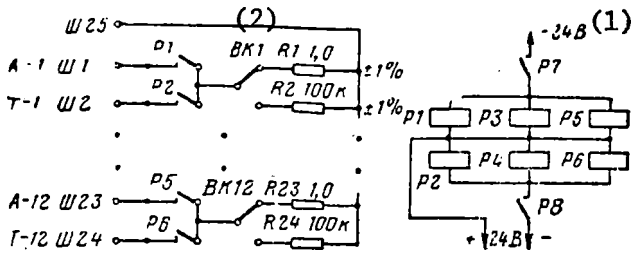

Figure 4.5. Schematic Diagram of Device for Electrical Calibration of Strain Amplifiers. Key: (1) 24 volts; (2) KV... switches

4.6. Analog-to-Digital Complex and the Programs for Automatic Experimental Data Processing

The analog-to-digital complex or automatic processing of experimental data (ATsVK) was built in the Railroad Car Division on the basis of applying a magnetic recording, the analog computer and digital computer. For several years the data were processed on the loading regimes of the undercarriages of freight cars of different types in operation and at increased speeds. The block diagram of the analog-to-digital complex is presented in Figure 4.6.

The ATsVK includes the following devices and instruments: 1--a tape recorder on which the signals of the dynamic processes are reproduced from the magnetic tape; 2--a sound amplifier through which the signal of the sound accompaniment is reproduced from the service track of the tape recorder; 3--an electronic oscillograph, on the screen of which visual inspection of the process signal is possible; 4--the analog computer; 5--the module of digital voltmeters (type F204/3); 6--the F595-KM digital printer; 7--the module of digital voltmeters (type VK-7-10A); 8--two-channel

coupler for coupling the analog computer to the punch; 9--PL-80 or PL-150 tape punch; 10--data input unit from the punch tape to the digital computer; 11--Nairi-S digital computer; 12--device for printing out the processing results.

The signal of the process reproduced from the magnetic tape goes to the analog computer where it is aligned, filtered and fed on the required scale to the processing system. All the basic functions of the analog part of the automated processing is conversion of the signals to a form convenient for measurement by digital voltmeters. The control of the conversions in the analog computer and the readout of the measured values is realized either from the processing itself (with its repetition frequency), or by quantization with respect to time from the signal of an outside oscillator. In the first case the signals go through special circuits before measurement by the digital voltmeters V_4 and V_5 [19], which generate the maximum values of the process, between two adjacent intersections of the null level. When reading out the values with the frequency of the external generator signal, the processes are fed to the input V_4 and V_5 directly, and they are read out by the signals of the analog computer control circuit. The results of measuring the values of the process with respect to positive and negative poles using a two-channel coupler are punched out successively on the punch tape in binary-decimal code. In order to punch the digital data, four bits of the punch tape are used; in the fifth bit the number division punch is made. The value of each tenth bit is punched in one row. In this way each number made up of the current values of the process with respect to plus

and minus is completely punched on the punch tape in five rows, inputting the division between adjacent numbers.

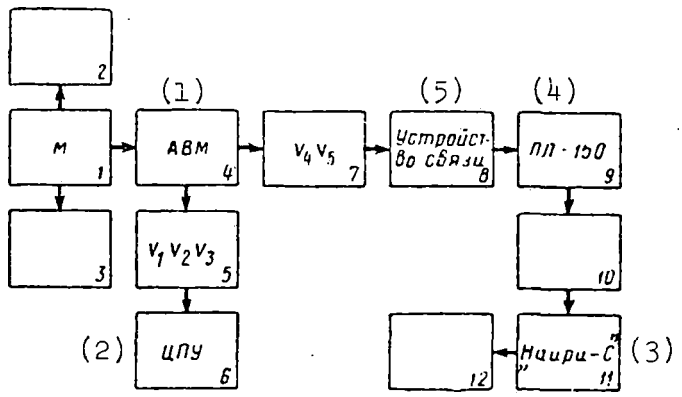

Figure 4.6. Block diagram of an analog-to-digital computer complex.

Key: 1. Analog computer

2. Digital printer

3. Nairi-S computer

4. PL-150 tape punch

5. Coupler

On completion of the experiment, a provisional experiment separation code is punched on the punch tape (for example, a code for the speed or nature of the section) by which the data are classified in the digital computer.

In addition to the amplitude measurements (or instantaneous values), during the process of reproducing the signals from the magnetic tape the analog computer determines the dispersions of the instantaneous values and the absolute maxima with respect to two signs. These three values are measured by the digital voltmeters V_1-V_3 and they are automatically printed out on a form of the ditigal printer.

When processing the complex process requiring preliminary calculations (for example, in order to determine the coefficient γ) or when performing a regression analysis of two processes, the computation and the logical operations are performed on the analog computer. The signal prepared in this way is fed to the circuit for making the measurements and punching out the data on the punch tape, after which it goes to the last stage--mathematical processing of the data punched on the punch tape, calculation of the dynamic indices and other operations performed by the Nairi-S digital computer. The data input to the digital computer is realized using a photoreader. The processing programs were developed by the Automation Laboratory of the Railroad Car Division of the institute in such a way that the classification of the data (distribution by levels) takes place in the process of accelerated input and the ready-access memory of the computer does not overflow when processing experiments of "unlimited" duration. The calculation of the basic distribution parameters and dynamic indices is accomplished on completion of the input of the data of the next experiment. A detailed description of the block diagrams and also the programs for processing the various processes is presented in [6, 15, 19, 21]. In Table 4.2 a list of programs is presented which were used when processing the data with the application of the ATsVK.

Table 4.2

Type of Data Processing	Result
Aligning	The constant component is excluded

Table 4.2 (continued)

Type of Data Processing	Result
Filtration	The high-frequency harmonics are excluded
Amplitude analysis	Amplitude distribution X_a, σ_a, $X_{max}^{(+)}$, $X_{max}^{(-)}$
Analysis of the instantaneous values	Distribution of the instantaneous values σ^2, $X_{max}^{(+)}$, $X_{max}^{(-)}$
Calculation of the index of smoothness of the behavior	W_z, W_y for each experiment
Calculation of the coefficient γ by deformations of the truck frame	Distribution of instantaneous values of γ, H, R, printout of the instantaneous values of H, R, γ_{max}
Calculation of the coefficient γ by deformations of the wheel webs	Same
Regression analysis	Correlation coefficients, linear regression coefficients, printout of the pairs of numbers

In order to expand the possibilities of the analog-to-digital computer complex (ATsVK) in the coupler between the analog computer and the punch provision is made for the possibility of punching out the data on the punch tape in the code of the M-6000 digital computer.

The card catalog of data processing programs using this computer is analogous to that presented in Table 4.2, and at the present time it is being expanded

and improved.

4.7. Systems for Complete Automation of the Processing of the Data From Dynamic Strength Testing of Railroad Cars

Along with many advantages, the ATsVK developed and used in the given studies to process experimental data have a number of deficiencies: a) no more than two processes are processed simultaneously; b) high-frequency processes cannot be processed; c) the processing program is limited. Therefore the Railroad Car Division of the Central Scientific Research Institute of the Ministry of Railways has worked on improving the methods of machine processing of data, the basis for which is the use of a specialized digital computer of the Dispersiometr type, the basic technical specifications of which are presented in Table 4.3. This machine is designed for calculating the statistical characteristics (the stationary and nonstationary ones with respect to mathematical expectation), and also for constructing the mathematical models (identifications) of complex, including nonlinear dynamic systems. The specialized digital computer Dispersiometr permits the solution of a broad class of problems which reduce to calculating the estimates: the one-dimensional and two-dimensional probability densities of the instantaneous and extremal values of the random processes; autocorrelation and mutual correlation functions; autodispersion and mutual dispersion functions; autospectral and mutual spectral densities; pulse transition functions of the linear systems; degree of nonlinearity of the system; provisional and nonprovisional of the first four moments; values of the pseudorandom series with given probability characteristics.

The basis for obtaining the estimates of the statistical characteristics is the principle of their indirect determination--in terms of the nonparametric instruments of the probability densities. Thus, first estimates of the two-dimensional probability density are obtained considering all of the available information, and then all of the necessary characteristics are found by these estimates.

The specialization of the computer consists in realizing systems program processing of the data. As a result of specialization, the time in the stage of density formation has been sharply reduced, which is most frequently a recurrent operation.

On the basis of the Dispersiometr specialized computer, the Railroad Car Division has created a system for complete automation of the processing of the data (SPAOD) from the dynamic strength testing of rolling stock. The SPAOD is a set of measuring devices, computer engineering means and a software system which permits the statistical probability processing and analysis of the random dynamic processes (with respect to any advance-given program) recorded on various sections of track at various speeds.

Table 4.3

Form of representation of the numbers	With fixed point
Number of processor instructions	16 (basic)
Word length of the numbers, binary bits	18
Processor speed, thousands of operations/sec	40

Table 4.3 (continued)

Effective speed, operations/sec	$0.5 \cdot 10^6$
Capacity of the ready-access memory (18-bit words)	8,192
External memory on magnetic tape, bits	$64 \cdot 10^6$
Number of channels for communication with the target	20
Number of recorded data with respect to one channel (8-bit words)	10,000
Solution time of the identification problem of average complexity (10 recordings of parameters)	2-3 hrs
Printout speed, characters/sec	400
Types of connected sensors	Standardized signals 0-5 milliamps, 0-10 volts
Rate of interrogation of the sensors, 1/sec	2,000
Input on punch cards	UVVK 601

The system completely excludes the operator from the processing and transfers his functions to the computer. This relieves the operator of tedious and monotonous operations and excludes subjective errors. This system greatly reduces the processing time, it increases the precision, it more completely extracts the useful information from the experimental data, and it reduces the cost of the experiment itself, increasing the rates of the

studies.

The effective use of the SPAOD is possible only on automatic measurement and recording of the data. The data must be recorded using the precision magnetic recording equipment. This recording system permits combination of the advantages of light beam recording (great smoothness, visual control) with the possibility of automation of the input of these data to the computer. In addition, when recording the dynamic processes it is necessary to record the service data on the tape recorder tape. The block diagram of the SPAOD is presented in Figure 4.7.

The service information is coded for subsequent automatic classification of the experiments by defined attributes. These attributes are the beginning and end of the experiment, the calibration sign, the characteristic of the section of track (a straight line, left curve, right curve, station tracks, and so on), the speed, and the number of the group of sensors.

The software for the system for complete automation of the processing of the data from dynamic strength tests and also the software for the system for partial automation of the processing of the data represented in a form different from analog (graphs, tables, and so on) have been developed. The software of the system for complete automation of the data processing includes special programs and the basic control program (OUP) which organizes the entire processing process. The OUP realizes multichannel input of the data and its distribution in the memory; it performs an analysis of the service information to determine the equivalent attributes, scaling,

filtration and smoothing; it controls the errors occurring during recording and reproduction of the processes on the tape recorder; it classifies the results of the processing with respect to the equivalent attributes. It controls the operation of the special processing programs; it forms the library of standard programs; it prints out the processing results or constructs graphs, and so on.

The special processing programs, in addition to calculating the statistical errors, are used to calculate the statistical estimates of the dynamic indices of the rolling stock: the distribution functions of the coefficient of resistance of the wheels to derailment and its parameters; the distribution functions of the coefficient of smoothness of travel and its parameters; the line regression coefficients, and so on.

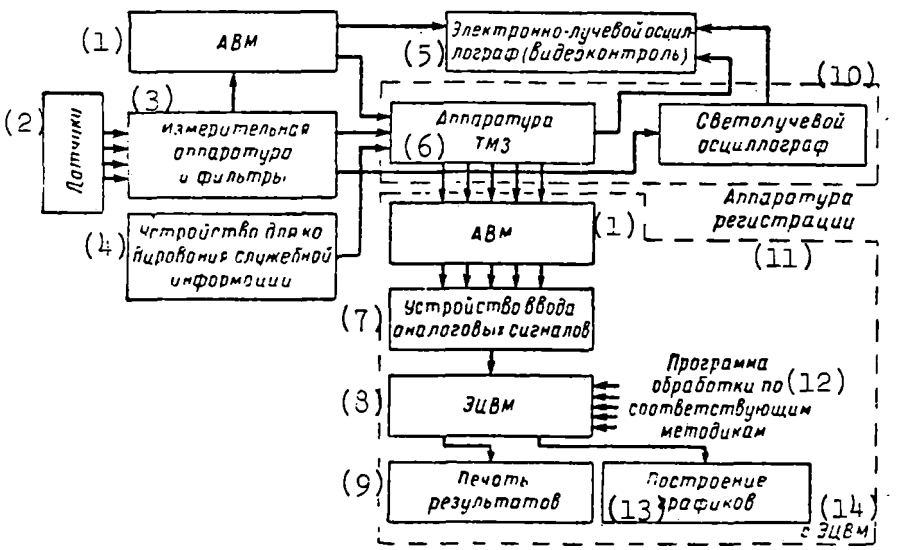

Figure 4.7. Block diagram of the SPAOD [System for Complete Automation of Data Processing].

Key: 1. Analog computer 2. Sensors

Key to Figure 47 (continued)

3. Measuring equipment and filters
4. Device for encoding service information
5. Cathode-ray oscillograph (video control)
6. TMZ equipment
7. Analog signal input device
8. Digital computer
9. Printout of the results
10. Light beam oscillograph
11. Recording equipment
12. Processing program with respect to the corresponding procedures
13. Graph construction
14. From the digital computer

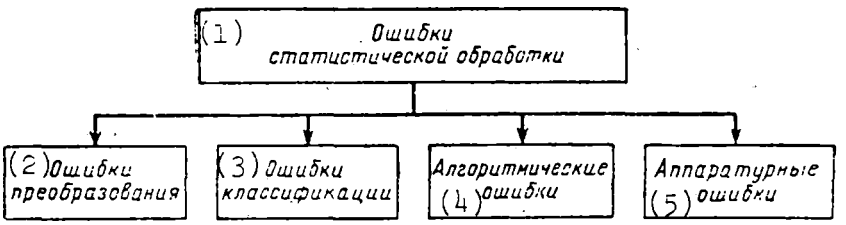

Figure 4.8. Classification of the errors in the statistical data processing.

Key: 1. Statistical processing errors
2. Conversion errors
3. Classification errors
4. Algorithmic errors
5. Hardware errors

The SPAOD software also includes programs for testing statistical hyptheses (zero and competitive), equalization of the empirical distribution, construction of the fiducial intervals, performing factor analysis, and so on.

The results of the numerous tests of rolling stock for different divisions of the institute were processed on this system.

The development of data processing and measurement automation has led to the occurrence of the problem of metrological support which includes the analysis and the normalization of the measurement and experimental data processing errors. Obtaining the statistical probability characteristics without estimating the precision can lead to significant errors, especially with a small volume of experimental data. Accordingly, the problem of classifying the processing errors and effective measures to eliminate them was solved (see Figure 4.8).

A more difficult problem is the protection from errors occurring during the measurements and data recording. The system provides for methods of discovering errors connected with failure of the sensors and the amplifier and low-quality magnetic recording.

The appearance of modern small third-generation computers completely solves the problem of selecting the hardware for the SPAOD. Their use in the SPAOD significantly increases the dynamic and frequency bands and will permit expansion of the class of investigated random processes.

Here the main problem remains the solution of the procedural problems connected with the general problem of statistical processing. The procedural principles with respect to qualitative and reliability analysis of the processing results are becoming constantly more complex. Accordingly, the Railroad Car Division is working on the problems of creating new methods of estimating various quality indices of the operation of the rolling stock, the scientific organization of experimental studies.

4.8. System for Automation of the Experimental Studies of Rolling Stock

The further improvement of the experimental research must proceed along the path of creating a system for automation of experimental studies of rolling stock (SAEIPS) using the mathematical apparatus of scientific experimental planning in the stage of preparing the experiment. The SAEIPS is designed for controlling the preparation and performance of the experiments by estimating the dynamic qualities of the rolling stock on a real time scale. The creation of the SAEIPS is unthinkable without using the most modern computer engineering means. The SAEIPS will permit the researchers to obtain not only the experimental results during the testing process, but, depending on them, also to direct the course of the experiment. The use of the system will also offer the possibility of testing the rolling stock in the limiting regimes.

Only the modern control computer can deal with this broad set of problems. This type of computer, in addition to the ordinary computer functions (the operative processing of the data, experimental planning, and so on) can

take on the control of the recording equipment, the calibration process, scaling, detection and elimination of emergencies, tracking of the test regime, and so on. In our country there is experience in the creation of such systems using specialized equipment and automation means.

The specialized equipment can solve specific problems optimally, but these automation systems are characterized by certain deficiencies: they can be used only for linear objects and stationary ergodic processes; the amount of equiment used increases proportionally to the number of simultaneously investigated processes and the number of estimate criteria used; the improvement and measurement of the estimate criteria require modification of the old equipment or creation of new equipment; the complexity of creating the automation system considering the specifics of each test.

The automated systems based on the computer are more flexible, for the calculation of all the parameters of the criteria of estimating the random processes is realized on them by programming. The appearance of new estimate criteria is connected only with the writing of new programs. The most effective can be the automation systems where the processing of certain high-frequency processes with respect to complex algorithms is performed under the control of the digital computer by specialized devices. Therefore the Railroad Car Division of the Central Scientific Research Institute of the Ministry of Railways decided to create the SAEIPS based on the control computer. For this purpose, the M-6000 ASVT-M computer was selected. On this machine the set of technical means is a set of unit modules executed on the elements of microelectronic engineering, and it is designed for the

composition of the control computer systems by design operating on a real time scale; there are couplers with the object for input of analog signals and also for input-output of digital data; the small dimensions of the structures will permit installation of the computer on the laboratory car. The small intake power of the computer can be set aside by the power system of the laboratory car. This computer is constantly improved. The Scientific Research Institute of Control Computers (NIIUVM) is developing improved processes: M-6010, M-7000, program compatible with the M-6000 processor and operating with the same peripheral devices.

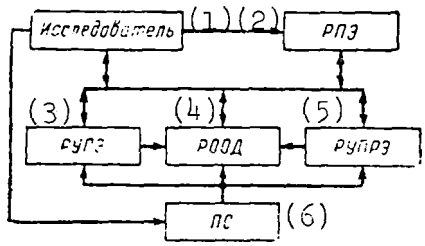

Figure 4.9. Generalized algorithm for operation of the SAEIPS: PS is the rolling stock.

Key: 1. Researcher

2. RPE [experimental planning mode]

3. RUPE [control of preparation of the experiment mode]

4. ROOD [operative data processing mode]

5. RUPRE [control of the performance of the experiment mode]

6. PS [rolling stock]

The hardware and software of this machine must provide for operation of the SAEIPS in the following modes: experimental planning (RPE), control of preparation of the experiment (RUPE), operative data processing (ROOD),

control of the performance of the experiment (RUPRE). The generalized algorithm for the operation of the system is illustrated in Figure 4.9.

The RPE must provide for the input of data on the performed experiment and selection of the optimal plan for performing the tests. The RPE prepares data for the operation of the system in the remaining modes. Here the data input must be convenient for the operator, and the form of the output, for use in the remaining modes.

The RUPE is used, for example, when determining the sensitivity of the strain gauges, during scaling, during preparation for the operation of the strain amplifiers, and so on. The data on the calibration and scaling are then used in the ROOD mode. Thus, the system hardware must provide for the possibility of monitoring and control of the tensometric equipment and also the input of data on the standard loads during calibration. The output data must be represented in a form that is convenient for visual monitoring and further use.

The ROOD must provide for estimating the dynamic qualities of the railroad car in real time. The technical equipment of the system must provide for commutation of the investigated processes, conversion of them from analog to digital code, transmission of the code to the processor and processing by the corresponding algorithms. The processing results must go to the researcher in a form which is convenient for their further quantitative and qualitative analysis.

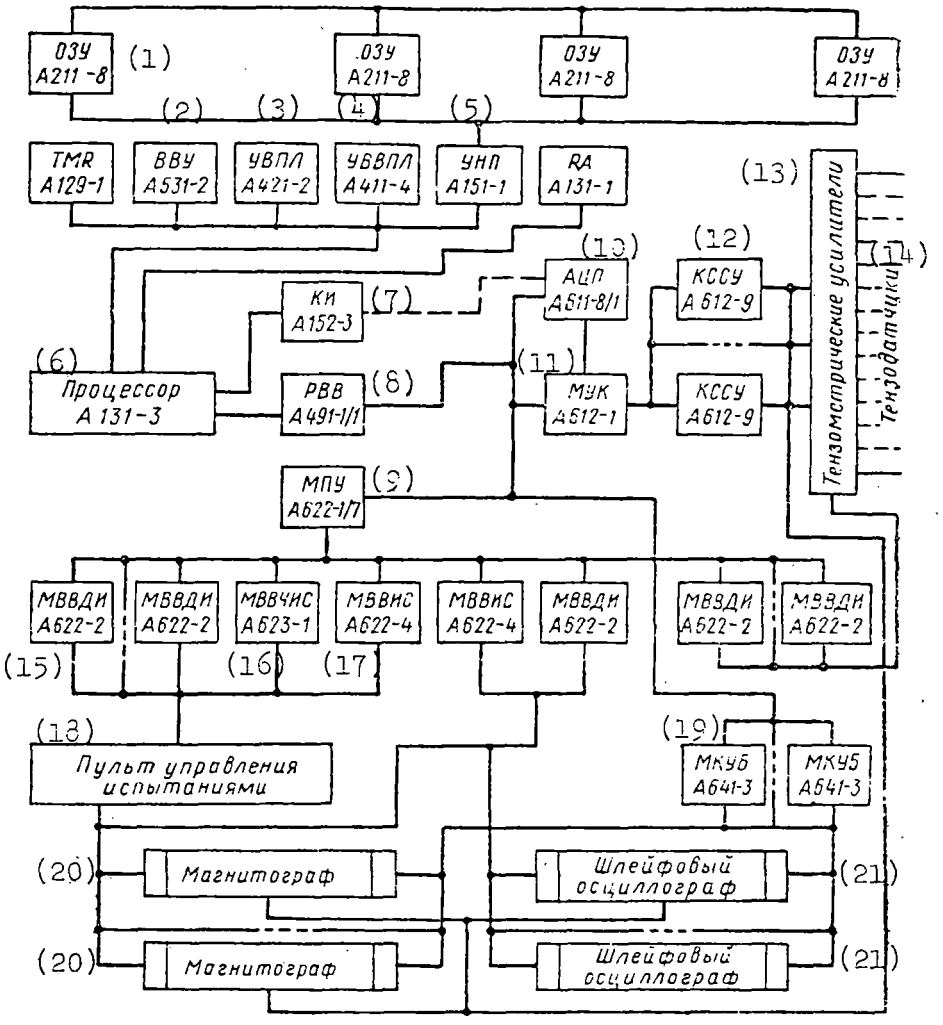

Figure 4.10. Structure of the SAEIPS system [System for Automation of Experimental Studies of Rolling Stock].

Key:
1. Ready-access memory
2. Input-output device
3. UVPL
4. UVVPL
5. UNP
6. Processor
7. KI
8. RVV
9. MPU
10. Analog-to-digital converter
11. MUK
12. KSSU

Key to Figure 4.10 (continued)

13. Tensometric amplifiers
14. Strain sensors
15. MVVDI
16. MVVChIS
17. MVVIS
18. Test control panel
19. MKUB
20. Tape recorder
21. Loop oscillograph

The RUPRE must provide for control recording of the investigated processes, normal functioning of the system, performance of the test by the plan selected in the RPE, that is, the system hardware must provide for monitoring and control of the tensometric and recording equipment, control of the test parameters and communications about operating failures of the system.

The software of the SAEIPS must realize autonomous operation of the system in the RPE and the RUPE modes and simultaneous operation in the ROOD, RUPRE modes. Here the fitness of the system in the RPE, RUPE and RUPRE modes is determined only by the presence of the hardware, and in the ROOD mode, it depends also on the technical specifications.

The logical composition of the system (determination of its composition, the relations between the unit modules entering into the system, operating regimes) was turned out beginning with its functional purpose considering

the realization of all the operating modes of the system.

In the L-6000 computer complex which is part of the SAEIPS, it is possible to isolate the following component parts: the nucleus of the complex, the input-output device, the analog signal input system, the digital data input system, the digital data output system.

The structural diagram of the SAEIPS is illustrated in Figure 4.10. The nucleus of the complex is the A131-3 processor designed for the processing of the instructions for arithmetic and logical data processing, input-output control. The word length of the words is 16 binary bits, the null single address instruction system, speed to 200,000 address operations per second and up to 1.8 million addressless operations per second. During the operation of the processor jointly with the arithmetic expander 131-1, the hardware execution of the instructions for multiplication, division and shifts of a binary word is possible. Up to eight input-output devices (here the 2K coupling is used) are connected directly to the processor. The use of one, two or three of the A491-1 RVV input-output expanders will permit an increase in this number to 22, 38 or 54. Interrupts are possible from the input-output devices and on errors in the system operation. The processor can operate with two ready-access memories, the A211-8 OZU [ready-access memory] with a capacity of 4,096 18-bit words each. The A151-1 UNP memory expansion unit provides for connecting up to eight of these memories to the processor.

The system includes the following input-output devices, the A411-4 UVVPL punch tape input unit, the A421-2 UVPL punch output unit, the A531-2 VVU symbolic data input-output unit, the A121-1 TMR timer.

The analog signal input system has the following structure: the A611-8 ATsP analog-to-digital computer (converts electric signals to 10-bit digital code, conversion time 20 microseconds) is connected to the RVV. The analog-to-digital converter is connected to the A612-1 MUK commutator control module in which up to eight 16-channel contactless commutators for medium-level signals A612-9 KSSU (input voltage range ±5 volts) can be installed. The commutation address comes to the MUK from the processor. The analog-to-digital converter (ATsP) can also be connected to the processor through the A152-3 KI increment channel which is designed for automatic increasing of the contents of the OZU cell by one, the address of which goes to the input of the device.

The A622-2 MVVDI digital data input module which is part of the digital data input system permits a 16-bit parallel code to be input to the processor from the two-position passive and active sensors. The A622-4 MVVIS initiative signal input module is designed for data input to the processor over eight channels from the initiative and emergency signal pickups and also from the sensors which rarely change their position. The A623-1 MVVChIS number pulse signal input module is designed for the reception, storage and input of data to the processor from the number pulse signal sensors. The MVVDI, MVVIS, MVVChIS are located in the A622-1 MGU group control module which is connected to the RVV. The MGU can have 22 modules of the digital

data input system.

The MKUB-3 contactless code control module is used for the reception and storage of data coming from the processor, and output of the control inputs in the form of a parallel 5-bit code to the target.

The couplings between the modules entering into the computer complex and also between the computer complex and the other devices entering into the SAEIPS are shown in Figure 4.7.

The limiting admissible operating conditions and also the operating experience during testing of rolling stock of the electronic and mechanical equipment indicate that the M-6000 and ASVT-M unit modules are workable under the conditions of the rolling laboratory car.

At the present time the software for the operative data programming mode has already been developed, and the software is being developed for the remaining operating modes of the system.

The fact that the estimate of the dynamic qualities of the rolling stock must be made by the SAEIPS in the ROOD mode in real time imposes definite requirements on the choice of the algorithms for processing the processes occurring on a moving train. In estimating the dynamic qualities of the rolling stock, it is necessary constantly to deal with the calculation of the probability densities (PV) of the stationary random processes (SSP), and, consequently, the ROOD mode, executing its functions, must provide for estimation of the probability density of the stationary random processes or

combinations of them in real time. Knowing the probability density, i possible to calculate certain other statistical parameters of the process

In practice, in order to estimate the probability density function of the stationary random processes, values of the empirical probability density (EPV) have been defined. One of the methods of determining the empirical probability density is to construct the numerical histogram (ChG). Here the range of input data is broken down into g intervals of magnitude Δ. When constructing the ChG, it is determined what number of observations of a given realization will fall in one interval or another. When using the M-6000 computer hardware for constructing the ChG, each interval is assigned one or several ready-access memory cells. In the M-6000 processor a program analysis is performed to determine what interval corresponds to the digital code received from the analog-to-digital converter, the address of the ready-access memory cell is formed corresponding to this interval, and a one is added to the contents of this cell. When determining the multidimensional EPV or for simultaneous investigation of several processes, the addresses of the histogram channels are formed as a function of the channel number over which the information was received.

For the possibility of executing this algorithm for constructing the ChG on a computer in real time (the ready-access processing) satisfaction of the following condition is required:

$$\Delta t_{int} \geq t_{conv} + t_{switch} + t_{form} + t_{org},$$

where t_{int} is the time interval between two adjacent interrogations of the channels;

t_{conv} is the conversion time of the analog-to-digital converter of voltage to digital codes;

t_{switch} is the switching time of the channels;

t_{form} is the time for analyzing the conversion code and changing the contents of the intervals;

t_{org} is the time for organizing the interrogation of the next channel.

The conversion time t_{conv} and the switching time t_{switch} are determined by the speed of the analog-to-digital converter and the commutator used in the given system.

When investigating one SSP the interrogation interval Δt_{int} is equal to the digitalization interval Δt_d for realization of the random process which is related to the upper boundary frequency f_B of the process spectrum by the expression

$$\Delta t_d = 1/kf_B,$$

where k =2-10 depending on the purpose of the investigation.

For parallel investigation of several random processes with different f_B the interrogation interval can be uniform and depend on the organization of the interrogation.

If the operative processing of the data is possible on the given computer, then the carrying capacity of the given system is determined as the minimum

possible interrogation interval $\Delta t_{int}^{\text{minimum possible}}$. Since in the formula t_{conv} and t_{switch} are constants, the increasing carrying capacity of the system can be achieved only by decreasing $(t_{form} + t_{org})$ as a result of using optimal procedures and algorithms and also as a result of their effective execution on a given computer. The standard software for the analog signal input system of the M-6000 cannot be used for organization of the operative processing, for the required algorithms are not available in it.

The algorithm for the organization of the operative processing was selected considering the fact that each investigated process can be processed with respect to any required algorithm or by several algorithms. Thus, for example, both the processing with respect to instantaneous values and with respect to the minima and maxima can be carried out immediately.

The program for organizing the operative processing permits the following functions: organization of the switching of the channels and ensurance of the required interrogation intervals; transfer of control to the processing programs; ensurance of the required lengths of the realizations of the investigated processes; transition to the programs for final data processing.

The preparation of the files for organization of the switching of the channels and ensurance of the required interrogation intervals are carried out by a special program for which the input data are the number of channels of the investigated processes and their f_B.

The programs for operative and final processing permit us to obtain all of the necessary statistical estimates of the processes occurring in the rolling stock (see 4.7). The duration of the SAEIPS will permit simultaneous calculation of five margin of stability coefficients or determination of 30 indices of smoothness of travel.

Chapter V. Selection of Experimental Objects and Test Procedure

5.1. Procedure for Selecting the Test Objects

The selection of the test objects in the stated problem is highly complex. Freight cars, in addition to great variety of types and sizes, have different technical conditions (from new ones that have just come from the car-building plant to the worn-out ones that have already been through one capital or medium repair).

In order to reflect the entire variety of the operating fleet of cars, it would be necessary to investigate very many objects and expend a great deal of time and means. Therefore for the tests it is necessary to select the minimum possible number of objects which will reflect the most characteristic average network condition of the operating fleet.

The technical condition of the cars ensuring safe operation at maximum admissible speeds is regulated by the technical operating rules of the railroads of the USSR (PTE) and the instructions with respect to the norms for maintenance of the most important assemblies of the cars. These norms, just as the tolerances on the manufacture and assembly of new undercarriages have

quite broad limits.

The running characteristics of the car estimated by the level of dynamic forces acting on the car are determined primarily by the technical condition of the following assemblies: a) the condition of the rolling surface of the wheel; b) the longitudinal and transverse clearances between the axle box and the guides of the side frames of the truck; c) longitudinal and transverse clearances in the assembly for coupling the beam above the springs to the lateral frame; d) the condition of the vibration extinguishers.

The dimensions of the basic truck assemblies and the range of variation of these dimensions in operation are presented in Tables 5.1 and 5.2. Let us consider the effect of each of the above enumerated factors briefly.

Table 5.1. Basic Dimensions of the Assemblies of New Trucks Considering the Technical Specifications and the Manufacturing Tolerances

Assembly (Part)	Rated Value, mm	Min, mm	Max, mm	Δ, mm
Wheel diameter with respect to the rolling circle	950.0	950.00	964.00	14
Admissible difference in diameters of the wheel pairs under one truck	--	--	--	6
TsNII-Ts3-0 truck base	1,850	1,852	1,858	16
MT-50 truck base	1,800	1,796	1,806	10
Foot diameter, D_p	300	298.65	--	--

Table 5.1 (continued)

Assembly (Part)	Rated Value, mm	Min, mm	Max, mm	Δ, mm
Center plate diameter, D_{pp}	303	--	303.35	--
Difference of the diameters, $D_{pp} - D_p$	3	2	4.70	--
Clearances between slide blocks	--	2	20.00	--
Clearances in the coupling assemblies of the truck frame:				
Longitudinal in the axle box assembly				
a) slide bearings	--	1	9.00	--
b) roller bearings	--	2	12.00	--
Transverse in the axle box assembly				
a) slide bearings	--	1	7.00	--
b) roller bearings	--	4	14.00	--
Longitudinal in the spring-mounted assembly of the MT-50 truck	3	1	10.00	--
Transverse in the spring-mounted assembly of the MT-50 truck	4	4	10.00	--

Table 5.2. Condition of the Wedge System of the TsNII-Kh3-0 Trucks in Operation

Measurement	Mean Statistical Value, x, mm	Maximum Value, x_{max}, mm
Increasing the level of wedges with respect to the spring-mounted beam	4.0	11.0

Measurement	Mean Statistical Value, x, mm	Maximum Value, x_{max}, mm
Spacing between the friction cleats	633.0	638.0
Slope of the friction cleats	1.0	4.4
Wear of the friction cleats	0.8	2.5
Completeness of the wedge*	229.0	236.0
Wear of the vertical surface of the wedge*	4.0	9.9

* The wear is determined with respect to the rated sizes of the wedges.

The studies by the Central Scientific Research Institute of the Ministry of Railways established that the uniform rolling of the wheels not exceeding the admissible, is felt favorably in the dynamics of the car, it leads to a reduction in the amplitudes of the twisting motion of the trucks and a decrease in the horizontal forces [19]. Such wheel defects as nonuniform rolling and saddle profile of the rolling surface, the slide block, the built-up metal, and so on which cause increased dynamic forces at the contact of the wheels with the rails constitute a small proportion in the operating fleet and are not the object of this investigation. Thus, for the set of statistical data on the values and the recurrence rate of the dynamic forces occurring during normal operating conditions, the new wheel pairs or wheel pairs with significant wear of the rolling surface are of the greatest interest.

For normal operation of the TsNII-Kh3-0 and the MT-50 type trucks which do not have rigid transverse coupling between the side frames, the clearances

between the axle box and the pedestal horns of the opening the side frame have great significance (see Table 5.1). In order to improve the quality of the running of the truck, these clearances must be minimal. However, with minimal clearances, pinching of the axle box in the opening is possible as a result of swinging of the side frames, which can lead to the appearance of high stresses in the end section of the side frame and the vicinity of the axle box opening and also to a reduction in bearing life. Calculations show that for total clearances between the axle box and the side guides of 6 mm along the car and 5 mm across the car, the possibility of pinching the axle box is excluded. Therefore according to the latest recommendations of the Central Scientific Research Institute of the Ministry of Railways for new trucks and also trucks undergoing capital repairs, these clearances are limited to 6-12 and 5-10 mm, respectively.

In operation the clearances fluctuate within a quite broad range. The arithmetic mean values of these clearances along the car are equal to 9 mm and across the car, 14 mm. Large transverse clearances are especially unfavorable for the running characteristics of the car, for they lead to sliding of the side frame and the occurrence of impacts during transfer of the horizontal forces.

The clearances in the assembly above the springs (between the beam above the spring and the columns of the side frames) also play a significant role in the formation and the transmission of horizontal dynamic forces. The dimensions of these clearances must be tied to the horizontal rigidity of the spring suspension in order to offer the possibility of elastic pickup

of the horizontal forces transmitted to the body of the car from the wheel pairs. The greater the clearances, the greater the displacement that can be realized by the operation of the elastic suspension force.

However, for significant horizontal forces, usually the clearance gets taken up, and this leads to an impact nature of transfer of horizontal forces. The studies of the Railroad Car Division of the Central Scientific Research Institute of the Ministry of Railways establish that for small clearances which are taken up at low speeds, the level of the horizontal forces is somewhat higher, but the buildup of these forces with an increase in speed takes place monotonically. For large clearances the total force level is lower down, but the individual maximum values of the horizontal forces differ significantly from the basic set of forces. These peaks appearing as a result of the effect of single unevennesses of the track (or switch crossings) have decisive significance when estimating the traffic safety. At operating speeds which are permissible for freight cars, these clearances must be about 8-10 mm.

The fitness of the vibration dampers in the MT-50 trucks is determined by the condition of the leaf spring, and in the TsNII-Kh3-0 trucks, by the wear of the wedge system and it is quantitatively estimated by the relative friction coefficient.

The greater the wear of the wedge friction system, the lower the effectiveness of extinguishing the vibrations. The generalized index of the total wear of all of the elements of the wedge system of the TsNII-Kh3-0 truck

is the position of the bearing surface of the wedges with respect to the beam above the springs (see Table 5.2). According to the technical specifications for the assembly of new trucks, the difference between the bearing surfaces of the wedges and the beam above the spring must not exceed +4 mm (high) and -8 mm (low). In the case of average wear, these values amount to +6 and -8 mm, respectively. The trucks were selected for testing by these tolerances.

5.2. Test Objects and Technical Specifications of the Trucks

On the basis of analyzing the technical condition of the operating fleet of cars and the effect of maintenance of the undercarriages on the running characteristics for the 1969-1973 tests, two four-axle gondolas on the TsNII-Kh3-0 trucks and two gondolas on the MT-50 trucks, two tank cars on the TsNII-Kh3-0 trucks and two tank cars on the MT-50 trucks were taken out of operation. In addition, the eight-axle tank car and two eight-axle gondolas manufactured at the Kryukovskiy Car Plant (KVZ) and the Ural Railroad Car Plant (UVZ) which are the most productive structural designs, were also tested. These eight-axle cars had single-type four-axle trucks made up of two series TsNII-Kh3-0 trucks connected by a connecting beam. The diameter of the center plate was 450 mm. After construction, the eight-axle tank car was operated for 6 months on the Transcaucasian railroad, and the eight-axle gondolas underwent rolling tests at the experimental ring of the Central Scientific Research Institute of the Ministry of Railways after the plant strength tests. At the experimental ring they were run 20,000 to 23,000 km loaded. The four-axle trucks were almost new, without wear in

the coupling assemblies of the frame elements and with the fitted elements of the friction wedge system in the spring suspension. All the cars were equipped with axle box assemblies with roller bearings (see Table 5.3).

Table 5.3. Test Objects

(1) Тип вагона и номер	(2) Грузоподъемность	(3) Масса, брутто т	(4) Тип тележки	(5) Год испытаний
(6) Четырехосный полувагон № 657-5413	64 т	79, 7, (7) щебень	(8) ЦНИИ-Х3-О	1969
Четырехосный полувагон № 627-7193	64 т	82,7, щебень	МТ-50	
(9) Четырехосная цистерна № 735-9358	60 м³	83,1	ЦНИИ-Х3-О	1971
Четырехосная цистерна № 746-1406	60 м³	83,1	ЦНИИ-Х3-О	
Четырехосная цистерна № 756-4078	50 м³	73,0	МТ-50	
Четырехосная цистерна № 752-4162	50 м³	68,0	МТ-50	
Четырехосный полувагон № 679-7620	64 т	81,09, щебень	ЦНИИ-Х3-О	1973
Четырехосный полувагон № 674-1725	64 т	81,52	МТ-50	
(10) Восьмиосная цистерна № 790-4043	120 м³	173,3	Четырехосные (11)	1972
(14) Восьмиосный полувагон (12) № 001 (КВЗ)	120 т	171	»	1973
(13) Восьмиосный полувагон № 690-0141 (УВЗ)	120 т	172,3	»	

Key:
1. Type of car and number
2. Load capacity
3. Gross weight, tons
4. Type of truck
5. Test year
6. Four-axle gondola
7. Gravel
8. TsNII-Kh3-O
9. Four-axle tank car
10. Eight-axle tank car
11. Four-axle
12. No 001 (KVZ)
13. No 690-0141 (UVZ)
14. Eight-axle gondola

Table 5.4. Results of Weighing Experimental Cars (kg-force)

Номер оси и нагрузка на тележку (1)	(2) Четырехосный полувагон									
	№ 657-5413			№ 627-7193			№ 679-7620			
	(3) Левая сторона	(4) Правая сторона	(5) Всего на ось	Левая сторона	Правая сторона	Всего на ось	Левая сторона	Правая сторона	Всего на ось	Левая сторона
1	10450	9375	19800	9300	11200	20500	9400	11250	20650	8320
2	9275	10050	19325	10150	11300	21450	10100	10400	20500	9000
	19725	19425	39125	19450	22500	41950	19500	21650	41150	17320
3	11275	9425	20700	9250	10850	20100	11000	9190	20190	9250
4	10425	9475	19900	9750	10900	20650	9900	9800	19700	9550
	21700	18900	40600	19000	21750	40750	20900	18990	39890	18800
5	—	—	—	—	—	—	—	—	—	—
6	—	—	—	—	—	—	—	—	—	—
	—	—	—	—	—	—	—	—	—	—
7	—	—	—	—	—	—	—	—	—	—
8	—	—	—	—	—	—	—	—	—	—
	—	—	—	—	—	—	—	—	—	—
Всего	41400	38325	79725	38450	44250	82700	40400	40600	81090	36120

(6) Восьмиосный полувагон									
№ 674-1725		№ 001			№ 690-0141			№ 790-4043		
Правая сторона	Всего на ось	Левая сторона	Правая сторона	Всего на ось	Левая сторона	Правая сторона	Всего на ось	Левая сторона	Правая сторона	Всего на ось
11500	19820	11350	10600	21950	10850	9850	20700	10400	10800	21200
11150	20150	11200	10200	21400	10600	10300	20900	10800	10400	21200
22650	39970	22550	20800	43350	21450	20150	41600	21200	21200	42400
11400	20650	10500	10200	20700	12850	9900	22750	11450	10850	22300
11350	20900	10450	10700	21150	11450	10350	21800	11750	11150	22900
22750	41550	20950	20900	41850	24300	20250	44550	23200	22200	45200
—	—	10750	11250	22000	11050	11150	22200	9900	11100	21000
—	—	11750	11100	22850	11000	11400	22400	10150	11950	22100
—	—	22500	22350	34850	22050	22550	44600	20050	23050	43100
—	—	10700	10200	20900	10100	10550	20650	10800	10800	21600
—	—	9900	10150	20050	10450	10450	20900	10400	10600	21000
—	—	20600	20350	40950	20550	21000	41550	21200	21400	42600
45500	81520	86600	84400	171000	88350	83960	172300	85650	87650	173300

Key: 1. Axle number and load on the truck
2. Four-axle gondola
3. Left side
4. Right side
5. Total per axle
6. Eight-axle gondola

Table 5.5. Total Clearances in the Pedestal Horns and in the Spring-Loaded Assembly

Тип вагона и номер (1)	Зазор и прокат, мм (2)	(3) Сторона вагона (по ходу движения) (4) правая				(5) левая			
		1	2	3	4	01	02	03	04
Четырехосный полувагон (6) № 657-5413	Суммарный поперечный (7)	10,0	9,0	—	—	9,5	9,0	—	—
	Суммарный продольный (8)	13,5	10,0	—	—	14,5	9,5	—	—
(9)	Прокат колесных пар	0,5	2,0	—	—	0,5	1,5	—	—
То же (10) № 627-7193	Суммарный поперечный	9,0	9,0	—	—	9,0	11,0	—	—
	Суммарный продольный	14,0	12,0	—	—	13,5	10,5	—	—
(11)	Поперечный между надрессорной балкой и боковой рамой	6,5	5,0	—	—	4,5	5,5	—	—
(12)	Продольный между надрессорной балкой и боковой рамой	9,0	10,0	—	—	11,0	10,0	—	—
	Прокат колесных пар	0,5	2,5	—	—	0,5	3,5	—	—
Четырехосная цистерна (13) № 735-9358	Суммарный поперечный	8,0	9,0	—	—	11,0	7,0	—	—
	Суммарный продольный	10,0	12,0	—	—	9,0	8,0	—	—
	Прокат колесных пар	0	0	—	—	0	0	—	—
То же № 756-4078	Суммарный поперечный	10,0	9,0	—	—	5,0	9,0	—	—
	Суммарный продольный	11,0	8,0	—	—	10,0	9,0	—	—
	Поперечный между надрессорной балкой и боковой рамой	3,5	4,2	—	—	3,0	3,5	—	—
	Продольный между надрессорной балкой и боковой рамой	2,5	3,0	—	—	1,0	4,5	—	—
	Прокат колесных пар	0	0	—	—	0	0	—	—
Четырехосная цистерна № 746-1406	Суммарный поперечный	10,0	9,0	—	—	5,0	11,0	—	—
	Суммарный продольный	8,0	8,0	—	—	3,0	5,0	—	—
	Прокат колесных пар	0	0	—	—	0	0	—	—
То же № 752-4162	Суммарный поперечный	9,0	10,0	—	—	8,0	13,0	—	—
	Суммарный продольный	4,0	5,0	—	—	10,0	11,0	—	—
	Поперечный между надрессорной балкой и боковой рамой	3,0	4,0	—	—	3,5	4,0	—	—
	Продольный между надрессорной балкой и боковой рамой	3,0	4,5	—	—	2,5	3,5	—	—
	Прокат колесных пар	0	0	—	—	0	0	—	—

Table 5.5 (continued)

Тип вагона и номер (1)	Зазор и прокат, мм (2)	(3) Сторона вагона (по ходу движения)							
		(4) правая				(5) левая			
		1	2	3	4	01	02	03	04
Восьмиосный полувагон (14) № 001	Суммарный поперечный (7)	9,0	14,0	9,0	10,0	14,0	11,0	13,0	10,0
	Суммарный продольный (8)	9,0	10,0	10,0	10,0	10,0	6,0	8,0	7,0
(9)	Прокат колесных пар	0,2	0,5	1,3	1,1	0,6	1,2	1,1	1,0
То же (10) № 690-0141	Суммарный поперечный	12,0	13,0	13,0	10,0	13,0	10,0	12,0	12,0
	Суммарный продольный	7,0	10,0	7,0	9,0	8,0	8,0	9,0	7,0
	Прокат колесных пар	0	0	0,4	1,0	1,1	1,0	0	1,0
Четырехосный полувагон (6) № 679-7620	Суммарный поперечный	12,0	13,0	—	—	11,0	12,0	—	—
	Суммарный продольный	8,0	9,0	—	—	7,0	8,0	—	—
	Прокат колесных пар	1,1	0,9	—	—	1,3	1,0	—	—
То же № 674-1725	Суммарный поперечный	11,0	13,0	—	—	12,0	10,0	—	—
	Суммарный продольный	9,0	10,0	—	—	10,0	8,0	—	—
(11)	Поперечный между надрессорной балкой и боковой рамой	8,0	7,0	—	—	3,5	6,0	—	—
(12)	Продольный зазор между надрессорной балкой и боковой рамой	5,0	7,0	—	—	6,0	8,0	—	—
	Прокат колесных пар	0,5	1,1	—	—	0,8	1,0	—	—

Key: 1. Type of car and number

2. Clearance and wheel tread wear, mm

3. Side of car (with respect to direction of travel)

4. Right

5. Left

6. Four-axle gondola

7. Total transverse

8. Total longitudinal

9. Wheel pair tread wear

10. Same

Key to Table 5.5 (continued)

11. Transverse between the spring-suspended beam and the side frame

12. Longitudinal between the spring-suspended beam and the side frame

13. Four-axle tank car

14. Eight-axle gondola

15. Eight-axle tank car

Table 5.6. Position of the Spring-Suspension Wedge

Тип и номер полувагона (1)	1		01		2		02		1	01	2	02
	Y_1	Y_2	Y_{01}	Y_{02}	Y_3	Y_4	Y_{03}	Y_{04}	$\Delta Y_i = \frac{Y_i + Y_{i+1}}{2}$			
Четырехосный (2)												
№ 657-5413	—6	—1	—4	—1	—	—	—	—	—3,5	—2,5	—	—
» № 735-9358	—	—	—	—	—	—	—	—	16	12,5	—	—
» № 746-1406	—	—	—	—	—	—	—	—	—9	—10,5	—	—
» № 679-7620	0	—2	12	4	—	—	—	—	—1	8	—	—
Восьмиосный № 001	3	1	9	11	7	10	7	9	2	10,0	8,5	8
(3) » № 690-0141	7	3	11	8	3	12	0	13	5	9,5	7,5	6,5

Note: The minus sign denotes raising the wedges with respect to the spring-loaded beam, the plus sign means the lowering of the wedges.

Key: 1. Type and number of gondola

2. Four-axle

3. Eight axle

Wheel-by-wheel weighing of the railroad cars at the weigh station of the Central Scientific Research Institute of the Ministry of Railways was carried out before the tests (see Table 5.4). The four-axle tank cars constituted an exception. It was assumed that the tank cars with symmetric boiler and uniformly distributed net load has in practice identical axial loads. However, the results of weighing the eight-axle tank car did not confirm this.

From Table 5.4 it is obvious that in the four-axle gondolas the difference between the loads on the center plate of the trucks was 1.2-1.58 ton-force. The difference between the loading of the four-axle trucks in the eight-axle tank car was 1.9 tons. In the eight-axle gondolas the load in the beds was distributed uniformly, and the loads transferred to the center plates of four-axle trucks were equal. The nonuniformity of loading between the wheel pairs and also between the two-axle trucks in the four-axle truck with respect to the average load was: between the two-axle trucks 2-5 percent; between the wheel pairs of one truck 3-7 percent; between the wheels of one wheel pair 4-10 percent.

The order of these values arises from the tolerances on the rigidity and the dispersion of the frictional forces in the spring complexes.

Before testing, the undercarriages of the experimental objects were also measured. The measurement data are presented in Table 5.5 and Table 5.6.

From Table 5.5 it is obvious that the clearances in the axle box assemblies correspond to the existing tolerances for the manufacture and assembly of the trucks and are close to their arithmetic mean operating clearances. The clearances in the spring-suspended assembly of the MT-50 trucks are also in the region corresponding to the mean operating level.

The tread wear of the wheel pairs was especially selected small in order to ensure more intense wobble of the trucks and to obtain the highest lateral forces.

In Table 5.6 the magnitudes of the lowering (raising) of the bearing surface of the friction wedges with respect to the spring-suspended beam are presented. It is known that some of the specialists functionally relate the value of the possible frictional force in the spring complex to this value. With respect to the technical specifications for the manufacture, the lowering of the wedges must be within the limits of 4-12 mm. It is obvious from Table 5.6, the greater part of the spring complexes of cars had limiting values of the lowering. At the same time, the spring complexes of the four-axle gondola No 657-4413 and the four-axle No 746-1406 tank car had significant raising of the wedges. However, no absolute values of the lowering (raising) of the wedges or their dispersion was reflected in practice on the relative friction coefficients obtained for static calibration of the spring suspension of these cars. Thus, for the four-axle tank car No 746-1406 having almost limiting raising of the wedges of 9.0-10.5 mm, the relative friction coefficient was 10.5-11.5 percent, respectively, and for the four-axle tank car No 735-9358 with lowering of the wedges of 16-12.5 mm for the right and left complexes this coefficient was 8-12 percent.

Thus, the conditions of contact of the most working surfaces and the degree of their fit and not the position of the bearing surface of the wedges with respect to the spring-suspended beam have the greatest significance for the level of frictional forces in normal operation of the spring suspension.

5.3. Procedure for Generalizing the Experimental Data for 1969-1973

During the study of the dynamic loading regimes of the undercarriages of the four-axle gondolas and tank cars both on the TsNII-Kh3-0 trucks and on the MT-50 trucks and also the eight-axle gondolas and tank cars, the dynamic tests were performed in the winter and the summer.

In the winter the experimental trips were made on freight trains at the operating speeds on the Moscow-Kuybyshev-Chelyabinsk-Novosibirsk-Irkutsk-Sverdlovsk-Perm'-Kirov-Yaroslavl'-Moscow and Moscow-Kuybyshev-Chelyabinsk-Inskaya-Irkutsk sections, and in the summer on the Moscow-Kuybyshev-Chelyabinsk-Sverdlovsk-Perm'-Kirov-Yaroslavl'-Moscow and Moscow-Gor'kiy-Kirov-Yaroslavl'-Moscow-Kiev-L'vov-Moscow sections. In addition, experimental trips with an individual locomotive with increased speeds (to 100-120 km/hr) were made on the Novosibirsk-Omsk, the Sverdlovsk-Bogdanovich and the Kirov-Yar sections.

A comparison of the loading regimes obtained for individual types of cars in the same sections of track in the winter and summer demonstrated the coefficients of vertical dynamics and frame forces acting on the undercarriages of the cars are somewhat higher under summer conditions. Therefore the dynamic testing of the eight-axle gondolas was done only in the summer.

The dynamic overloads of the axles which, as a rule, are higher in the winter as a result of the effect of the inertial forces from the nonspring-mounted parts of the truck were studied in detail previously when creating a new method of strength calculation of the axle. Therefore in the present

studies only the actual overloads of the axles determined for a number of sections were compared with the calculated values.

Accordingly, the operating conditions of the axle are estimated at the present time.

During operation testing in 1969 and 1973 on the indicated sections of track, broad material was obtained on the running characteristics of the experimental objects, the anslysis of which revealed the effect of both the speed of the trains and the technical condition of the cars and operating sections of the track on the buildup of dynamic loads. It was discovered that independently of the test sections, the effect of the technical condition of the track on the growth of the dynamic vertical and horizontal forces exceeds by approximately two times the effect of the increase in speed, and the effect of the technical condition of the undercarriages essentially is not felt in the variation in level of the dynamic forces.

In analyzing the test results in 1969-1973, it was established that the maximum dynamic forces were obtained for the four-axle gondolas both on the MT-50 trucks and on the TsNII-Kh3-0 trucks (by comparison with the tank cars).

The frame forces of the eight-axle tank car and the eight-axle gondolas are practically identical, and the maximum coefficients of vertical dynamics for an eight-axle tank car are 30 percent higher than for the gondola.

Considering the possibility of the operation and maintenance of the rolling stock over closed routes, the decision was made not to average the dynamic loading data obtained by different types of cars on the same trucks and to present the worst of them.

Therefore in this paper data are presented on the four-axle gondola on MT-50 trucks, the four-axle gondola on TsNII-Kh3-0 trucks, the eight-axle gondola and the eight-axle tank car obtained on the Kirov-Yar section of the Gor'kovskaya railroad.

With respect to technical condition, as the studies have demonstrated, this section corresponds to the average network condition of the track sections.

As much as the estimate of the dynamic loading regime of the undercarriages of the freight cars is the most important for the existing (80 km/hr) and prospective (100 km/hr) level of maximum operating speeds, the generalized data are presented primarily for these two velocity gradations.

Chapter VI. Vertical Dynamic Forces Acting on the Side Frames of the Trucks

6.1. Four-Axle Gondola on the MT-50 Type Trucks

For the railroad cars on the MT-50 type trucks having rigid spring suspension with insufficient frictional forces for extinguishing the vibrations, the natural vibrations of the bouncing and galloping of the railroad car on the springs with the basic tone frequency of about 3.2-3.5 Hz are characteristic which coincides with the calculated data. The high-frequency vibrations of the nonspring-loaded masses with a frequency of 40-50 Hz are superimposed on the basic tone vibration.

In Figure 6.1 the maximum values are presented for the dynamic load coefficients k_d^{max} as a function of the speed (with respect to one point from the realization lasting 20 seconds) for the basic vibration tone (Figure 6.1a) and the total values of these coefficients are given considering the high-frequency component (Figure 6.1b). At a speed of up to 80 km/hr, the largest of the maximum values of k_d^{max} are equal to +0.8 (overload) and +0.6 (unloading of the spring suspension). At a speed of 100 km/hr the overwhelming majority of these values do not exceed +1.1 and +0.9; the unit values of the overload in the given tests were +1.7 and +1.9 (for one point).

The envelopes of the line on the graph characterize the level of the maximum values of the dynamic load coefficients in the sections of track in good condition (the lower line) and satisfactory condition (the upper line).

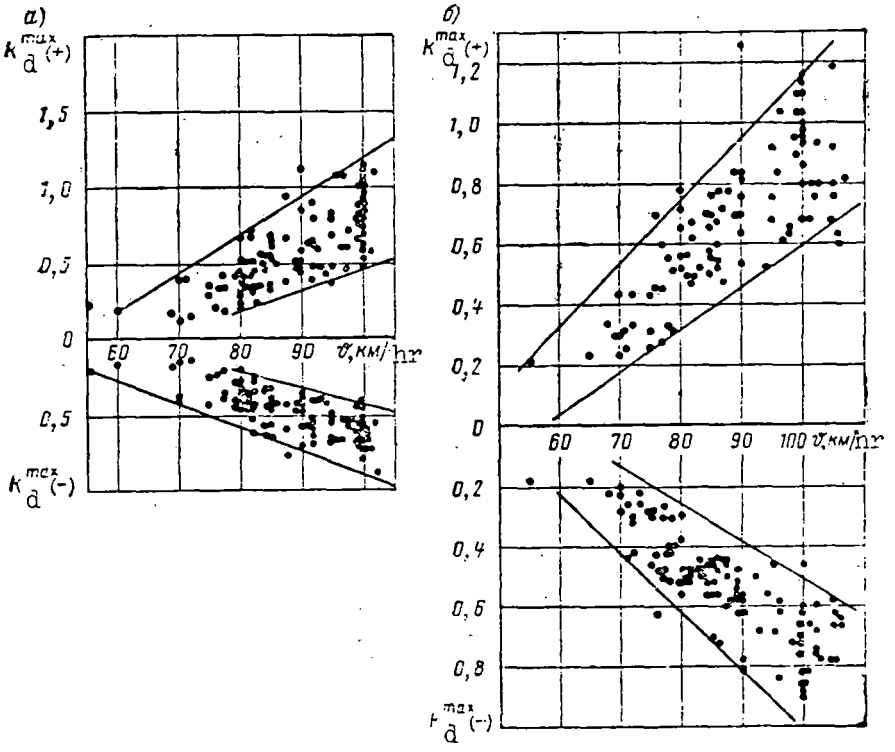

Figure 6.1. Maximum coefficients of vertical dynamics as a function of the speed of a four-axle gondola on MT-50 trucks: a--for processing with respect to the basic tone ($f \leq 10$ Hz); b--considering the high-frequency components.

The maximum values of k_d^{max} included between these lines reflect the effect of the technical condition of the track on the force loading of the undercarriages. A comparison of the relative increment of the dynamic load coefficients with an increase in speed by 20 km/hr with dispersion of the absolute values of these coefficients at constant speed indicates that the

effect of the technical condition of the track is 1.5-2.0 times greater than the effect of the indicated increase in velocity.

From the graphs it is also obvious that the maximum values of k_d^{max} obtained when processing by the basic tone of the vibrations on the total dynamic forces obtained when processing considering the high-frequency vibrations in practice coincide, which is characteristic of the suspension systems with a low degree of extinguishing of the vibrations.

The statistical distributions of the coefficients of the vertical dynamic forces are presented in Figure 6.2a. They agree visually well both with the exponential and the logarithmic normal distribution law. However, the hypothesis of the exponential distribution of the coefficients of vertical dynamic forces was deflected, for the testing of this hypothesis demonstrated the significant difference of theoretical and experimental distribution parameters.

The testing of the proposition of the logarithmically normal distribution of the coefficients of dynamic forces by the Pearson number demonstrated that this law quite closely describes the empirical distributions.

On the basis of the data obtained, the distribution of the general set of coefficients of vertical dynamic forces of the four-axle gondolas on the MT-50 trucks can be characterized by the following statistical parameters:

Speed, km/hr	80	100
Mean value, k_d	0.175	0.310
Standard deviation, σ	0.220	0.220

In accordance with the indicated calculation parameters, the probable value of the maximum coefficient of dynamic forces, for example, for v = 100 km/hr, is

$$\lg k_{\text{д}}^{\max} = \lg \bar{k}_{\text{д}} + 3\,\sigma = 0{,}1394; \qquad k_{\text{д}}^{\max} = 1{,}4.$$

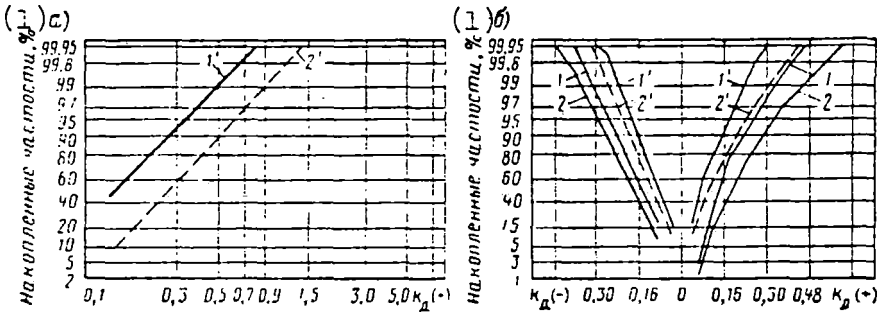

Figure 6.2. Distribution of the coefficients of vertical dynamic forces: a--acting on the frame of the MT-50 trucks; b--acting on the frame of the TsNII-Kh3-0 trucks; 1 and 1'--v = 80 km/hr; 2 and 2'--v = 100 km/hr, respectively, with and without consideration of the high-frequency components.

Key: 1. Accumulated frequencies, %

The unit extremal values of the coefficients of vertical dynamic loads going beyond the limits of probable values of the logarithmically normal distribution occur as a result of impact on closure of the coils of the springs in the spring suspension.

The change in nature of operation of the springs implies a change in the distribution law of the loads on the undercarriages. Therefore the probability of the occurrence of such values cannot be estimated by the

distribution parameters of the general set of dynamic loads occurring during vibrations of the cars on the springs.

6.2. Four-Axle Gondola on the TsNII-Kh3-0 Trucks

An analysis of the vibration frequencies of the four-axle gondola by the oscillograms demonstrated that for this type of gondola the average vibration frequency basically was 4.5 Hz, which is twice the calculated value of the natural vibration frequency on the springs. The high-frequency harmonics with a frequency of 40-50 Hz are superposed on the vibrations of the basic tone.

The quantile diagrams of the distributions of the coefficients of the vertical dynamic forces acting on the side frames of the TsNII-Kh3-0 type truck of the four-axle gondola are presented in 6.2b. The largest of the maximum values of k_d^{max} (with respect to one point from each realization) are presented on the point graphs in Figure 6.3; hence, it is obvious that the largest of the maximum coefficients of vertical dynamics recorded in the experiments were equal to 0.45 for v = 80 km/hr and 0.55 for v = 100 km/hr. Thus, as a result of the more improved suspension for this type of running gear the absolute values of k_d^{max} are appreciably lower than for the MT-50 type truck. However, in this case the same nature of the dependence of the dynamic loads on the increase in speed and the technical condition of the track is retained. For the railroad cars on the TsNII-Kh3-0 type trucks the effect of the technical condition of the track also exceeds the effect of the increase in speed by 20 km/hr by 2.0-3.0 times.

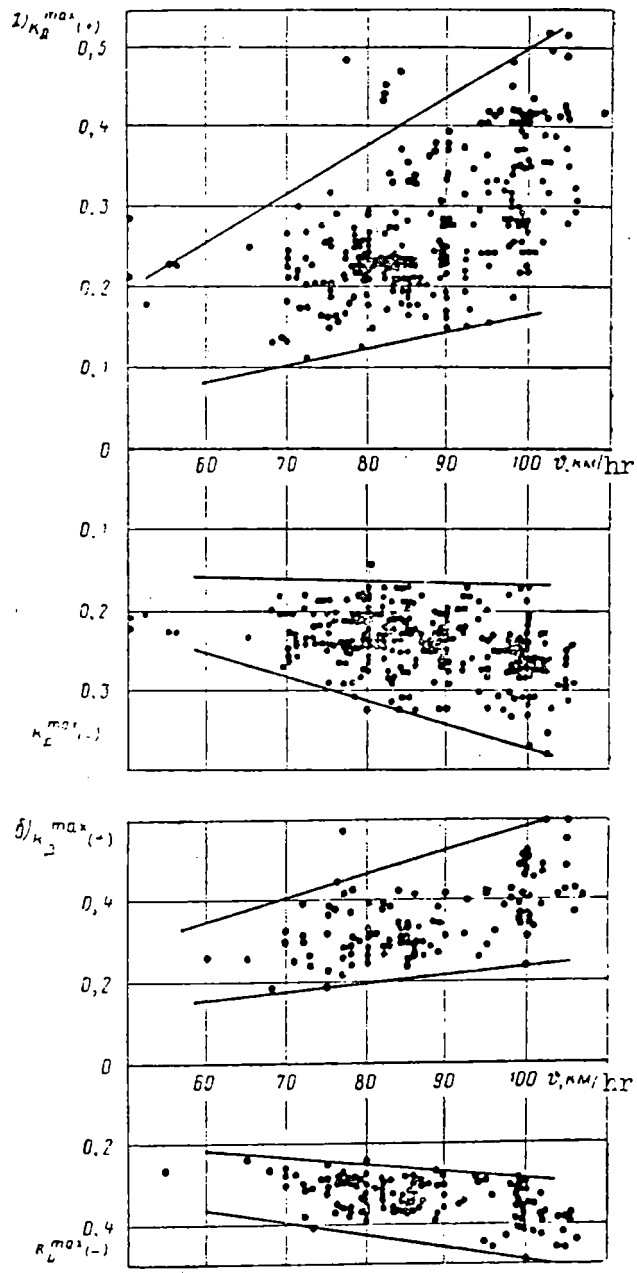

Figure 6.3. Maximum coefficients of vertical dynamics as a function of the speed of the four-axle gondola on the TsNII-Kh3-0 trucks.

The processing of the amplitudes of the coefficients of vertical dynamic forces with respect to the basic tone of the vibrations and considering their high-frequency components demonstrated that the high-frequency component k_d for the TsNII-Kh3-0 trucks is about 40 percent of the amplitudes of the basic vibration tone.

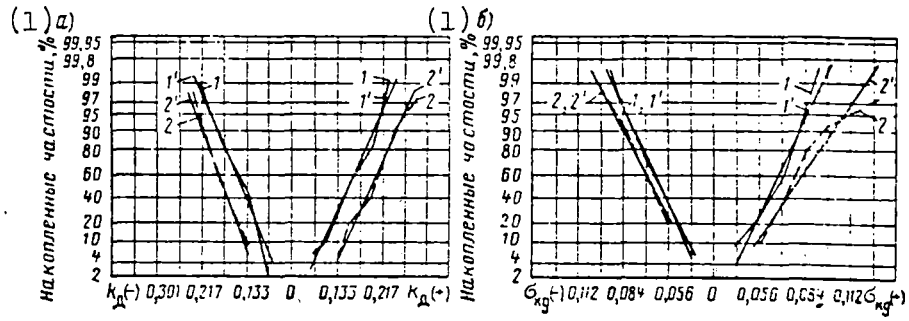

Figure 6.4. Distribution of the coefficients of vertical dynamic forces of the four-axle gondola on the TsNII-Kh3-0 trucks: a--mean values; b--mean square deviation; 1 and 1'--v = 80 km/hr; 2 and 2'--v = 100 km/hr experimental and theoretical curves, respectively.

Key: 1. Accumulated frequencies

The distribution of the coefficients of vertical dynamic forces is close to the normal law. Therefore in order to obtain the statistical distribution characteristics of these forces, the distributions of the mean values of k_d and standard deviations were constructed. Under the assumption that they are distributed normally, the theoretical frequencies of the values of the mean and standard deviations were determined (Figure 6.4). The further testing of this hypothesis by the Pearson number demonstrated that the normal

distribution law quite closely describes the empirical distributions. On the basis of these data, the distributions of the coefficients of vertical dynamic forces (the basic type of vibration) acting on the side frames of the TsNII-Kh3-0 trucks under the four-axle cars can be characterized by the following statistical parameters:

Speed, km/hr	80	100
Mean value of $\bar{k}_d$	0.154	0.195
Standard deviation from the mean values of $\sigma\bar{k}_d$	0.037	0.033
Mean standard deviation of the general set $\bar{\sigma}$	0.064	0.077
Deviation from the mean values of the standard $\bar{\sigma}_{\bar{\sigma}}$	0.013	0.018

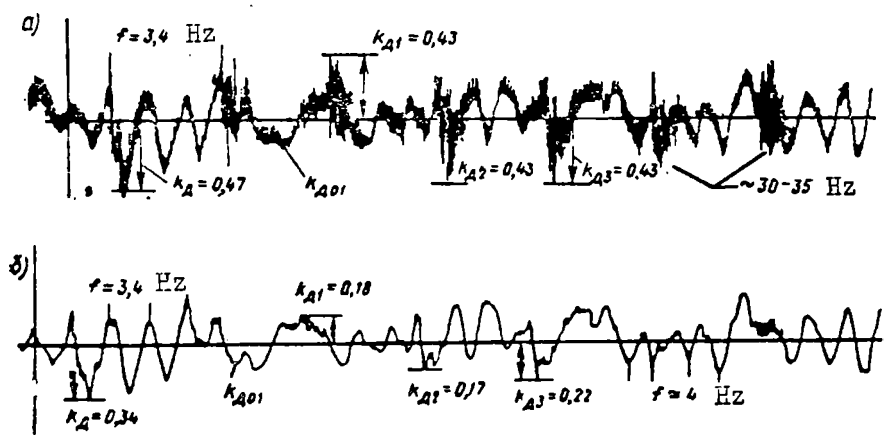

Figure 6.5. Examples of oscillograms of the coefficients of vertical dynamic forces of the eight-axle gondola at a speed of v = 100 km/hr: a--without low-frequency filter; b--with low-frequency filter for a cutoff frequency f = 10 Hz.

On the basis of these data, the calculated probable value of the maximum coefficient of vertical dynamic forces, for example, for v = 100 km/hr is

$$k_{\tilde{d}}^{max} = \overline{k}_{d}^{max} + 3\sigma^{max} = 0,7,$$

which agrees very well with the results of numerous dynamic (running) tests of these trucks.

6.3. Eight-Axle Railroad Cars

The running characteristics of the eight-axle railroad cars with the series-type TsNII-Kh3-0 trucks are distinguished qualitatively from the properties of the four-axle cars on the same trucks. This difference is determined by the presence of the connecting beam of the four-axle truck which serves not only as a type of equalizer decreasing the amplitudes of the long unevennesses in the track but also an element which rigidly transmits the impacts from all of the four wheel pairs to the frame elements of the truck on passage over short unevennesses. This gives rise to the relatively high level of high-frequency components of the vibrations for the eight-axle railroad cars with frequencies of about 30-40 Hz.

The oscillograms of the coefficients of vertical dynamic forces acting on the lateral frame of the truck of the eight-axle gondola are presented in Figure 6.5. On the oscillograms, the zones of passage of the four-axle truck over the joints which along the length exactly correspond to the distance between the four wheel pairs of the truck of 5.05 meters are clearly obvious. Between the joints, the high-frequency component in practice is absent, but there are sections of the track where the high-frequency components are continuously superposed on the basic tone and have quite significant amplitudes, the peaks of which nevertheless occur for the joints.

From the presented oscillogram it is also obvious that the frequency of the vibrations recorded by the upper strip of the side frame has a quite broad spectrum, from which the following are isolated most clearly: the basic predominant vibrations with frequency of 0.6-1.0 Hz connected with the side rolling of the car body; the often encountered wobble vibrations on the springs with a frequency of about 2-2.5 Hz; the most frequently encountered vibrations having the highest (with respect to the basic tone) amplitudes with a frequency of about 3.5 Hz, the nature of which still is unclear; the quite clearly expressed (but with low amplitudes) vibrations with a frequency of 4-4.5 Hz; the high-frequency vibrations from the effect of the joints and the short unevennesses with a frequency of 30-40 Hz.

The average frequency of the basic vibration tone calculated roughly as the quotient from the division of the number of amplitudes for the experiment by the duration of the realization (20 seconds) is 2.5 Hz for the side frames of the truck of an eight-axle railroad car at v = 80 km/hr and approximately 3.25 Hz at v = 100 km/hr. This indicates that at lower speeds the low frequencies predominate, and at speeds over 80 km/hr, the vibrations with a frequency of 3-3.5 Hz predominate.

It must be noted that the equivalent deflection corresponding to frequencies 3.5-4.0 Hz must be 20-15 mm, at the same time as the calculated static bending of the spring suspension is 45 mm, that is, the spectrum of the vertical vibrations of the eight-axle cars is caused not by the vibrations on the springs, but obviously by the quite high total flexibility of the frame elements of the four-axle truck and bed.

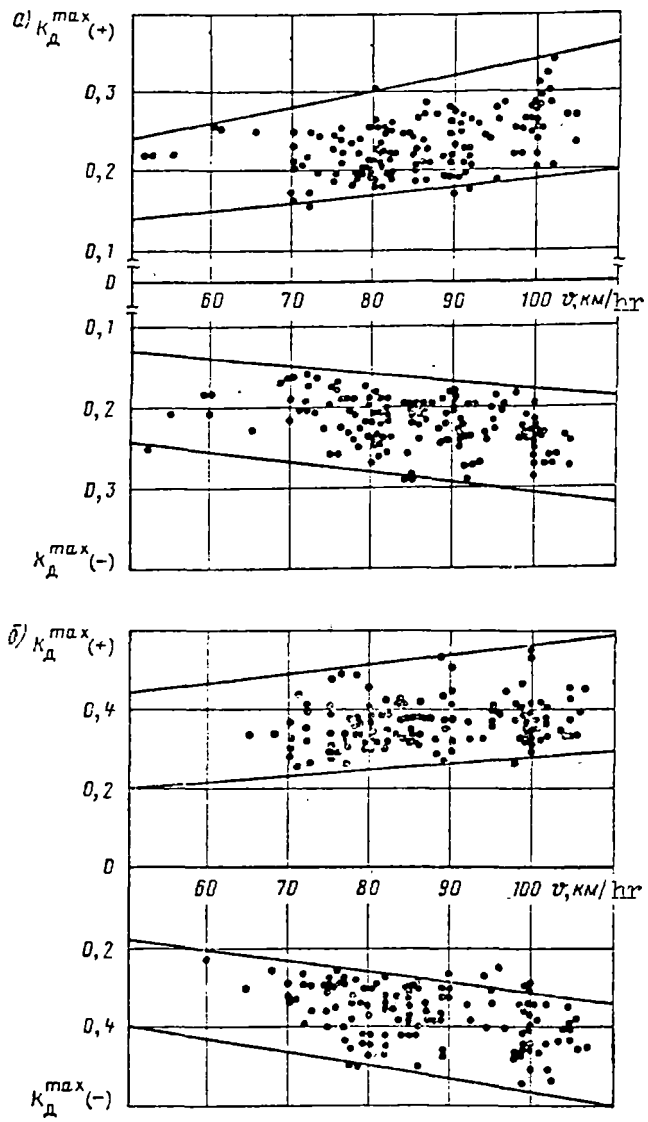

Figure 6.6. Maximum vertical dynamic coefficients of the function of the speed of an eight-axle gondola: a--when processing with respect to the basic tone ($f \leq 10$ Hz); b--considering the high-frequency components.

The point graphs of the largest maximum coefficients of vertical dynamic forces (with respect to the basic vibration tone) obtained for v = 70-100 km/hr on the Kirov-Yar section of the Gor'kiy railroad are presented in Figure 6.6.

These data indicate that the general level of the vertical dynamic forces of the low vibration tone does not exceed 30-40 percent of the static load, it depends little on the speed and reacts weakly to the track conditions.

As has already been mentioned, these dynamic forces are determined not by the vibrations from the track unevennesses and the sagging of the springs, but the predominance in the eight-axle cars of qualitatively different types of oscillations, including the side roll of the body on the foot. Considering that high-frequency vibrations which are significant with respect to absolute values of the amplitudes were noted, along with the ordinary processing with respect to the basic tone, the recordings were also processed without the low-frequency filter (in the frequency band from 0-50 Hz) (see Figure 6.6b). The reading of the amplitudes in both cases was done by the basic vibration tone, that is, out of the group of high-frequency amplitudes, actually only one was taken into account--the largest after the basic tone half-period.

When estimating the traffic safety, the primary role is played by the statistical parameters of the low-frequency tone vibrations. At the same time the total forces have great effect on the fatigue strength of the undercarriages of the car. The quantile diagrams indicate how high the effect

of the high-frequency components of the vibrations on the overload of the side frames of the trucks of the eight-axle cars is (Figure 6.7). For example, the maximum amplitudes of k_d with respect to the basic tone are within the limits of 0.28-0.36, and the total maximum amplitudes reach values of 0.48-0.56, that is, 1.5-1.7 times higher. Therefore, hereafter when studying the loading regimes of the truck frame elements by the high-frequency vertical forces, it is necessary to process the processes considering the recurrence rate of all of the amplitudes k_d.

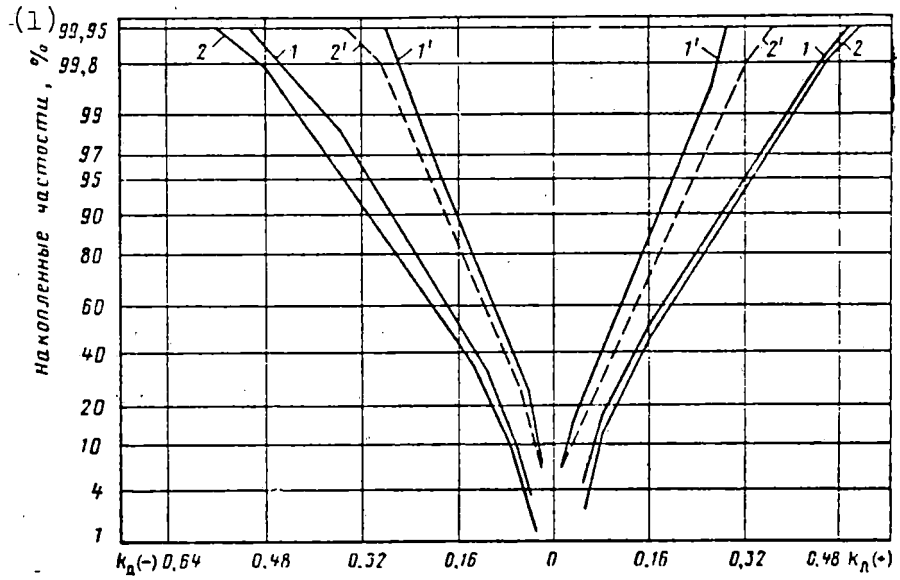

Figure 6.7. Distribution of the coefficients of vertical dynamic loads of the eight-axle gondola. The notation is the same as in Figure 6.2.

Key: 1. Accumulated frequency, %

In order to estimate the statistical distribution characteristics of the coefficients of dynamic vertical forces of the basic vibration tone, the

distributions of the mean values of $k_д$ and the standard deviations (Figure 6.8) were constructed, and the theoretical frequencies of these distributions were determined under the assumption that they were distributed normally. Further testing by the Pearson criterion demonstrated that there are grounds for talking about the normal distribution $k_д$ and σ.

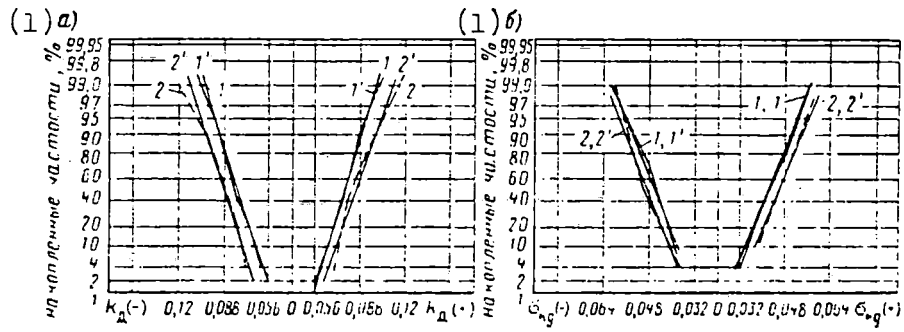

Figure 6.8. Distribution of the coefficients of vertical dynamic forces of the eight-axle gondola: a--mean value; b--mean square deviations; 1 and 1'--v = 80 km/hr; 2 and 2'--v = 100 km/hr, the experimental and theoretical curves, respectively.

Key: 1. Accumulated frequencies, %

A close statistical relation was established between the mean values of the dynamics coefficients and the corresponding standard deviations of the partial samples (realizations). The correlation coefficient determining the relation between these random variables is 0.8 and 0.9 for all types of cars, including the cars on the MT-50 trucks.

Thus, the distribution of the vertical dynamic coefficients can be represented as a two-dimensional distribution estimated by five parameters: the mean value and the standard deviation of the mean value of $k_д$, the mean value

and the standard deviation of the standard and the correlation coefficient. On the basis of these data, the distribution of the general set of coefficients of vertical dynamic forces (the basic vibration tone) acting on the side trucks of the eight-axle cars can be characterized by the following statistical parameters.

For the eight-axle gondola:

Speed, km/hr	80	100
Mean value $\overline{k}_d$	0.098	0.108
Standard deviation from the mean values $\sigma\overline{k}_d$	0.012	0.012
Mean standard deviation of the general set $\overline{\sigma}$	0.056	0.060
Standard deviation from the mean values $\overline{\sigma}_{\overline{\sigma}}$	0.007	0.008

For the eight-axle tank car, these forces turned out to be somewhat higher than for the eight-axle gondola.

For the eight-axle tank car:

Speed, km/hr	80	100
Mean value $\overline{k}_d$	0.084	0.096
Standard deviation from the mean values $\sigma\overline{k}_d$	0.026	0.029
Mean standard deviation of the general set $\overline{\sigma}$	0.041	0.049
Standard deviation from the mean values $\overline{\sigma}_{\overline{\sigma}}$	0.009	0.013

Thus, the calculated probable value of the maximum coefficient of vertical dynamic forces of the basic vibration tone, for example, for v = 100 km/hr will be:

For the eight-axle gondola $k_d^{max} = \bar{k}_d^{max} + 3\sigma = 0.39$

For the eight-axle tank car $k_d^{max} = \bar{k}_d^{max} + 3\sigma = 0.50$

These values agree well with the data obtained on the line.

Chapter VII. Horizontal (Frame) Forces

7.1. Four-Axle Gondola on the MT-50 Trucks

The point graphs of the maximum frame forces are presented in Figure 7.1 as a function of the speed of the car on the MT-50 trucks for the Kirov-Yar section of the Gor'kiy railroad (with respect to one point with a realization lasting 20 seconds for the even and odd directions of motion of the experimental train). For a speed of 80 km/hr the highest values of the forces on the straight sections of the track do not exceed 2.0 tons, and on the curves, 3.5 tons; for a speed of 90 km/hr the forces increase respectively to 3.0 (4.5) tons, and for 100 km/hr, to 5.6 (6.0) tons. The unit extremal values of the forces for 100 km/hr reach 8.0 (9.6) tons. It is necessary to remember that with respect to the traffic safety conditions and the stability of the track with respect to shear the maximum frame forces must not exceed 40 percent of the axial static load. For a loaded gondola with an axle load of 21.0 tons, the maximum admissible value is 0.4 x 21.0 = 8.4 tons.

Thus, for the gondola on the MT-50 trucks the set of amplitudes of the frame forces (with the exception of one value, 9.6 tons, obtained at the entrance to the curve) at a speed of 100 km/hr is below the admissible values.

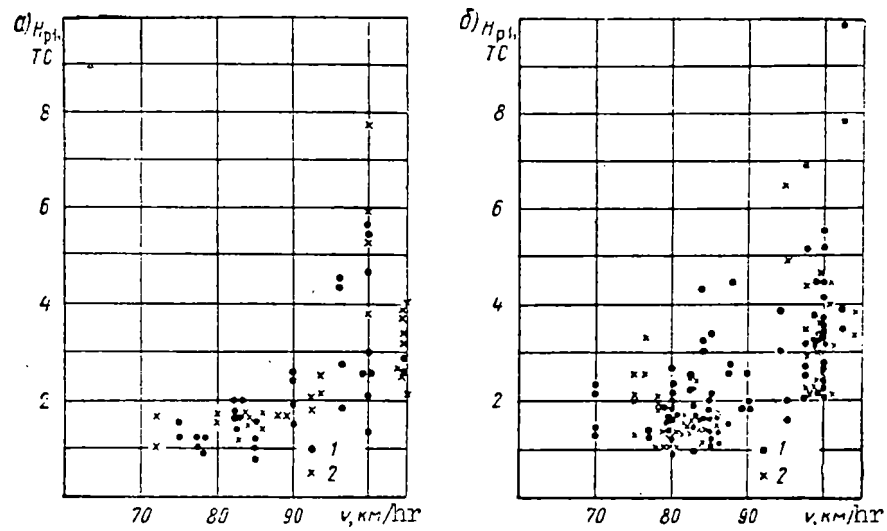

Figure 7.1. Dependence of the maximum values of the frame forces on the speed of a four-axle gondola on the MT-50 trucks (the Kirov-Yar section): a--straight sections of the tracks; b--curves; 1--first trip; 2--second trip.

The largest frame forces obtained in various segments of the experimental section of track are presented on the point graphs (see Figure 7.1). The lower boundary of the points pertains to the sections with different maintenance of the track, and the upper, to sections having deviations in the trueing of the track close with respect to the point estimate to satisfactory.

From the graphs it is obvious that for the sections with a good track condition, increasing the velocity leads to insignificant growth of the maximum forces. With an increase in velocity by 20 km/hr the maximum frame forces increase in these sections from 1.0 to 2.0 tons. The level of the largest frame forces itself in the sections of the track with good condition is

extraordinarily low even for cars on trucks having unsatisfactory running characteristics.

The dispersion of the points for constant feed characterizes the difference in the segments of the track with respect to maintenance. This dispersion of the maximum forces is especially significant for a speed of 100 km/hr and it fluctuates from 2.0 to 5.0 tons. Thus, the technical state of the track exceeds the effect of the increase in speed by several times. The nature of variation of the amplitudes of the frame forces during the process of movement indicates that significant amplitudes of the forces appear not in connection with their continuous buildup as a result of intense wobbling, but as a result of the effect of single unevennesses, which leads to single surges of amplitudes.

In order to estimate the probability of the appearance of the highest forces, a study was made of the statistical laws characterizing the overall level of loading of the undercarriages by horizontal forces (Figure 7.2, 7.3).

From the graphs of the statistical distributions of the set of amplitudes of the frame forces H_p it is also obvious that the four-axle car on the MT-50 trucks is more sensitive to the presence on the track of individual unevennesses than to the increase in speed. This follows from the nature of variation of the modal values of $\overline{H}_p$ and the standard deviations (see Figure 7.3). Thus, the modal values of the amplitudes of the frame forces reflecting the mean static level of the dynamic interaction vary with an increase in speed insignificantly. For example, for v = 80 km/hr, $\overline{H}_p$ = 0.64 ton, and for

v = 100 km/hr, $\bar{H}_p$ = 1.0 tons at the same time as the maximum values of the frame forces determined by the standard deviation which depends on the variation of the conditions of interaction differ highly significantly. Thus, the 99.5 percent quantile of the investigated force distributions in the speed range of 80-100 km/hr is distinguished by approximately 2.0 tons. For the forces having recurrence of less than 0.2 percent, this difference is 3.0 tons or more. The low order of the modal values of the frame forces indicates the weak effect of the speed. However, with an increase in speed as a result of more intense wobbling motion of the car, the probability that the wheel pair will encounter an unevenness in the track increases which is caused by an increase in the deviation from the modal values.

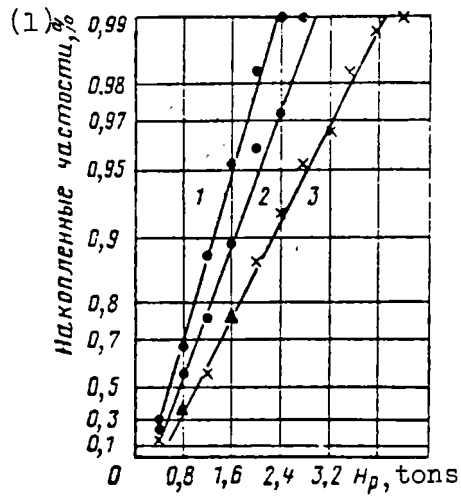

Figure 7.2. Amplitude distribution of the frame forces acting on the front wheel pair of the MT-50 truck with standard spring complex (Yar-Kirov): 1--v = 76-85 km/hr; 2--v = 86-95 km/hr; 3--v = 96-105 km/hr.

Key: 1. Accumulated frequencies, %

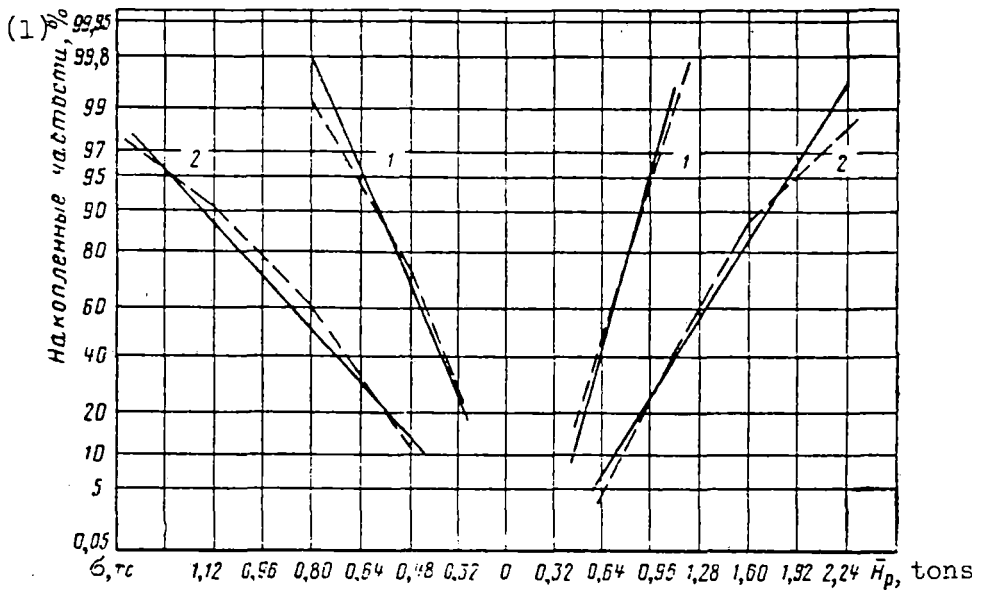

Figure 7.3. Distribution of the mean $\bar{H}_p$ and mean square deviations σ of the frame forces acting on the lateral frames of the MT-50 truck (Kirov-Yar): 1--v = 80 km/hr; 2--v = 100 km/hr; the dotted lines are the experimental curves and the solid lines, the theoretical curves.

Analogous results were obtained in the sections with excellent and good condition of the track (Omsk-Inskaya of the Western Siberian railroad), where increasing the speed to 100 km/hr did not lead to a noticeable increase in either the modal or the maximum values of the frame forces.

A study of the distribution law of the amplitudes of the frame forces indicates that approximately 95 percent of all of the amplitudes are quite close to a normal distribution law. The amplitudes of H_p, the values of which lie above approximately 35 percent quantile agree with the exponential distribution law quite well.

Testing the hypothesis of normal distribution of the mean and standard deviations of the amplitudes of the frame forces by the Pearson criterion demonstrated that the normal law quite closely describes the investigated empirical distributions.

As a result of the analysis performed for the four-axle cars on the MT-50 trucks, the following statistical distribution parameters were obtained for speeds of 80 and 100 km/hr:

Speed, km/hr	80	100
Mean value of the frame force $\overline{H}_p$, tons	0.663	1.198
Standard deviation of the mean values of the frame force $\sigma\overline{H}_p$, tons	0.170	0.381
Mean standard deviation of the general set of amplitudes of the frame forces $\overline{\sigma}$, tons	0.404	0.780
Standard deviation from the mean values $\overline{\sigma}_{\overline{\sigma}}$, tons	0.133	0.299

In accordance with the presented parameters, the calculated probability maximum frame force, for example, for v = 100 km/hr will be

$$H_p^{max} = \overline{H}_p^{max} + 3\sigma^{max} = 7.3 \text{ tons.}$$

The calculated value of H_p^{max} that was obtained agrees well with the maximum probable values measured in the experiments. The unit extremal frame forces equal to 8.0 and 9.6 tons (not repeating in other trips) obviously were obtained on the track unevennesses which, in turn, are not embedded in

the statistical distribution law of the unevennesses of the section of track from Kirov to Yar. It is possible that with respect to the point description, these unevennesses corresponded to the "unsatisfactory" condition of the track requiring a speed limit, which was not checked out during the process of the experiment.

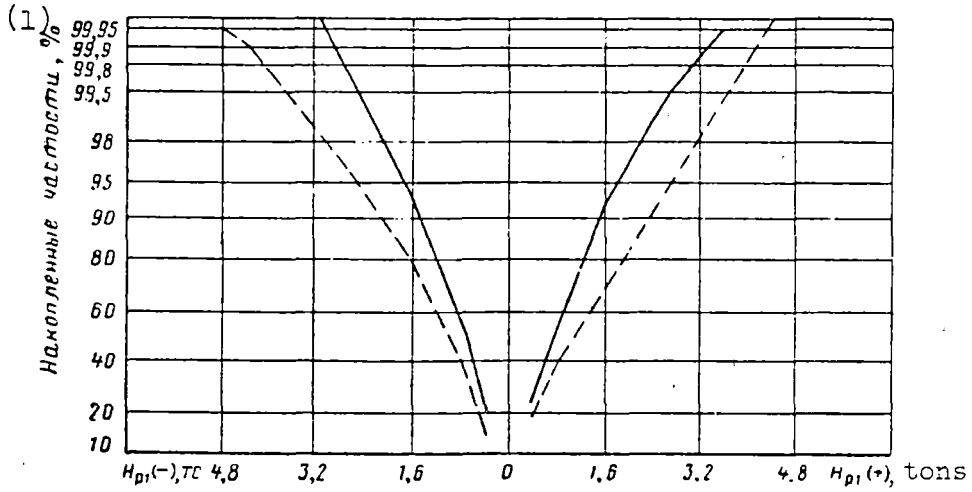

Figure 7.4. Amplitude distribution of the frame forces for the four-axle gondolas on the TsNII-Kh3-0 trucks (Kirov-Yar): solid curve v = 80 km/hr; dotted curve v = 100 km/hr.

Key: 1. Accumulated frequencies, %

7.2. Four-Axle Gondola on the TsNII-Kh3-0 Trucks

The quantile diagrams of the statistical distributions of the amplitudes of the frame courses for the four-axle gondola on the TsNII-Kh3-0 trucks are shown in Figure 7.4.

The freight cars on trucks of this type, as a result of the high degree of connectedness of the truck frame in plan view and the presence of damping of the lateral vibrations react more weakly to the increase in speed and

to the unevennesses in the plan view than the cars on the MT-50 trucks. This was exhibited in significantly smaller standard deviations from the mean amplitudes of the frame forces and the mean values of the amplitude dispersion.

It is of interest that the mean values of the frame forces and the dispersion are very close for the four-axle cars on trucks that differ so much with respect to structural design. For speeds to 80 km/hr, the cars on the MT-50 trucks has smaller mean indices by approximately 15-20 percent, and at a speed of 100 km/hr these indices are approximately 5 percent lower for the car on the TsNII-Kh3-0 trucks. This agrees with the existing concepts of the effect of the frictional forces in the spring suspension system on the dynamic processes. In the case of insignificant disturbances the frictional forces raised the level of the forces, and for strong perturbations, they decreased them, absorbing the excess energy.

The analysis of the amplitude distribution of the frame forces acting on the side frames of the TsNII-Kh3-0 trucks demonstrated that they are close to a normal law. The testing of the distribution of the mean and standard deviations of the frame forces by the Pearson criterion confirmed the closeness of the empirical distributions to the normal law.

On the basis of the data obtained for the four-axle cars on the TsNII-Kh3-0 trucks, the statistical distribution parameters of the amplitudes of the frame forces have the following values:

Speed, km/hr	80	100
Mean value of the frame force $\overline{H}_p$, tons	0.791	1.144
Standard deviation of the mean values of the frame force $\sigma\overline{H}_p$ tons	0.187	0.263
Mean standard deviation of the general set of amplitudes of the frame forces $\overline{\sigma}$, tons	0.488	0.706
Standard deviation from the mean values $\overline{\sigma}_{\overline{\sigma}}$, tons	0.096	0.152

Thus, the calculated probable value of the maximum frame force, for example, for v = 100 km/hr will be

$$H_p^{max} = \overline{H}_p^{max} + 3\sigma^{max} = 5{,}42 \text{ tons},$$

which agrees entirely with the results of numerous tests.

7.3. Eight-Axle Cars

On the eight-axle gondola, the horizontal (frame) forces were measured for the front four-axle truck: for the first H_{p_1}, for the second H_{p_2} and the fourth H_{p_4} wheel pairs, with respect to the direction of travel.

The statistical amplitude distributions of the frame forces with respect to all the axles are similar to each other. The general level of the frame forces of the eight-axle gondola at speeds to 100 km/hr is low: the greatest of the maximum values is 3.4 and 3.6 tons. The quantile amplitude distribution diagrams of the frame forces acting on the first wheel pair are presented in Figure 7.5.

An analysis of the quantile diagrams of the amplitude distributions of the frame forces for the eight-axle gondola and the eight-axle tank cars demonstrated that the repetition frequency of the single values of the frame forces for the eight-axle tank car is somewhat higher than for the eight-axle gondola, but the overall level of the maximum forces is in practice identical for them.

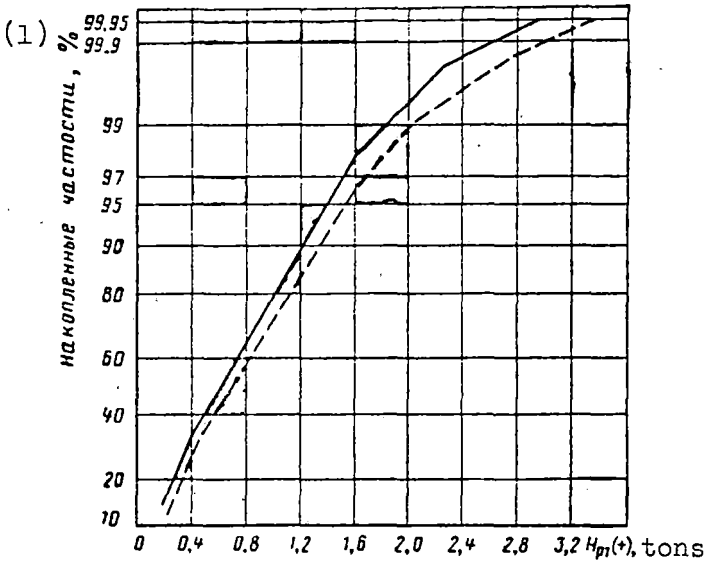

Figure 7.5. Amplitude distribution of the frame forces acting on the first wheel pair of the eight-axle gondola with respect to the direction of travel. The notation is the same as in Figure 7.4.

Key: 1. Accumulated frequencies, %

In order to obtain the statistical amplitude distribution characteristics of the frame forces, the distributions of the mean and standard deviations were constructed, and the theoretical frequencies of the values of these variables were defined. The test with respect to the Pearson criterion demonstrated that there are grounds for talking about the normal distribution

of the values of the frame forces.

Accordingly, for the eight-axle cars, the following statistical distribution parameters of the frame forces were obtained:

Speed, km/hr	80	100
Mean value of the frame force $\bar{H}_p$, tons	0.46	0.58
Standard deviation of the mean values of the frame force $\sigma\bar{H}_p$, tons	0.12	0.15
Mean standard deviation of the general set of amplitudes of the frame forces $\bar{\sigma}$, tons	0.34	0.41
Standard deviation from the mean values $\sigma_{\bar{\sigma}}$, tons	0.10	0.12

With respect to these parameters the calculated probable maximum frame force, for example, for v = 100 km/hr will be

$$H_p^{max} = \bar{H}_p^{max} + 3\sigma^{max} = 3{,}25 \text{ tons},$$

which agrees quite well with the statistical distributions obtained. The comparisons of the parameters of the statistical distributions of the frame forces for the eight-axle and four-axle cars on the TsNII-Kh3-0 trucks indicates that the mean values of these parameters are approximately 4 percent lower for the eight-axle railroad cars. The standard deviations from the mean values of the parameters differ little for the two types of cars and have very small values, which indicates the weak reaction of these cars to the unevennesses of the track in plan view.

The parameters obtained for the statistical distributions of the amplitudes of the frame forces permit reliable and objective information of the effect of an increase in speed on the growth of the frame forces depending on the type of undercarriages. For example, for a speed of 100 km/hr by comparison with 80 km/hr all the statistical characteristics increase: for the car on the MT-50 trucks, approximately double; for the car on the TsNII-Kh3-0 trucks, an increase by 1.5 times; and for the eight-axle car, 1.2-1.25 times.

Chapter VIII. Dynamic Forces Acting on the Wheels and Axles of the Wheel Pairs of Freight Cars

8.1. Vertical Dynamic Forces Acting on the Wheels of Freight Cars

The application of the tensometric wheel pair made it possible to obtain broad data on the loading of the wheels of freight cars by vertical forces measured directly by the deformations of the wheel webs. It was discovered that the vertical forces acting on the wheels of the freight cars vary within significantly greater limits than the forces acting on the side frames of the trucks. This is explained by the effect of the inertial loads and the effect of the frame forces causing additional overloads of the wheels.

Figure 8.1 shows the quantile distribution diagrams of the vertical dynamic forces acting on the wheel of an eight-axle gondola obtained for trips in the section from Yar to Kirov. In Table 8.1 the values are presented for the mean, mean square and maximum loads obtained in operation and on trips with increased speeds. The range of variation of the vertical dynamic forces R is on the average 4-25 tons for all sections.

The analysis of the data obtained indicates that the distributions of the instantaneous values of the vertical dynamic forces R are close to the normal law, although for the four-axle freight cars, the speeds of which exceed 80 km/hr, the deviations from the normal law increase. Thus, the mean square deviations of the vertical dynamic forces R from the mean value increase from 1.7 tons at a speed of 80 km/hr to 2.8 tons at a speed of 110 km/hr.

Table 8.1

Вагон (1)	Участок (2)	Величина (3)	(4) Скорость движения, км/ч 40	50	60	70	80	90	100	110
(5) Четырехосная цистерна ЦНИИ-Х3-О	Инская—Омск	R_{max}	—	—	—	17	18	23	24	24
(6) Четырехосная цистерна МТ-50	То же	R_{max}	—	—	—	14	23	25	24	—
(7) Четырехосный полувагон ЦНИИ-Х3-О	Киров—Яр	$\overline{R}$	—	—	—	—	11,5	11,6	11,7	11,4
		σ	—	—	—	—	1,7	2,43	2,75	2,80
		R_{max}	—	—	—	—	—	22	24	19
(8) Четырехосный полувагон ЦНИИ-Х3-О	Эксплуатационный участок Киров—Москва	$\overline{R}$	10,4	10,9	10,8	11,1	11,5	—	—	—
		σ	1,2	1,4	1,5	1,65	1,7	—	—	—
		R_{max}	14	16	17	17	18	—	—	—
(9) Восьмиосная цистерна	Киров—Яр	R_{max}	—	—	18,5	18,5	19	20	21,5	—
	Эксплуатационный участок Москва—Челябинск	$\overline{R}$	11,6	11,9	12	11,9	12	—	—	—
		σ	1,55	1,67	1,9	1,87	1,9	—	—	—
		R_{max}	—	—	17,5	22,5	22,5	—	—	—
(10) Восьмиосный полувагон	Киров—Яр	$\overline{R}$	8,8	9,0	9,1	9,5	9,5	9,7	10,0	—
		σ	1,0	1,1	1,1	1,3	1,4	1,5	1,5	—
		R_{max}	15	18	16	20	22	22	25	—

Key: 1. Car

2. Section

3. Value

4. Speed, km/hr

5. Four-axle tank car, TsNII-Kh3-O; Inskaya-Omsk

6. Four-axle tank car, MT-50; same

Key to Table 8.1 (continued)

7. Four-axle gondola, TsNII-Kh3-0; Kirov-Yar
8. Four-axle gondola, TsNII-Kh3-0; Operating section from Kirov to Moscow
9. Eight-axle tank car; Kirov-Yar, operating section from Moscow to Chelyabinsk
10. Eight-axle gondola; Kirov-Yar

At the same time, the increase in speed of the eight-axle gondola from 80 to 100 km/hr in practice has no effect either on the distribution parameters or on the maximum values (see Figure 8.1 and Table 8.1).

The eight-axle cars react weakly to the disturbances from the track unevennesses. The distributions R are presented in Figure 8.2 for the eight-axle gondola obtained on several trips on the Yar-Kirov section. In spite of the fact that the data were recorded on random sections of the track, the distributions R in practice coincide.

A similar distributions stability of the vertical dynamic forces R was noted also for the eight-axle tank cars. Estimating the values obtained for the vertical forces, it is necessary to note that they correspond to the conditions where there are no defects (creep, built-up metal, and so on) on the rolling surfaces of the wheels causing additional forces. In addition, as the analysis of the accelerations of the axle box assemblies of the cars has demonstrated, the sections on which the trips were made created small inertial overloads on the short unevennesses in the track. The problems of the effect of the inertial forces on the overloads of the

undercarriages of the cars were investigated in other studies and were not studied in the given case.

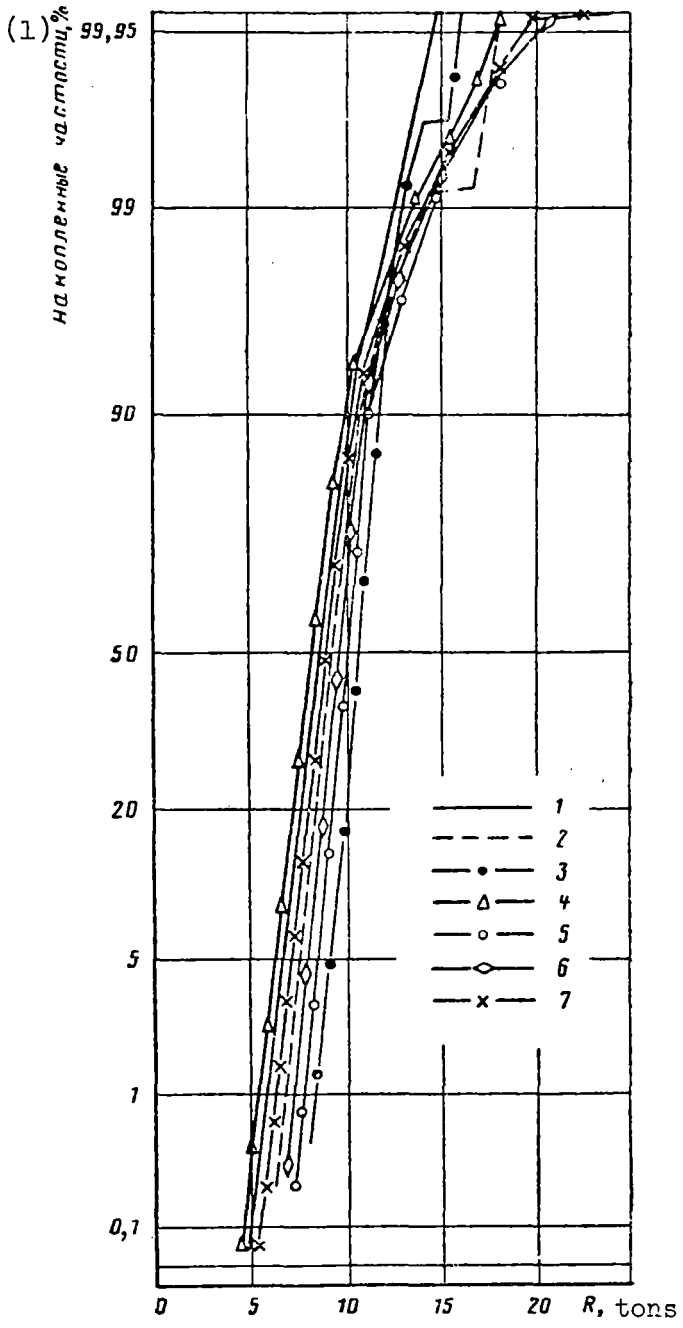

Key: 1. Accumulated frequencies, %

Figure 8.1. Quantile distribution diagrams of the vertical dynamic forces R acting on the wheel of an eight-axle gondola for various

Figure 8.1. (continued) speeds (in km/hr) in the Kirov-Yar sections: 1--v = 40, n = 279; 2--v = 50, n = 122; 3--v = 60, n = 301; 4--v = 70, n = 1,014; 5--v = 80, n = 4,365; 6--v = 90, n = 3,952; 7--v = 100, n = 7,749.

8.2. Horizontal Dynamic Forces Acting on the Webs of Railroad Car Wheels

The measurement of the horizontal dynamic forces by the deformations of the wheel webs made it possible to expand the concept of the processes occurring during interaction of the wheel with the rail to a significant degree. The qualitative analysis of the recordings of the horizontal forces D_γ demonstrated that for movement without colliding with the rail the frictional forces of spreading, directed outside the track, are in operation [6]. The reason for the appearance of these forces is the bending of the axle of the wheel pair under the effect of the vertical forces. The frame force in this case is within the limits of the frictional forces of the wheels on the rails and it is determined by their difference.

In the case where one of the wheels runs against the rail the tensometric measurement circuit on the web records the force acting inside the track. These events are defining with respect to the resistance of the wheel to derailment.

The web of the opposite wheel which rolls without colliding records a force at this time also directed inside the track. The cause for the appearance of the force in this direction is the friction between the surfaces of the colliding wheel and rail. Measuring the horizontal and vertical forces

acting on the wheel rolling without colliding simultaneously, it is possible to determine the frictional coefficients under the moving car.

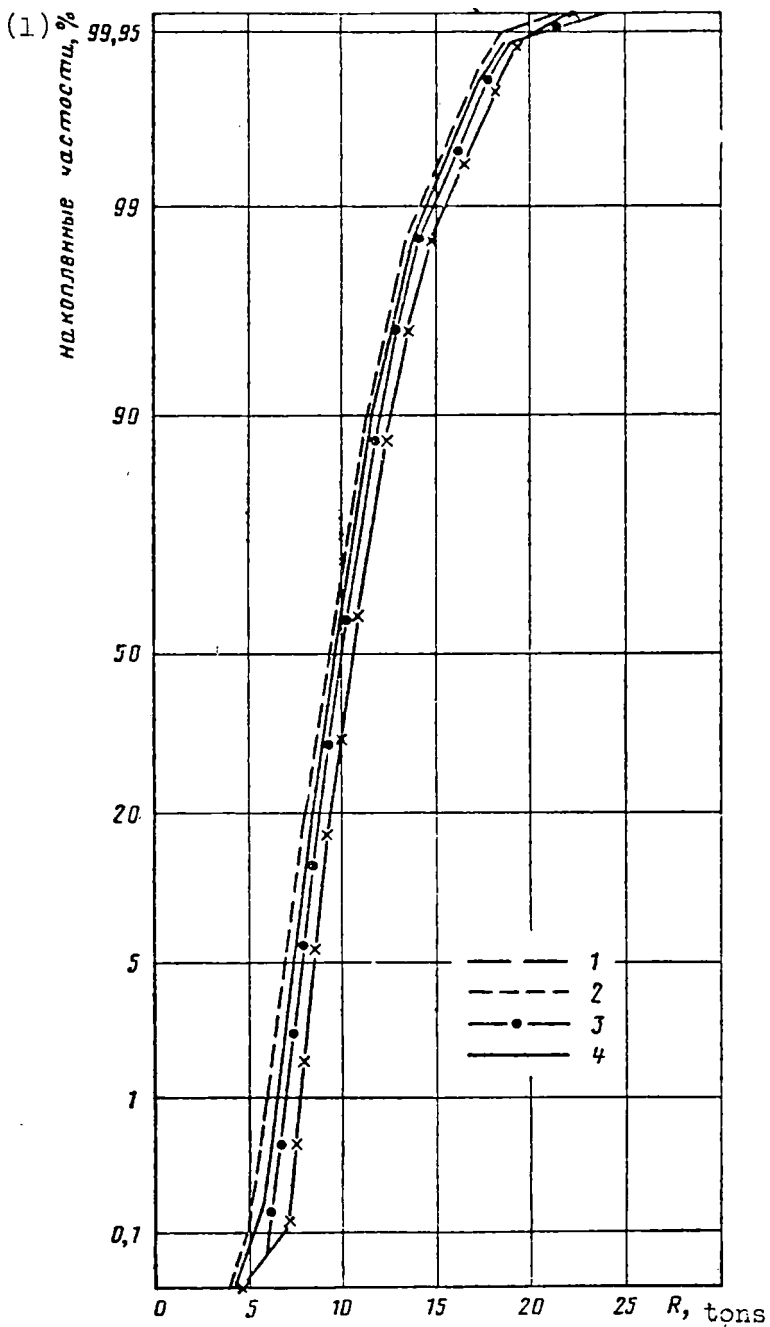

Figure 8.2. Quantile distribution diagrams (summary) of the vertical dynamic forces R acting on the wheel of an eight-axle gondola

Figure 8.2. (continued) in the Kirov-Yar section: 1--high-speed trip I, n = 16,380; 2--high-speed trip II, n = 11,084; 3--high-speed trip III, n = 9,136; 4--high-speed trip IV, n = 18,052.

Key: 1. Accumulated frequencies, %

The measurement of the horizontal forces with respect to the web deformations of the wheel pair made it possible to establish that the frictional forces of spreading do not exceed the value of $H_{friction}$ = 2.5 tons in operation. The horizontal forces acting on the wheels when colliding with the rail vary within broader limits.

In Figure 8.3 histograms are presented as an example for the distributions of the horizontal forces for the eight-axle gondola obtained on the Yar-Kirov section. The maximum values of the indicated forces obtained for various trips in all the tested cars are presented in Table 8.2. The distribution parameters are also presented here for the eight-axle gondola.

The analysis of the data obtained indicates that the distribution law of the instantaneous values of the horizontal forces is close to normal. Therefore the values of the forces considering the probability of their repetition can be determined by two parameters: the mean and mean square.

The comparison of the horizontal forces obtained in the different sections demonstrated that the least values were recorded on the Omsk-Inskaya section (see Table 8.2). Thus, even for the four-axle tank car on the MT-50 trucks the greatest value at a speed of 100 km/hr did not exceed 5 tons.

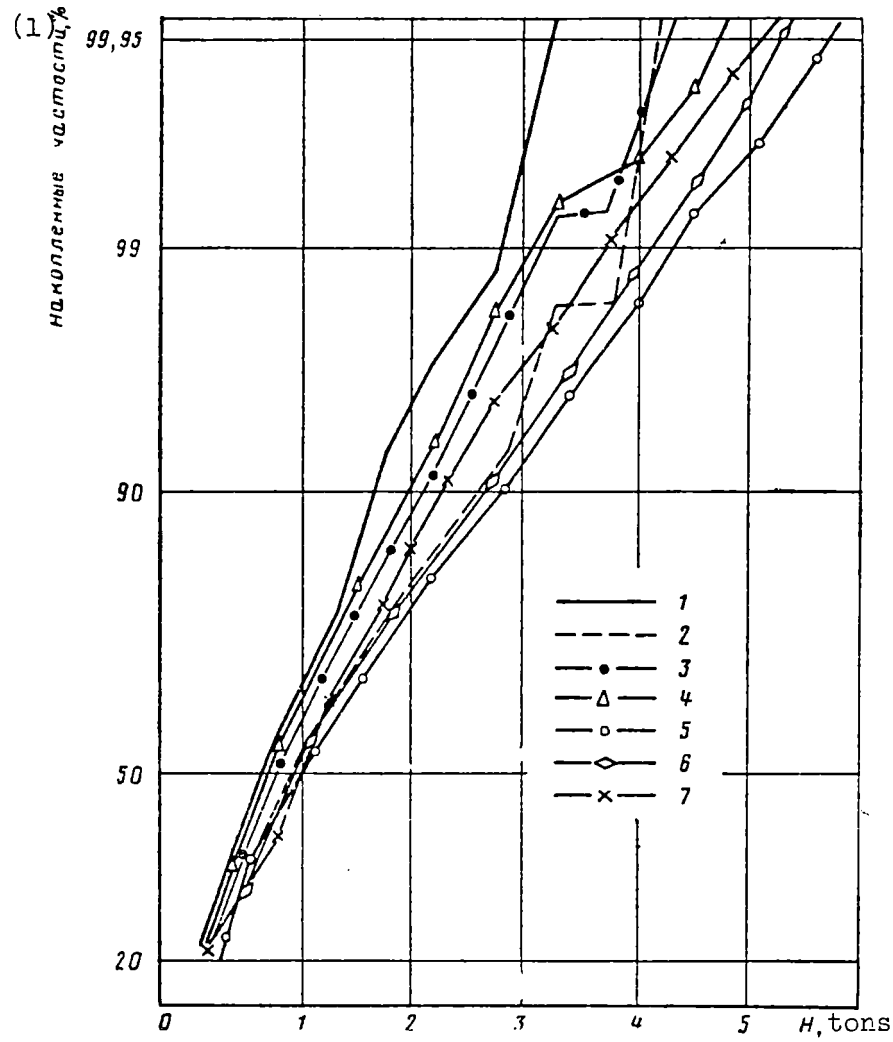

Figure 8.3. Quantile distribution diagrams of the horizontal dynamic forces H acting on the wheel of the eight-axle gondola at various speeds (in km/hr) on the Kirov-Yar section: 1--v = 40, n = 141, 2--v = 50, n = 57; 3--v = 60, n = 155; 4--v = 70, n = 480; 5--v = 80, n = 2,495; 6--v = 90, n = 2,146; 7--v = 100, n = 3,754.

Key: 1. Accumulated frequencies, %

Table 8.2

Вагон (1)	Участок (2)	Величина (3)	(4) Скорость движения, км/ч 40	50	60	70	80	90	100	110
(5) Четырехосная цистерна ЦНИИ-Х3-О	Омск—Инская	H_{max}	—	—	—	—	2,8	3,1	4,3	3,8
(6) Четырехосная цистерна МТ-50	То же	H_{max}	—	—	1,8	1,8	3,6	4,7	4,8	—
(7) Четырехосный полувагон ЦНИИ-Х3-О	Киров—Москва	H_{max}	—	2,4	3,9	3,7 (4,4)	3,2	—	—	—
(8) Восьмиосная цистерна	Москва—Челябинск	H_{max}	3,8	4,8	4,8	4,5	—	—	—	—
(9) Восьмиосный полувагон	Яр—Киров	$\overline{H}$	0,7	0,95	0,7	0,7	0,95	1,0	1,0	—
		σ	0,75	1,2	1,0	1,0	1,3	1,25	1,15	—
		H_{max}	3,2	4,2	4,2	4,8	5,9	5,3	5,3	—

Key: 1. Car

2. Section

3. Value

4. Speed, km/hr

5. Four-axle tank car, TsNII-Kh3-O; Omsk-Inskaya

6. Four-axle tank car, MT-50; same

7. Four-axle gondola, TsNII-Kh3-O; Kirov-Moscow

8. Eight-axle tank car; Moscow-Chelyabinsk

9. Eight-axle gondola; Yar-Kirov

It is necessary to note some difference in the nature and values of the horizontal forces acting on the wheels of the four-axle and the eight-axle railroad cars: a) out of the entire set of measured values of the horizontal forces, the forces acting inside the rails (corresponding to the collision of the wheels with the rail) for the four-axle car amount to about 20

percent, and for the eight-axle car, about 45 percent; b) with respect to absolute value the lateral forces for the four-axle car are somewhat lower than for the eight-axle car (by approximately 0.75 ton).

The inverse relation is noted for the frame forces: this force is somewhat larger for the four-axle cars.

8.3. Dynamic Overloads of the Axles

The axle of the wheel pair is one of the most responsible elements of the undercarriages of the railroad car. It operates under complex force and stress conditions. On the axle two characteristic zones for taking the external loads are noted: the overhanging sections and the midsection. In the former the bending stresses occur under the effect of the application of vertical forces to the journals. In the midsections the stresses arise, also, from the lateral forces applied to the wheels at the points of their contact with the rails. Therefore, in all the experiments the bending deformations of the axle of the dynamometric wheel pair were recorded in the sections before the hubs and after the hubs. The loading in each cross section was characterized by the dynamic overload coefficient k_d, that is, the ratio of the dynamic amplitude of the bending deformation to the static amplitude occurring on slow rolling of the car in the straight section of the track.

The most detailed study was made of the deformations of the axles of the four-axle gondola in 1969 on the Chelyabinsk-Inskaya section and the eight-axle gondola, in 1973, on the Kirov-Yar section of Gor'kiy railroad and

Lavochnaya-Volovets section of L'vov railroad. The quantile distribution diagrams of the coefficients k_d were constructed by the processing results.

Comprehensive studies were previously made of the dynamic overloads of the railroad car axles which in 1968 were completed by developing a new method of strength calculations of them [22]. Therefore the primary problem in the present study consisted in comparing the results obtained with the calculated values. This permits confirmation of the correctness of the force regimes adopted in the calculation and at the same time discovery of the operating conditions of the axles which were not taken into account in the calculation.

The analysis of the data obtained demonstrated the following: a) the overloads of the overhanging sections of the axles of the four-axle and eight-axle cars on the TsNII-Kh3-0 trucks depend weakly on the variation of the speed within the limits of 70-100 km/hr. The nature of the distributions of the coefficients k_{dsh} in practice is not influenced by the direction of motion of the car. With respect to its value, on both types of cars the coefficients k_{dsh} are practically identical. The maximum values of $k_{dsh\ max}$ in both cases reached values of 2.0; b) the overloads of the parts of the axle beyond the hub are appreciably higher than the overloads of the cantilevered parts, especially where the wheel pair is the head-on pair in the car (that is, the first or third in the direction of motion). The coefficients k_{dzch} for the eight-axle gondola in the Kirov-Yar section turned out to be less than the coefficients for the four-axle gondola obtained previously [4], but somewhat larger than in the 1969 tests. On the average they

must be considered in practice identical; c) at the Lavochnaya-Volovets pass during the descent in the 1973 tests, quantile diagrams were obtained for the distributions of the overload coefficients of the axle of the eight-axle gondola differing sharply from the ordinary ones (Figure 8.4). As a rule, the recurrence rate of the overload coefficients $k_d = 1.0$ (that is, the static load) is within the limits of 50-60 percent, and in the given case its quantile is shifted by 90 percent. The reason for this is the presence of a large number of small-radius curves in this section and the application of recovery when braking the freight trains on the extended downslopes. The compressive forces in the train cause the appearance of significant lateral forces and, as a consequence, overloads of the cross sections of the axles beyond the hub. The effect of these factors was felt in the sharp increase in overload coefficients k_{zdch} of the part of the axle beyond the hub. The largest value of these coefficients was reached at $k_{dzch} = 3.6$. This corresponds to bending stresses of $\sigma = 1{,}200$ kg-force/cm^2, which approaches the fatigue limit of the rolled axle ($\sigma_{-1} = 1{,}300$ kg-force/cm^2). The values of such large overloads of the part of the axle beyond the hub agreed completely with the large lateral forces measured on this section by the wheel webs. A comparison of the data obtained with the calculated values is shown in Figure 8.5. The calculated curve 2 corresponds to the amplitude distribution for the admissible margin of strength and equals 2.0 [22], the curve 2' corresponds to the analogous distribution of the amplitudes for the level of calculated accelerations of the axle box assembly decreased by two times. In our experiments, on the rolling surfaces of the tensometric wheel pair there were no defects. In the calculation it

was proposed that there are unevennesses on the rails and the wheels, and they cause identical accelerations. Therefore, the curves obtained in our experiments must be compared with curve 2'.

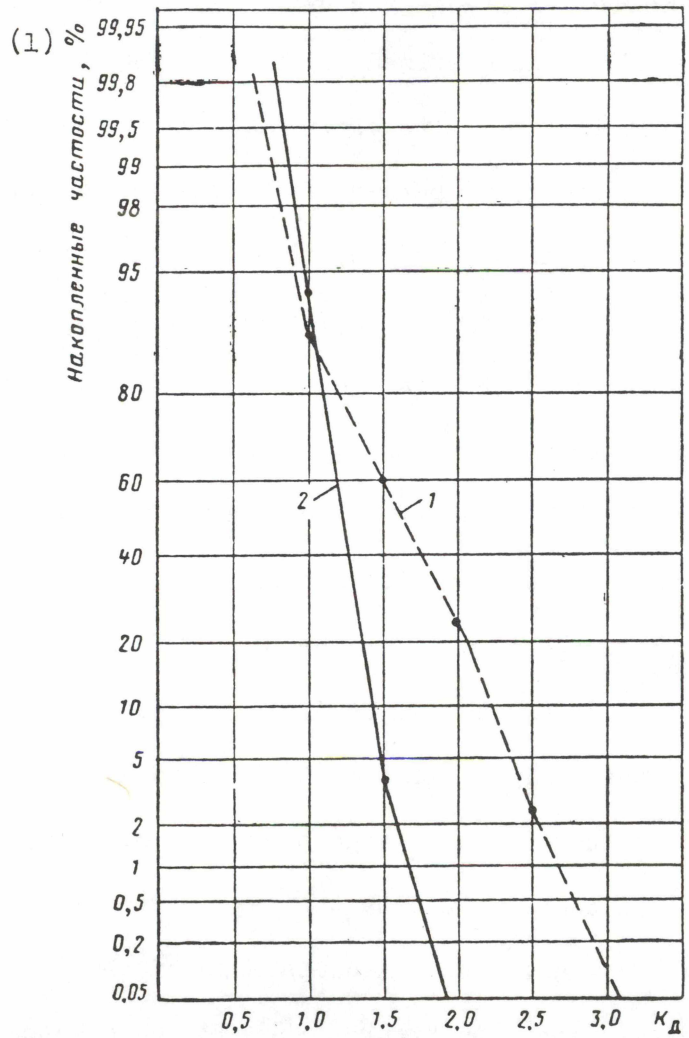

Figure 8.4. Quantile distribution diagrams of the overload coefficients of the axle of the eight-axle gondola on Lavochnaya-Volovets pass of the L'vov railroad: 1--k_{dzch}; 2--k_{dsh}.

Key: 1. Accumulated frequencies, %

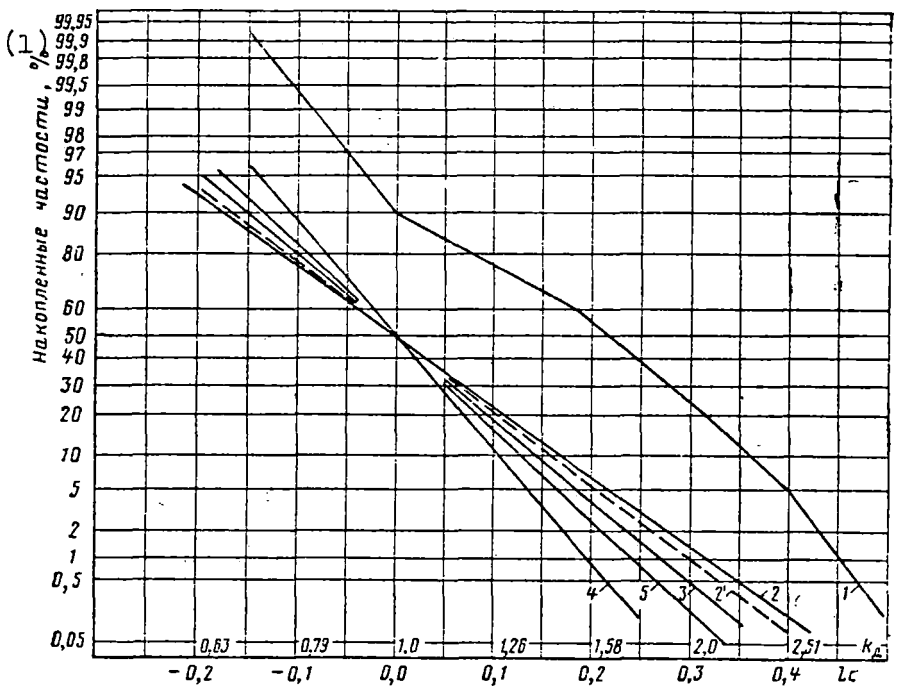

Figure 8.5. Quantile distribution diagrams of the overload coefficients of the axles: 1--eight-axle gondola, Lavochnaya-Volovets pass, 1973; 2--calculation for n = 2; 2'--calculation for diminished accelerations; 3--calculation for a speed of v = 80 km/hr; 4--Chelyabinsk-Inskaya, 1969; 5--Kirov-Yar, 1973.

Key: 1. Accumulated frequencies, %

The calculated curve 3 was obtained for a speed of the car of v = 80 km/hr.

The curves 1, 4 and 5 are the experimental quantile diagrams of the amplitude distributions of the overload coefficients of the axle cross sections beyond the hubs. The analysis of Figure 8.5 indicates that the experimental curves 4 and 5 are located below the calculated curves 2' and 3, which indicates the substantiation of the stress regimes of the axles adopted in

the calculation.

At the same time the experimental curve 1 runs appreciably above the calculated values.

The results of the experiments demonstrated the necessity for deeper study of the conditions of movement of the railroad cars in the mountainous sections of the railroads with small-radius curves.

The cars in the general network traffic get into these sections rarely. Therefore the proportion of increased overloads of the axles in the total number of loading cycles is low, and these overloads are not dangerous if we consider the available reserve (see Figure 8.5). However, if the car is designed for constant traffic in such a section or it circulates in a closed line where such a section exists, this must be taken into account and the minimum admissible diameter of the parts of the axles under the hubs must be increased.

Chapter IX. Ratio of the Vertical and Horizontal Forces Operating on the Undercarriages of Freight Cars

9.1. Regression Analysis of the Vertical and Horizontal Forces Acting on the Undercarriages of Freight Cars

The force regime of the loading of the lateral frames of the trucks of freight cars is determined by many factors. During movement of the car over an actual track the side frames of the trucks are subjected to the effects of horizontal and vertical forces, the appearance of which is caused by the interaction of the wheels with the rails and the horizontal and vertical vibrations of the body on the springs. In order to estimate the interrelation of these forces theoretically it is necessary to investigate the mechanical system having 15° of freedom.

When performing the dynamic tests of the freight cars usually the horizontal (frame) forces of interaction of the side frames of the truck with the wheel pairs (H_p) and the coefficients of vertical dynamic loading of the side frames (k_d) are recorded. These processes occur simultaneously and determine the complex force regime of the loading of the side frames.

The analysis indicates that on movement of the car the effect of the frame forces is usually accompanied by an additional vertical overload of the side frame of the truck in the direction of which the frame force is directed and the partial unloading of the opposite side frame. This indicates the presence of oscillations of the lateral rolling and the lateral deviation of the body which create additional overloads of the spring complexes and, consequently, the truck frame.

In addition, under the effect of various factors the body also has other forms of oscillations, of which the oscillations of hopping and galloping also create additional vertical overloads on the side frames which usually are not connected with the side oscillations of the car.

In its turn, this type of horizontal oscillation, as a rule, can be accompanied by the appearance of frame forces not connected with the additional vertical overloads of the side frames. Therefore, it can be expected that the relation between the vertical and horizontal forces acting on the side frames of the trucks must be most sharply exhibited in the case of predominance of the oscillations of the side rolling and the side deviation of the body of the car. The presence of the oscillations of the hopping and the galloping, in certain cases, the effect of the body determine the scattering of the points of the function $k_d(H_p)$.

What has been stated permits us to draw the conclusion of expediency of the statistical approach when estimating the relation of the experimentally measured values of the vertical and horizontal loads of the side frames of

the trucks. The simplest and most available means of this analysis at the present time is determination of the degree of correlation of two dynamic processes and calculation of the regression coefficients determining the linear dependence of the experimental values of k_d and H_p.

For this purpose, the group of experiments which is described when making high-speed trips with the eight-axle gondola and the section from Yar to Kirov was processed using the analog-to-digital complex by the program developed by the Laboratory of Automation of Experimental Data Processing.

The program provides for the possibility of input of the empirical values of two dynamic processes measured at one time to a digital computer, in the given case, the coefficients of vertical dynamics and frame forces. As a result of processing the file of values of k_d and H_p, the digital computer calculates their mean and mean square values, the empirical correlation coefficient and the linear regression coefficients.

By these data, it is possible to determine the degree of correlation of the indicators of the dynamic processes and also to obtain the expression for the linear empirical function k_d and H_p both in individual experiments and by the entire set of measured values. In Figure 1, an example of the regression line is presented for the file of experimental values of k_d and H_p measured in one of the experiments.

The analysis of the data obtained demonstrated that there is a dispersion of the centers of the distributions of the files of values of the vertical and horizontal loads on the side frames of the truck and various angles of

inclination of the regression lines. This indicates the predominance of certain types of oscillations of the body of the car during movement over a straight section of the track and around curves with different speeds. However, it does not appear possible to determine the stable laws of variation of the correlation coefficients and linear regression as a function of the plan of the track and the speed by the data from processing a limited number of experiments. Therefore, the estimate of the empirical correlation coefficient of the vertical and horizontal dynamic forces acting on the side frames of the two-axle truck of an eight-axle gondola which is in front with respect to the direction of motion was performed for the entire file of measured values (N ≈ 10,000) independently of the sections of track and the speed.

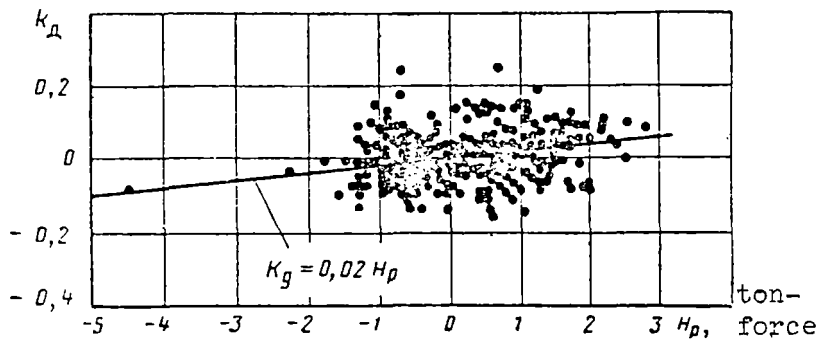

Figure 9.1. Regression line $k_d(H_p)$ and the file of experimental values of the vertical and horizontal forces acting on the side frame of the first two-axle truck of an eight-axle gondola with respect to the direction of motion (the Kirov-Yar section, the straight line v = 80 km/hr).

As a result, the following empirical correlation coefficients and the mean static linear relations for the loads on the side frames of the truck were obtained:

a) for the right side with respect to the direction of movement r = 0.27

$$k_{d1} = 0.025\ H_p; \tag{9.1}$$

b) for the left side with respect to the direction of movement r = 0.30

$$k_{d2} = 0.035\ H_p. \tag{9.2}$$

Testing the significance of the correlation coefficients obtained [23] indicates that it is possible with a probability of more than P = 0.999 to drop the possible proposition of noncorrelation of the values of k_d and H_p, for

$$|r|\sqrt{N-1} \approx 30 \gg H_{critical}. \tag{9.3}$$

Moreover, the correlation coefficients obtained turn out to be low, which indicates the presence of many factors influencing the dispersion of the experimental values of k_d and H_p with respect to the linear functions defined by expressions (9.1) and (9.2).

It is of great interest to study the interconnectedness of the horizontal and vertical forces acting at the contact points of the wheels with the rails, on the relation of which, in particular, the resistance of the wheel to running up on the rail head depends. The force diagram for the forces acting on the wheel pair with one of the wheels colliding with the rail is

presented in Figure 2.1.

In order to find the analytical relation of the horizontal and vertical forces acting on the colliding wheel at the point of contact with the rail, let us use the expressions obtained in Chapter II:

$$R_1 = \frac{a+2s}{2s} P_1 - \frac{a}{2s} P_2 + \frac{r_к}{2s} H_р + q_к ; \tag{9.4}$$

$$R_2 = \frac{a+2s}{2s} P_2 - \frac{a}{2s} P_1 - \frac{r_к}{2s} H_р + q_к . \tag{9.5}$$

If we consider that the vertical load on the side frame of the truck is distributed between the wheel pairs evenly, then the vertical forces acting on the journal of the wheel pair axle are defined by the expressions:

$$P_1 = \frac{1}{2}(P_{ст} + \Delta P); \tag{9.6}$$

$$P_2 = \frac{1}{2}(P_{ст} - \Delta P), \tag{9.7}$$

where $P_{СТ}$ is the static vertical load on one spring set;

ΔP is the dynamic variation of the vertical load on one spring complex.

After substitution of (9.6) and (9.7) in (9.4) and (9.5), we obtain:

$$R_1 = R_{ст} + \frac{2b}{2s} \frac{\Delta P}{2} + \frac{r_к}{2s} H_р ; \tag{9.8}$$

$$R_2 = R_{ст} - \frac{2b}{2s} \frac{\Delta P}{2} - \frac{r_к}{2s} H_р , \tag{9.9}$$

where R_{CT} is the reaction of the rail to the static load from the wheel equal to $R_{ст}=\frac{P_{ст}}{2}+q_к$; $2b=2a+2s$.

Substituting the values of 2b, 2s and r_k in (9.8) and (9.9), we obtain:

$$R_1=R_{ст}+0{,}644\Delta P+0{,}3\,H_р; \tag{9.10}$$

$$R_2=R_{ст}-0{,}644\,\Delta P-0{,}3\,H_р. \tag{9.11}$$

As weas demonstrated above, the dynamic addition of the vertical load on the side frames of the truck is a complex function of many factors and is not uniquely defined. However, the statistical approach when estimating the empirical values of k_d and H_p permits use of the methods of regression analysis to determine the simplified expressions for the dependence of these dynamic processes in the form

$$k_д=\pm a\,H_р, \tag{9.12}$$

where a is the linear regression coefficient.

Then the value of ΔP will be

$$\Delta P=k_д\,P_{ст}=a\,P_{ст}\,H_р=k\,H_р, \tag{9.13}$$

where $k = aP_{CT}$ is the constant coefficient for the given truck.

The horizontal force acting on the colliding wheel will be equal to the following considering (9.13)

$$H_1=H_р+\mu\,R_2=H_р[1-\mu(0{,}644\,k+0{,}3)]+\mu\,R_{ст}. \tag{9.14}$$

The vertical force acting from the rail on the colliding wheel, considering (9.13) is

$$R_1 = R_{ст} + (0{,}644\,k + 0{,}3)\,H_p. \qquad (9.15)$$

From (9.14), let us find the expression for the frame force and let us substitute it in (9.15). After the conversions we have

$$R_1 = \left[1 - \frac{\mu(0{,}644k + 0{,}3)}{1 - \mu(0{,}644\,k + 0{,}3)}\right] R_{ст} + \frac{0{,}644\,k + 0{,}3}{1 - \mu(0{,}644\,k + 0{,}3)}\,H_1. \qquad (9.16)$$

The expression (9.16) relates the vertical and the side forces acting on the colliding wheel at the point of its contact with the rail.

Using the results of the regression analysis of the function $k_д(H_p)$ and knowing the static load on the spring complex of the eight-axle gondola, we find k = 0.59. Taking this into account, expression (9.16) assumes the form

$$R_1 = \left(1 - \frac{0{,}68\,\mu}{1 - 0{,}68\,\mu}\right) R_{ст} + \frac{0{,}68}{1 - 0{,}68\,\mu}\,H_1. \qquad (9.17)$$

It is known that the transverse friction coefficient between the wheel and the rail has a significant effect on the values of the horizontal forces. The application of the tensometric wheel pair for measuring the horizontal and vertical forces acting simultaneously on the wheel webs permitted experimental evaluation of the friction coefficient μ under the moving cars under real conditions. In particular, such measurements were made on the experimental ring of the Central Scientific Research Institute of the Ministry of Railways in 1974 under the loaded four-axle gondola. The analysis

of the data obtained demonstrated that the friction coefficient μ varied on movement with constant speed within quite broad limits (0-0.33)

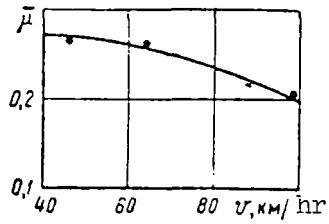

Figure 9.2. Mean value of the friction coefficient of the noncolliding wheel across the rail as a function of the speed of the railroad car.

In Figure 9.2 a graph of the variation of the mean alue of the friction coefficient when moving over the same section of track at different speeds is presented, which indicates that the friction coefficient μ essentially decreases with an increase in speed, especially for speeds about 80 km/hr.

The graphs of the function (9.17) for boundary values of the friction coefficient are presented in Figure 9.3.

It must be expected that the basic mass of the values of the lateral and vertical forces acting on the colliding wheel will be inside the interval formed by the straight lines 1 and 2.

In order to check this proposition and study the effect of speed and the nature of the track sections on the ratio of the vertical and horizontal forces a group of experiments set up for trips with the eight-axle gondola in the Kirov-Yar section were processed by the regression analysis program mentioned above.

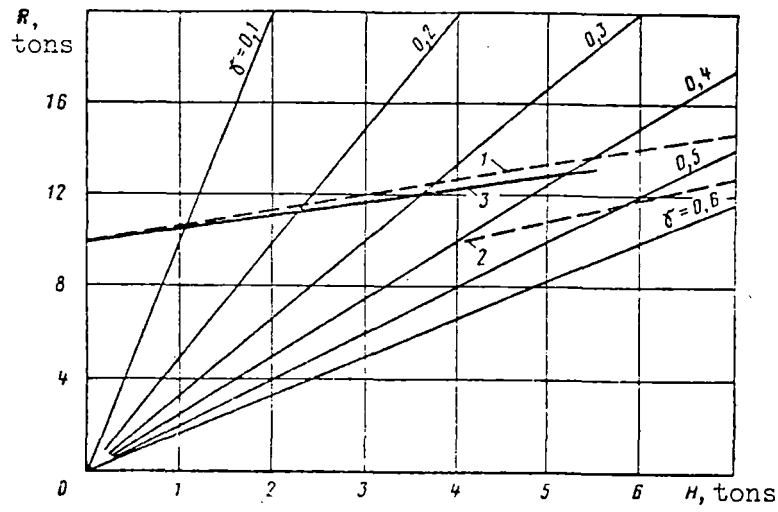

Figure 9.3. Analytical and empirical functions of the vertical and lateral forces acting on the wheel of an eight-axle gondola when it runs against the rail: 1--analytical function ($\mu = 0$); 2--the same ($\mu = 0.33$); 3--regression line $R = 9.9 + 0.67\ H$.

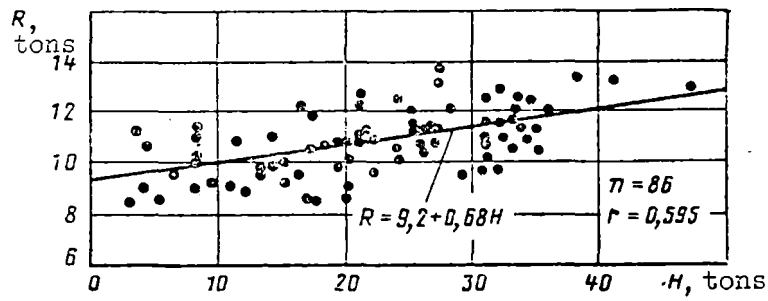

Figure 9.4. File of experimental values and regression line for the vertical and lateral forces acting on the wheel of an eight-axle gondola when it runs against the rail (Kirov-Yar section, right curve, v = 80 km/hr. The values of H (tons) must be multiplied by 10^{-1}).

As a result of the processing, the correlation coefficients and the coefficient of linear empirical regression of the vertical and horizontal forces acting on the wheel webs were obtained for speeds of 80-100 km/hr over the straight sections of track and around curves of different radius and direction. The analysis of the data obtained permits the following conclusions to be drawn:

1. The most strongly statistical relation of these variables is exhibited when moving around curved sections of the track, that is, in cases where collision of one of the wheels against the rail predominates. Under these conditions of motion, the correlation coefficients of R_{coll} and H_{coll} reached values of $r = 0.62$, which indicates the quite close relation of the vertical and lateral forces determining the margin of resistance to derailment.

2. When moving over straight sections, where both wheels alternately run against the rails, the statistical relation of the vertical and horizontal forces acting on the webs of the wheels is exhibited quite weakly ($r \approx 0.2$). This can be explained by the significant difference in the relation of the vertical forces to the horizontal forces when the wheel runs against the rail (the horizontal force is directed inside the track) and in the case where the wheel is not the colliding wheel, but the horizontal force of the same direction acts on it caused by the friction of the wheel against the rail. In the first case the correlation coefficient is positive and has a significant value; in the second case it is either close to zero or it is negative.

3. The statistical relation of the vertical and horizontal forces in practice does not depend on the speed of the eight-axle gondola.

A comparison of the straight line 3 of the averaged regression line R_H for the case of movement of the eight-axle gondola over curved sections of track with the straight lines 1 and 2 of the analytical function R(H) indicates that the results of the experimental estimate of the statistical relation of the values of these forces are close to the calculated values (see Figure 9.3).

In accordance with the graphs, with an increase in the horizontal forces the values of R_H are shifted into the zones of large coefficients γ for which the stability margin decreases.

In addition, the experimentally measured values of R and H have significant dispersion with respect to the regression line R_H (Figure 9.4). The reason for this dispersion is the vertical oscillations of hopping and galloping of the body which are not related to the horizontal forces, the effect of the friction between the rolling surfaces of the wheels and the rails and also the local unevennesses of the rails causing significant vertical inertial overloads of the wheel webs.

The scattering of the values of R_H, in particular, the significant unloading of the colliding wheel with large lateral forces can lead to a decrease in stability. However, on the whole the regression analysis of the experimental values of the vertical and lateral forces acting on the web of the wheel running against the rail indicates that the maximum values of γ which

can be expected for the most unfavorable comparisons of these forces in the speed range of 60-100 km/hr do not exceed $\gamma = 0.50-0.55$ for the eight-axle gondola. This corresponds to minimum values of the margin of stability $\eta = 2.0-1.8$.

9.2. Freight Car Derailment Coefficients

One of the basic safety criteria for the freight car traffic in operation is their resistance to derailment when the wheel runs against the rail.

By stability with respect to derailment here we mean the position of the colliding wheel with respect to the rail for which it, although it goes to a single point contact with respect to the lateral face of the flange of the wheel and the chamfer of the rail head, under the effect of dynamic forces, continuous sliding of the flange takes place until the point of contact is raised to the rolling surface of the wheel and the rail [25].

The condition of resistance to derailment in this case is not achieving the ratio of the lateral and vertical forces simultaneously acting on the colliding wheel and reduced to the contact point with the rail, the defined critical value for which the unfavorable combination of certain other factors can lead to the flange rolling up on the rail head and derailment of the train. This condition is described in the form

$$H/R < (H/R)_{critical}, \tag{9.18}$$

where H and R are the lateral pressure and the vertical force acting simultaneously on the flange of the colliding wheel from the rail.

The theoretical and experimental studies of the processes occurring when the wheel runs against the rail in the last decade in our country and abroad indicate that the critical value of this ratio is a function of such factors as the angle of inclination of the wheel flange, the frictional coefficient between the wheel and the rail, the presence and the ratio of the longitudinal and transverse sliding of the wheel, the angle of collision, the speed, and so on [13, 25].

However, in the special case of motion where the longitudinal sliding of the colliding wheel is absent, the magnitude of the ratio $(H/R)_{critical}$ has the minimum of all possible values not depending on the angle of contact of the wheel against the rail [13]:

$$(H/R)_{\text{min critical}} = \operatorname{tg}[\beta - \operatorname{arctg}(1 - 0{,}002\,v)\mu_0], \tag{9.19}$$

where β is the angle of inclination of the flange of the wheel to the surface of the rail;

v is the speed, km/hr;

μ_0 is the maximum coefficient for $v = 0$.

In Figure 9.5 the relations (9.19) are presented for the minimum critical ratio of the lateral and vertical forces as a function of the speed for several values of the friction coefficient μ_0.

The values of the ratios H/R bounded by the graph of their minimum critical value for the highest friction coefficient μ_0 under the given conditions and the x-axis are safe, and the corresponding region can be considered a

region of guaranteed stability.

Thus, if the basic purpose of the investigation is not establishment of the sufficient conditions of derailment on collision and, on the contrary, finding the conditions ensuring safety from derailment, it is expedient to limit ourselves to determining the ratio of the lateral and vertical forces acting on the colliding wheel at the point of its contact with the rail. Obviously, condition (9.18) can be considered in the sense of the sufficient condition of resistance at the wheel to derailment on collision if the value of $(H/R)_{\text{min critical}}$ is determined by the above-mentioned relation for the maximum value of the friction coefficient μ_0.

The time of effect of the forces, the ratio which is close to the critical value has no significance if it satisfies the condition 9(a), for here free sliding of the flange of the colliding wheel along the shoulder of the rail downward is ensured.

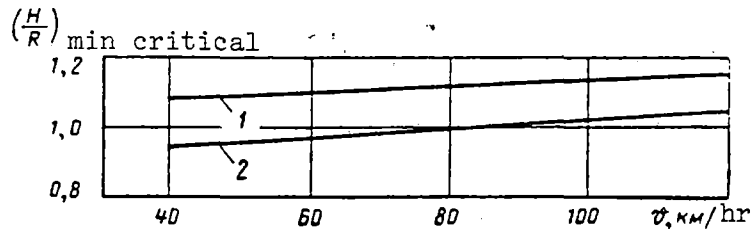

Figure 9.5. Minimum critical ratio of the lateral and vertical forces acting on the colliding wheel as a function of speed.

The estimation of the derailment coefficient of the freight cars of different types in the given study was made only by the ratio of the vertical and lateral forces acting on the wheel at the point of contact with the rail,

without considering the time of the effect of this ratio and the colliding angle.

The experiments performed in 1974 on the experimental ring of the Central Scientific Research Institute of the Ministry of Railways and also the numerous data obtained when performing dynamic tests of freight cars of different types on operating sections of the railroads within the scope of this study confirmed the recommendation made in [13] that when estimating the stability it is necessary to assume a maximum value of the friction coefficient of $\mu_0 = 0.33$. Therefore, the limiting value of the ratio H/R which guarantees safety from derailment adopted as the criterion in the given investigation is defined by the straight line 2 in Figure 9.5.

In cases where the operating conditions differ from the ordinary ones, for example, in mountainous sections with small-radius curves, where the application of sand during purely recovery braking leads to significant increase in the friction coefficient, the problem of ensuring stability of the cars with respect to derailment requires special study.

In order to estimate the stability, two different methods of measuring the horizontal and vertical forces at the points of contact of the wheels with the rails were used (see Chapter II).

In connection with the fact that the more improved method of measuring the lateral and vertical forces by the deformations of the webs of the tensometric wheel pair and determination of their relations [6] was developed in the process of the performance of this study and for a number of experimental

objects the data are missing or were obtained in limited volume, it did not appear possible to use it to estimate the stability of all types of freight cars, the loading regimes of the undercarriages of which were investigated. Therefore the stability was estimated by the method based on measuring the vertical and horizontal forces by the deformation of the truck frame [15].

After improvement of it permitting increased precision of calculating the coefficient γ equal to the ratio of the lateral load to vertical (see Chapter II), in 1974 and 1975, additional processing of the previously obtained recordings was carried out:

a) In the 1970 tests for the four-axle tank cars on the TsNII-Kh3-0 and MT-50 trucks in the Inskaya-Omsk sections.

Previously the tape recordings of the frame forces H_p and the coefficients of vertical dynamic k_d were copied from the VNIIE tape recorder to the YeMM-140 tape recorder. Here, as a result of poor quality of the recordings of H_p and k_d of the four-axle tank car No 752-4162 on the MT-50 trucks, on which on the trips in the Omsk-Inskaya section with increased speeds a tensometric wheel pair was located, analogous recordings of the other four-axle tank car on the MT-50 trucks (No 756-4078) of higher quality were processed;

b) In the 1973 tests for the eight-axle gondola in which the data were previously obtained on stability using the tensometric wheel pair.

In Table 9.1 the maximum values of the coefficients γ and their values for the accumulated recurrence rate of 99.9 percent are presented for all types of freight cars obtained by the method using the deformations of the side frames of the trucks (B), and for comparison, also by the method using the deformations of the wheel webs (D). In Figure 9.6 to 9.8, the corresponding quantile distribution diagrams of the coefficients γ are presented for the four-axle tank cars and gondolas on the TsNII-Kh3-0 and the MT-50 trucks and the eight-axle tank cars and gondolas.

The analysis of the distribution curves obtained demonstrated that the instantaneous values of the coefficients γ are subject to a logarithmically normal distribution law for all types of cars with the exception of the four-axle gondolas and tank cars on the MT-50 trucks at speeds above 80 km/hr.

For the existing level of speed (to 80 km/hr) all types of loaded freight cars have margins of stability with respect to derailment sufficient to ensure safety in all sections of the track where trips were made with the experimental objects. Here $\eta \geq 1.7$ (see Table 9.1).

It must be emphasized that, in spite of the fact that in the experiments with the operating speeds individual significant dynamic unloading of the side frames of the MT-50 trucks under the four-axle gondolas and tank cars were noted, this did not lead to a significant decrease in the margins of strength in view of the relatively low level of side forces. Nevertheless, the absolute peaks of the coefficients γ for these types of cars pertain to

the times of the greatest unloading of the colliding wheel.

A comparison of the stability of the freight cars during movement with operating speeds at different times of year (see Figure 9.6) demonstrated that the peculiarities of the loading of the undercarriages in the winter connected with increased rigidity of the track and growth of the inertial forces, do not have a significant effect on this safety index of motion.

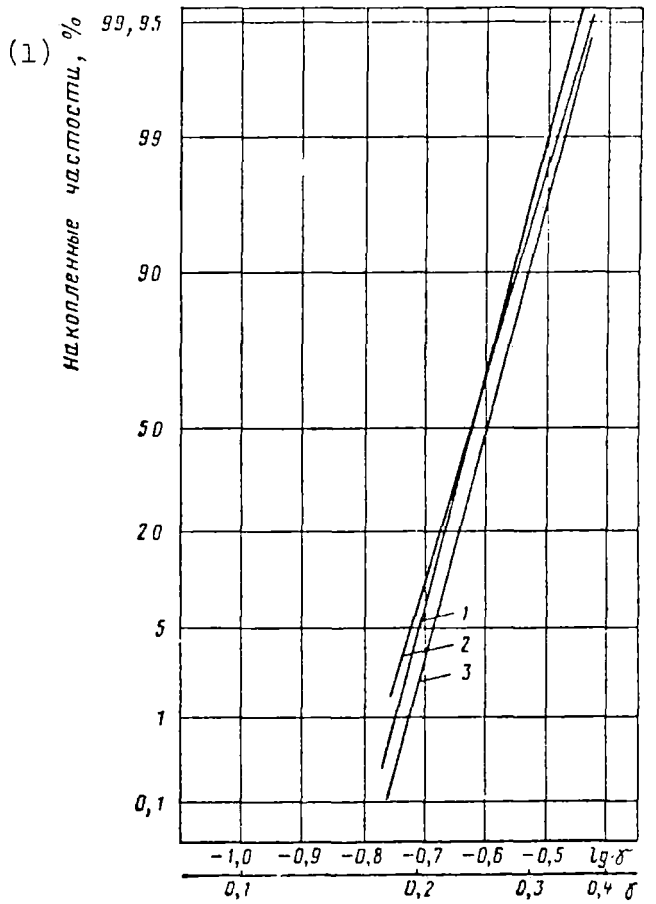

Key: 1. Accumulated frequencies, %

Figure 9.6. Quantile distribution diagrams of the coefficients γ: 1--eight-axle gondola, Moscow-L'vov, 1973; 2--eight-axle tank car, Yaroslavl'-Moscow, summer 1972; 3--eight-axle tank car, Yaroslavl'-Moscow, winter 1972.

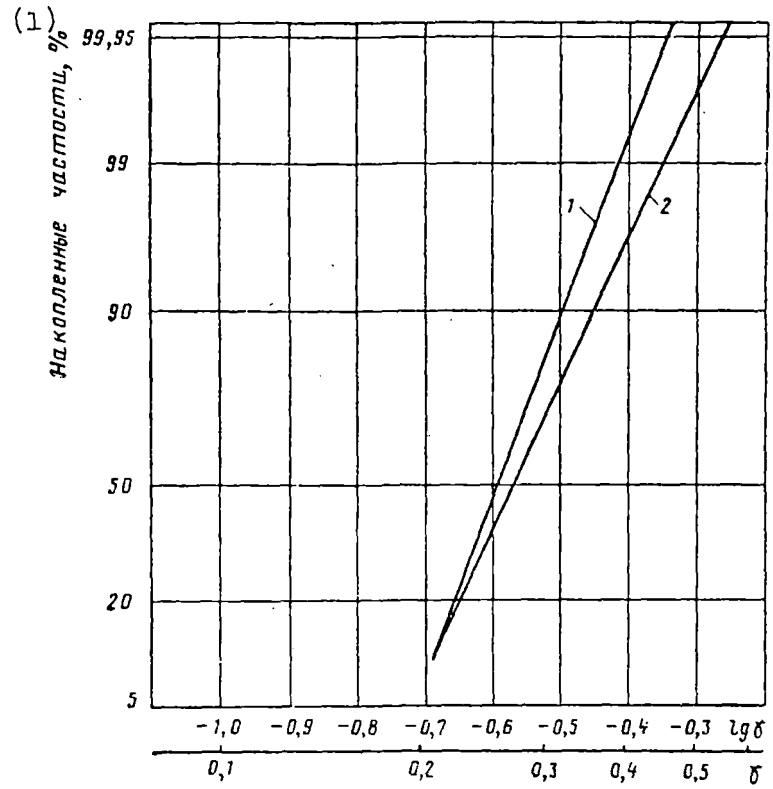

Figure 9.7. Effect of the direction of motion on the coefficients γ for a wheel pair of a four-axle gondola on TsNII-Kh3-0 trucks: 1--Kirov-Yar; 2--Yar-Kirov.

Key: 1. Accumulated frequencies, %

When moving at operating speeds, the effect of the increase in speed on the derailment coefficients is manifested weakly.

This situation can pertain to all types of tested freight cars.

The distribution curves of the coefficients γ of the four-axle gondola on the TsNII-Kh3-0 trucks when moving in the Yar-Kirov section in the forward and return directions (see Figure 9.7) indicate that the first wheel pair

in the direction of motion (oncoming) (the Yar-Kirov direction) takes the greatest horizontal dynamic forces, which is accompanied by an increase in the coefficients γ.

A comparison of the maximum values of γ measured by the deformations of the side frames and the wheel webs give good comparison of them (see Table 9.1). The data for the four-axle tank cars on the MT-50 trucks for which significant divergence of the results obtained on the Inskaya-Omsk section in the 1970 experiments is noted constitute an exception. Thus, for v = 100 km/hr, the tank car No 752-4162, by the web deformations $\gamma = 0.5$ was obtained, and for the tank car No 56-4078 by the deformations of the side frames of the truck (Figure 9.8a), $\gamma = 1.03$ was obtained.

The cause of this divergence obviously is instability of the dynamic characteristics of the railroad cars on the MT-50 trucks which leads to the fact that the different cars give sharply differing results and also that one and the same car on different trips and on different sections can give significant scattering of the data.

In the given case this divergence was also promoted by the fact that the deformations of the webs of the tensometric wheel pair in the mentioned experiments were recorded at another time and on different sections of the track than the frame forces and the coefficients of vertical dynamics, for they were in different recording groups.

Analogous divergences in the dynamic indices of the four-axle gondola on the MT-50 trucks at speeds above 85 km/hr were noted in the Yar-Kirov section

in 1973. Here, in several experiments of trip No 1 the values of the coefficient γ were recorded appreciably higher than in the other experiments and on the other trips. Therefore when estimating the dynamic qualities of the railroad cars on the MT-50 trucks connected with safety of motion, it is necessary to use the worst data, which was done when estimating the margin of resistance to derailment when the data for the first trip were taken (Figure 9.8b) in the Yar-Kirov section. In Table 9.1 the data are presented for the maximum values of the coefficient γ pertaining to this trip.

The analysis of the results of the trips with speeds of the four-axle gondola increased to 100 km/hr on the MT-50 trucks in the Yar-Kirov section with the least favorable combination of lateral and vertical forces demonstrated that for $v = 80$ km/hr, just as in the other sections at the operating speeds, this car had a margin of stability of no less than $\eta = 1.7$. With an increase in speed the margin of stability reduces. Nevertheless, for $v = 90$ km/hr, 99.9 percent of the values of the coefficients do not exceed $\gamma = 0.68$, which corresponds to a margin of stability of $\eta = 1.5$. In the individual experiments at this speed, individual cases of the appearance of maximum coefficients $\gamma = 0.95$ were noted, which corresponds to a margin of stability $\eta = 1.1$.

With a further increase in the speed to 100 km/hr the margins of stability disappear, and in order to estimate the traffic safety of this type of car it follows, in addition to the relation of the side and vertical forces, to consider the time of effect of this ratio, the angle of collision of the wheel with the rail and other factors.

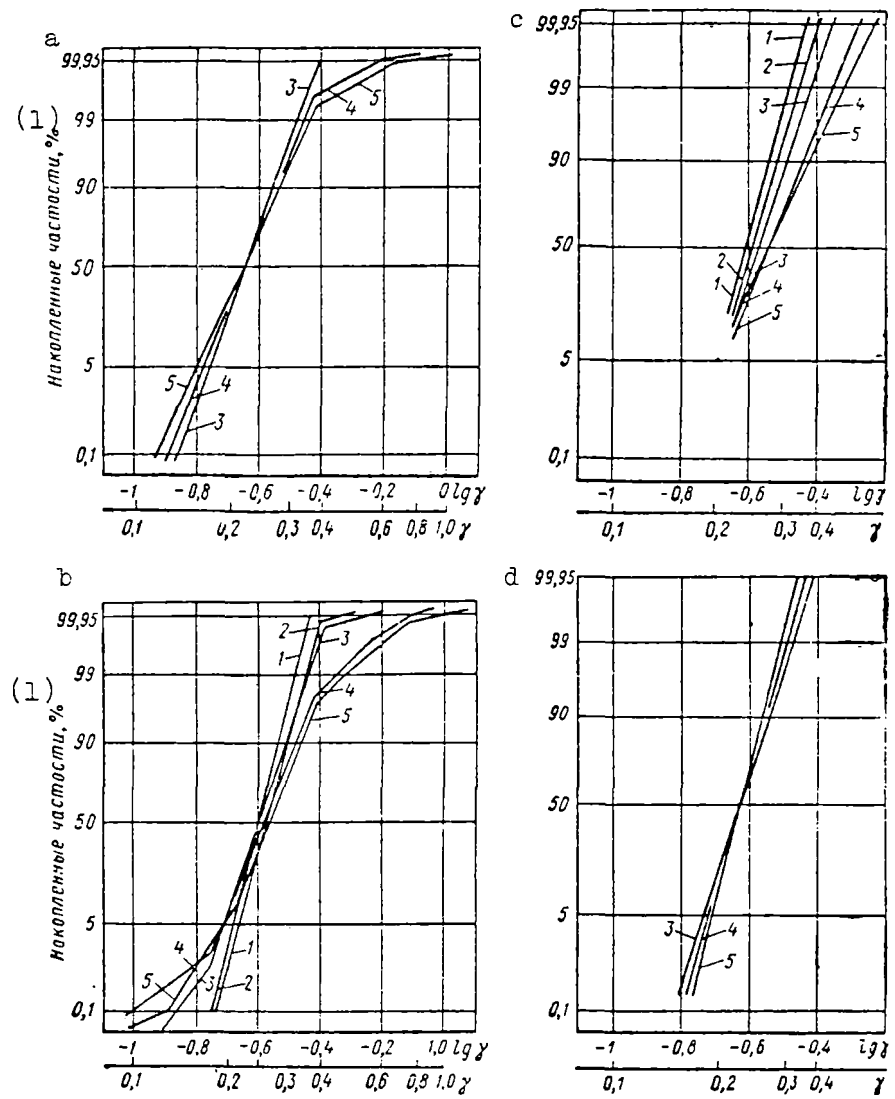

Figure 9.8. Quantile distribution diagrams of the coefficients γ at increased speeds: a--four-axle tank car on MT-50 trucks, Inskaya-Omsk, 1970; b--four-axle gondola on MT-50 trucks, Kirov-Yar, 1973; c--four-axle gondola on TsNII-Kh3-0 trucks, Kirov-Yar, 1973; d--eight-axle tank car, Kirov-Yar, 1972; 1--v = 60 km/hr; 2--v = 70; 3--v = 80; 4--v = 90; 5--v = 100 km/hr.

Key: 1. Accumulated frequencies, %

The four-axle tank cars and gondolas on the TsNII-Kh3-0 trucks have appreciably higher margins of stability. For example, for the four-axle tank car No 746-1406 in the Inskaya-Omsk section on trips at speeds of 80-120 km/hr the maximum value of the coefficient γ does not exceed 0.525 (η = 1.96).

The coefficients γ for the four-axle gondola No 676-1330 on the TsNII-Kh3-0 trucks measured on the trips on the Yar-Kirov section in 1972 at speeds of up to 100 km/hr turned out to be somewhat higher than for the four-axle tank car. Thus, at a speed of v = 100 km/hr the maximum value of the coefficient γ for this car (Figure 9.8c) was 0.75. The analysis of the curves in the same figure indicates that ar increase in the speed somewhat decreases the margins of stability. However, on the whole both the four-axle tank cars and the gondolas on the TsNII-Kh3-0 trucks have margins of stability of no less than 1.7 with speeds to 100-120 km/hr.

The direction of motion has a significant effect on the nature of variation of the horizontal dynamic forces acting on the wheels of the freight cars and the resistance to derailment.

Table 9.1. Importance of Coefficients γ of Freight Cars

Тип вагона и тележки (1)		(2) Поездки с повышенными скоростями, км/ч 60	80	90	100	120	(3) Эксплуатационные режимы движения
(4) Четырехосная цистерна ЦНИИ-Х3-О	Б	—	—	0,36/0,375	0,36/0,425	0,40/0,475	—/0,50
	Д	—	0,27/0,28	0,37/0,40	0,34/0,35	—	—/0,43
(5) Четырехосные цистерны МТ-50	Б[1]	—	0,375/0,425	0,50/0,90	0,62/1,03	—	—/0,50
	Д[2]	0,22/0,23	0,25/0,27	0,44/0,50	0,425/0,50	—	—/0,51
(6) Четырехосный полувагон ЦНИИ-Х3-О	Б	0,36/0,375	0,425/0,475	0,49/0,575	0,56/0,575	—	0,37/0,50
	Д	—	—	—	—	—	—
(7) Четырехосный полувагон МТ-50	Б	0,370/0,425	0,43/0,625	0,66/0,96	0,71/1,08	—	0,45/0,60
	Д	—	—	—	—	—	—
(8) Восьмиосный полувагон	Б	0,35/0,375	0,375/0,425	0,375/0,425	0,375/0,425	—	0,34/0,425
	Д	0,380/0,425	0,375/0,425	—	—	—	0,36/0,475
(9) Восьмиосная цистерна	Б	—	0,450/0,475	0,400/0,425	0,400/0,425	—	0,475/0,525
	Д	—	—	0,325/0,425	0,375/0,425	—	—

Note: B--for side frames; D--for web deformations. In the numerator for P = 99.9%; in the denominator--absolute maximum. 1--tank car No 756-4078; 2--tank car No 752-4162.

Key: 1. Type of car and truck

2. Trips at higher speeds, km/hr

3. Experimental traffic conditions

4. Four-axle tank car, TsNII-Kh3-O: B, D

5. Four-axle tank car, MT-50; B, D

6. Four-axle gondola, TsNII-Kh3-O; B, D

7. Four-axle gondola, MT-50; B, D

8. Eight-axle gondola; B, D

9. Eight-axle tank car; B, D

The study of the stability of the eight-axle freight cars at speeds increased to 100 km/hour demonstrated that the variation of the speed in the range of 60 to 100 km/hour in practice has no effect on the margins of stability of these types of freight cars. The maximum values of this coefficient both for the eight-axle gondola and for the eight-axle tank car in the Yar-Kirov section did not exceed 0.45 (Figure 9.8, b). The variation of the direction of motion also in practice has no effect on the margin of stability of these types of cars.

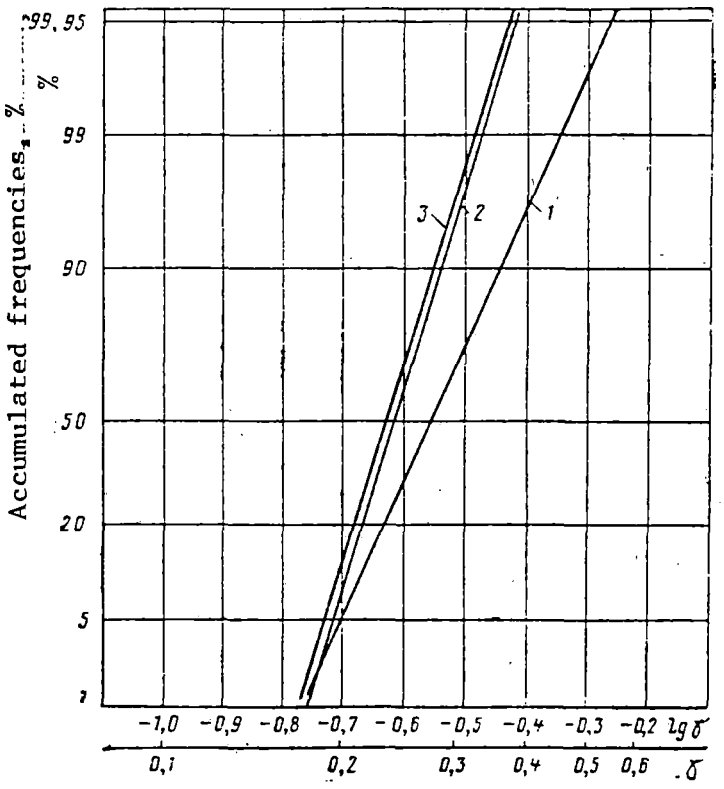

Figure 9.9. Quantile diagrams of the total distribution of the coefficients γ of the freight cars at increased speeds, Kirov-Yar, 1973: 1--Four-axle gondola on the TsNII-Kh3-) turck; 2--Eight-axle tank car; 3--Eight-axle gondola.

Thus, from the point of view of stability, the eight-axle cars have an advantage over all the remaining types of freight cars.

In Figure 9.9, the distributions of the coefficients γ of the eight-axle cars and the four-axle gondola on the TsNII-Kh3-0 trucks having the greatest margins of stability out of all of the four-axle freight cars are presented. The comparison indicates that the eight-axle gondolas and the tank cars have in practice identical margins of stability, and they are appreciably larger than for the four-axle gondola. Thus, the minimum margin of stability η of the eight-axle cars at speeds of up to 100 km per hour was no less than 2.1 as opposed to 1.7 for the four-axle gondola on the TsNII-Kh3-0 trucks.

On the whole, the studies demonstrated that both the eight-axle freight cars and the four-axle ones on the TsNII-Kh3-0 trucks have large derailment coefficients which do not disappear with an increase in the speeds of these types of cars to 100 to 120 km/hour.

Chapter X. Estimate of the Dynamic Loading of the Undercarriages of Freight Cars

10.1. Analysis of the Dynamic Loading Spectra of the Bearing Elements of Car Structural Elements

For the calculational-experimental estimate of the strength and the reliability indexes of the bearing elements of the structural elements of the cars in their stage of development or experimental operation, it is necessary to have reliable information available about the dynamic loading and the strength characteristics of the parts which can be obtained either in the process of performing the dynamic running tests or theoretically using the methods of statistical dynamics.

The goal of this study is analysis of the random processes of the variation of the stresses and the coefficients of dynamic overloads in the elements of the undercarriages, determination of the distribution functions of the peaks, the spectral density and the normalized correlation functions required for development of the method of bench testing for endurance and for calculation of the service lives.

In order to obtain the dynamic loading spectra, the running dynamic tests were performed on the cars in the Moscow-Kuybyshev-Chelyabinsk-Sverdlovsk-Perm'-Yaroslavl'-Moscow sections.

The eight-axle and four-axle gondolas constructed by the car building plants imeni Dzerzhinskiy in Nizhniy Tagil and Kremenchug and also the eight-axle tank car constructed by the plant in Z-danov were taken as the objects for the tests.

The stresses and also the dynamic overload coefficients were measured in the most responsible zones limiting the strength of the structural design. They were determined on the basis of the available operating experience or on the basis of the results of the bench fatigue tests.

In order to measure the stresses, the strain gauges of the ohmic resistance were used with the 10-20 mm base and resistance of 100 to 200 ohms, and for recording the dynamic loads operating on the nonspring-loaded and spring-loaded elements of the car and also the accelerations and deflections of the spring complexes, measuring instruments were installed. The stressed state of the following elements of the undercarriages were measured: the lateral frames of the two-axle trucks of the four-axle freight cars with respect to the axle-box and spring opening, the beams above the springs of the four-axle and eight-axle cars, the connecting beams of the cast and stamped-welded structural design. On the bodies of the eight-axle gondolas, the pedestals, the pivot assemblies, the ridge beams in the vicinity of the pivot assembly and the middle cross-section, the transverse beams, the pivot and intermediate uprights of the body.

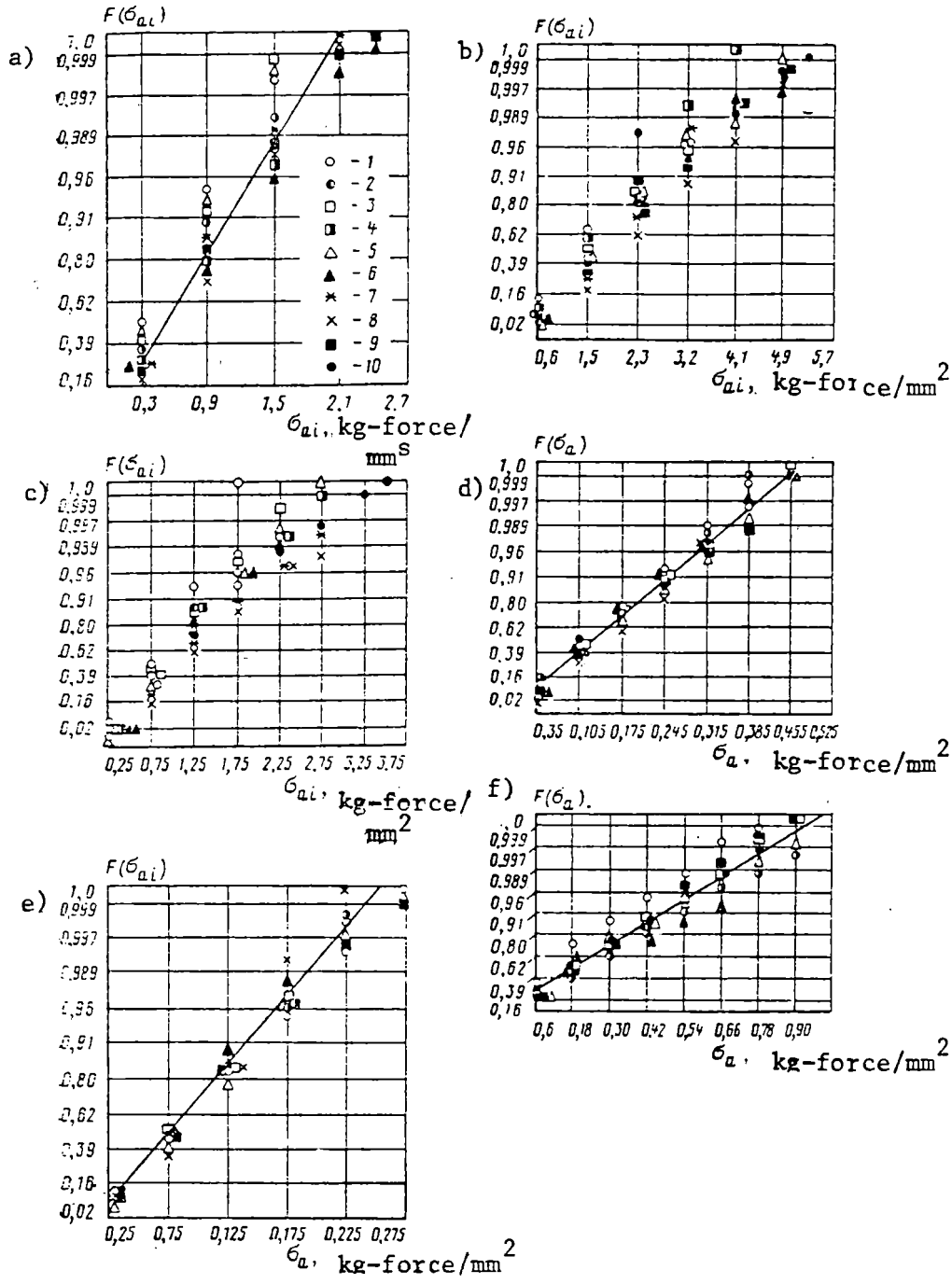

[See caption for Figure 10.1 on page 206]

[See Figure 10.1 on page 198]

Figure 10.1. Distribution function of the amplitudes of dynamic stresses in the middle cross-section of the lower web of the beam under the spring of the TsNII-Kh3-0 type truck (a); in the cross-section of the angle of the axle-box opening in the side frame (b); in the cross-section of the angle of the spring opening in the side frame (c); in the cross-section of the edge foot of the cast connecting beam (d); in the cross-section of the edge foot of the stamping and welding connecting beam (e); in the foot of the body of the eight-axle gondola (f).
1--Speed (in km/hr) 30 to 40; 2--41 to 50; 3--51 to 60; 4--61 to 70; 5--71 to 80; 6--81 to 90; 7--91 to 100; 8--101 to 110; 9--111 and higher; 10--Average considering the recurrence rate of the speed during the entire service life.

The position of determining the dynamic stresses in the investigated cross-sections of the parts during the service life was ensured by the representativeness of the information about the loading. The calculated basis for the strain gauging time was provided under the assumption that the loading process of the parts of the car can be described by the normal stationary random function having an ergodic property. For such process, it is recommended that the minimum strain gauging time be taken no less than 2,575 seconds (43 minutes) [24]. The actual recording time of the dynamic processes on the magnetic tape was from 3 to 8 hours for different processes.

The software of the recording time of the processes, in spite of the fact that the strain gauging time was small by comparison with the actual service life of the car permits determination of the statistical characteristics of the random loading process within the limits of given precision.

The statistical processing of the test materials in the form of recordings on a magnetic tape and oscillographic paper was carried out using the Dispersiometr computer, the Nairi computer and the analog-digital complex of the railroad car division of the Central Scientific Research Institute.

The process of dynamic loading of the undercarriages is characterized by the mean magnitude of the stress which varies insignificantly during the movement along the straight sections of the track and the dispersion which essentially depends on the speed of the car and the technical conditions of the track.

In Figure 10.1 the distribution functions are presented for the amplitudes of the dynamic stresses in various elements of the undercarriages for various

speed intervals and also the average functions obtained considering the recurrence rate of the speed intervals during their service time. It is obvious from the graphs, the reduced distribution functions of the dynamic stresses obtained as a result of processing the experimental data satisfy the Rayleigh distributions.

The amplitude distribution for the dimensionless aligned normal random process which coincides with the distribution of the peaks can be calculated

$$W(h)=\frac{1}{\sqrt{2\pi}}\left[\nu e^{\frac{-h^2}{2\nu^2}}+\sqrt{2\pi(1-\nu^2)}\,he^{\frac{-h^2}{2}}\Phi\left(\frac{\sqrt{1-\nu^2}}{\nu}\right)\right], \qquad (10.1)$$

where Φ (...) is the interval of the probabilities of normal distribution

$$h=\frac{\sigma_a}{\sqrt{D}};$$

σ_a is the random stress amplitude of the spectrum, kg-force/mm^2;

D is the process dispersion;

ν is the dimensionless parameter which depends on the width of the energy spectrum ($0\leqslant\nu\leqslant1$); for $\nu < 0.4$ their process is close to narrow band, and the distribution, with respect to [24], to Rayleigh.

The parameter entering into (10.1) is expressed in terms of the moments of the spectral density of the corresponding orders, and the moments, in turn, depend on the values of the correlation function k (τ) and its derivatives [24]:

$$\nu=\sqrt{1-\frac{M_2^2}{M_0M_4}},$$

where

$$M_0=\frac{1}{\pi}\int_0^\infty S(\omega)\,d(\omega)=-k(0);\quad M_2=\frac{1}{\pi}\int_0^\infty \omega^2 s(\omega)\,d(\omega)=k^{II}(0);$$

$$M_4=\frac{1}{\pi}\int_0^\infty \omega^4 s(\omega)\,d(\omega)=-k^{(IV)}(0).$$

The values of the maximum coefficients of the vertical dynamic forces for the parts of the cars are regulated by the corresponding normative.

The analysis of the coefficients of dynamic overloading defined as the ratio of the dynamic stresses to the static stresses ($k_{d.\ p} = \sigma_{dyn}/\sigma_{st}$), demonstrated that they are distributed within quite broad limits and can exceed the calculated values of the coefficients of vertical dynamics by several times.

In Figure 10.2 and Figure 10.3 the relations are presented for the maximum values measured in the experiment of the coefficients of dynamic overloading of the assemblies of the undercarriages and the bodies of the gondolas.

The largest dynamic overloading coefficients were recorded for the foot assemblies, and they are determined by the rolling oscillations of the body with respect to the spring-loaded masses.

For the central foot of the body $k_{d.p}$ reached 3.6 to 4.0; accordingly, for various parts the coefficients of asymmetry of the loading cycles vary within the limits from +0.5 to -0.5.

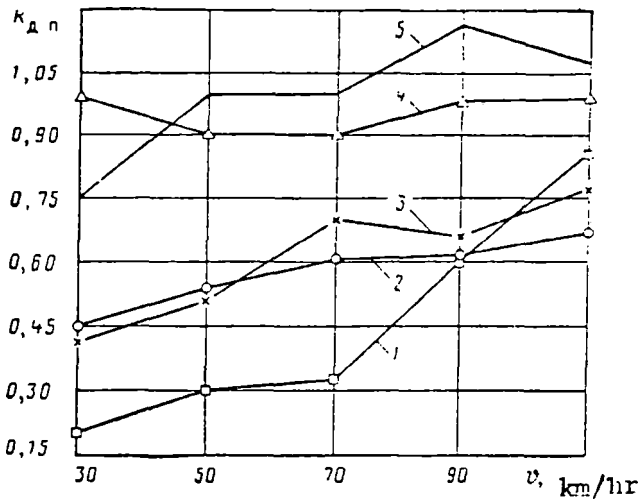

Figure 10.2. Coefficients of dynamic overloading of the assemblies of the body of an eight-axle gondola as a function of the speed: 1--Ridge beam in the central cross-section; 2--Intermediate upright of the body; 3--Pivot beam of the body; 4--Upper scan; 5--Ridge beam in the vicinity of the pivot assembly.

For the elements of the undercarriages where the stressed state of the rolling of the body is felt insignificantly, $k_{d.\ p}$ in practice coincide with the calculated coefficients of the vertical dynamic forces determined in accordance with the norms. It is possible to consider the beam above the spring of the truck (in the cross-section under the foot) and the ridge beam (with respect to cross-section in the middle of the body) as these elements.

It is necessary to note that the dynamic stresses in the assemblies determined by the simultaneous effect of the vertical and horizontal forces are characterized by different $k_{d.\ p}$. Therefore when performing the strength calculations for the undercarriages and the body it is necessary to consider the

components of the dynamic stresses from the effect of the lateral loads, especially if this is connected with the variation of the schematic of the application of the vertical loads such as, for example, in the foot assemblies and the bearing surfaces of the side frames on the housing of the axle box.

For analysis of the factors determining the dynamic overload of the body and truck elements, a spectral analysis was made of the stresses at the most characteristic points with respect to the procedure discussed in reference [24].

In Figure 10.4 the graphs are presented for the structural density of the stresses in the central foot of the housing, the connecting beam and the lateral frame of the truck of an eight-axle gondola, in the side frame and the beam above the spring of TsNII-Kh3-0 truck of the four-axle gondola. Let us note that in accordance with the applied procedure for constructing the graphs of the spectral density, the maximum value of the function in each of the graphs was provisionally taken as one.

From the analysis it follows that for the central foot of the body, the connecting beam and other elements the graphs of the spectral density have a clearly expressed peak with predominant frequency equal approximately to 1 hertz. In addition, it is possible to note the small surge of the spectral density on a frequency of 5 and 10 hertz which, considering its small value, cannot have a significant effect on the effective frequency.

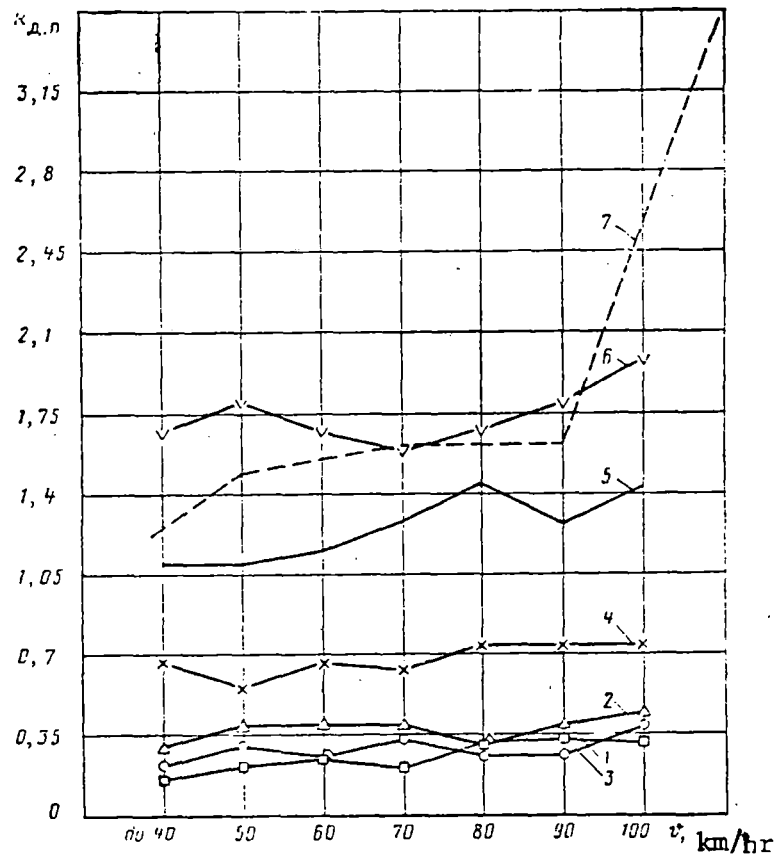

Figure 10.3. The coefficients of dynamic overload of the assemblies of the truck of an eight-axle gondola as a function of speed: 1--Beam above the spring in middle cross-section under the foot; 2--Connecting beam, middle cross-section under the foot; 3--Connecting beam; zone of inflection of the lower sheet above the axle of the wheel pair; 4--Side frame with respect to the inside angle of the axle-box opening; 5, 6--Connecting beams in the vicinity of the edge foot; 7--Central foot of the body.

The analysis of the graphs of the spectral density of the unsprung parts of the truck demonstrated that the loading processes are multifrequency. For the side frame of the truck of the four-axle gondola, loads are characteristic with a frequency of the effect of the truck which depends on the speed, the frequency of the hopping of the body of 2.5 hertz and the bending vibrations of the body of 5 to 6 hertz, and also the higher frequencies of 20.0 to 30.0 hertz.

For the side frame of the truck of the eight-axle gondola, the loading process with frequencies of 1.2 to 2.5 and 4 to 9 hertz is characteristic. In addition, to a greater degree than in the four-axle gondola here the oscillations are expressed with a frequency of 30 to 40 hertz occurring from the short unevenness of the rails. Loading of the beam above the spring of the TsNII-Kh3-0 truck is characterized by frequencies of 3 and 6 hertz, which is connected with the vibrations of the body on the spring suspension and the natural bending vibrations of the body of the all-metal car.

The width of the energy spectrum Δf_e usually is determined by the formula [24]

$$\Delta f_э = \frac{D}{s(\omega_0)}, \qquad (10.2)$$

where D is the dispersion of the loading process, kg-force x c^2/mm^4;

$s(\omega_0)$ is the maximum value of the spectral density, kg-$force^2$-sec/mm^4.

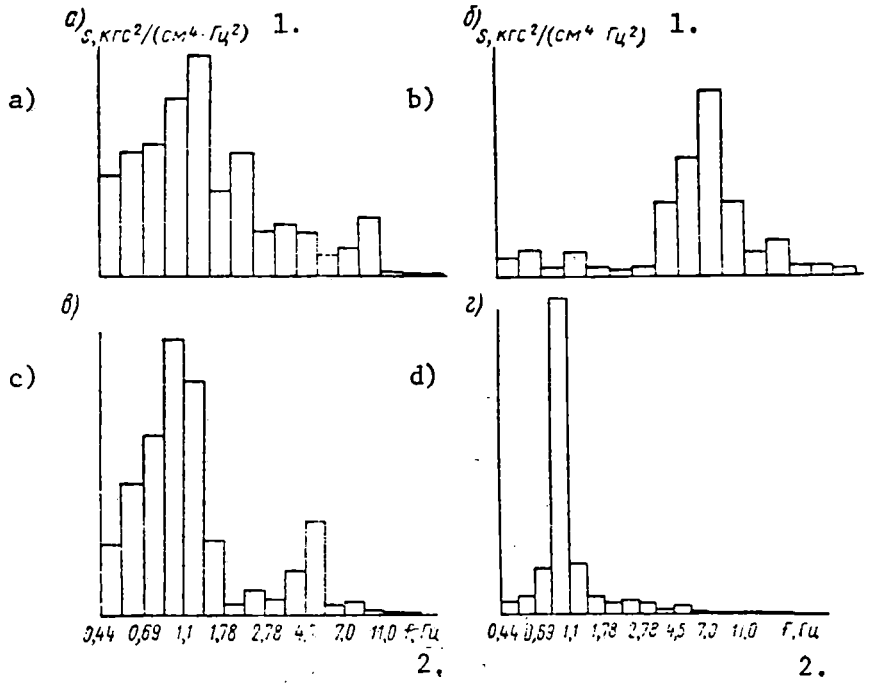

Figure 10.4. Graph of the spectral density of the stresses in the elements of the undercarriages for v = 80 to 100 km/hr: a--Side frame of the four-axle gondola; b--Side frame of the eight-axle gondola; c--Beam above the spring of the four-axle gondola; d--Connecting beam and central foot of the eight-axle gondola.

Key: 1. Kg-force^2/(cm^4-hertz^2); 2. Hertz.

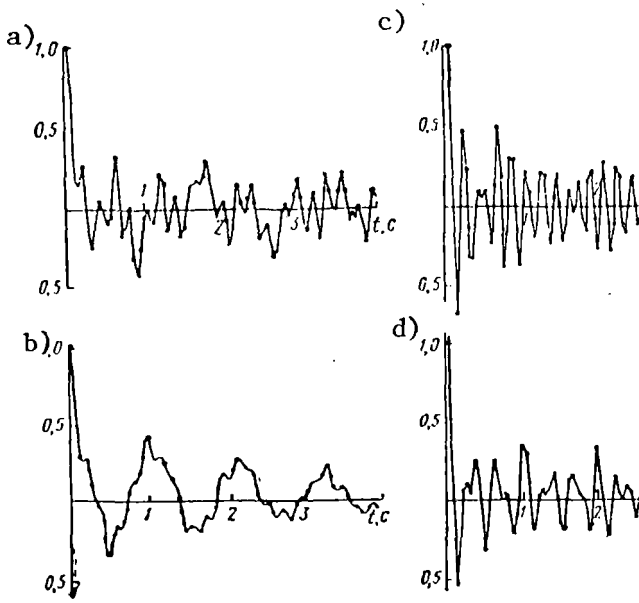

Figure 10.5. [See caption on following page]

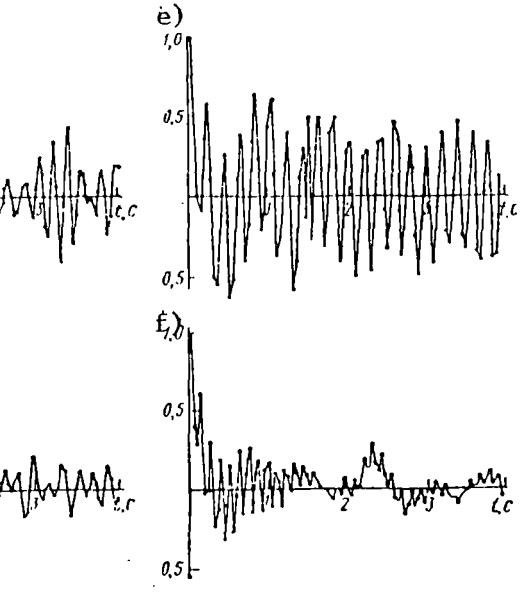
в)
1,0
0,5
0,5
1
2
3
4 с
б)
1,0
0,5
0,5
1
2
3
4 с

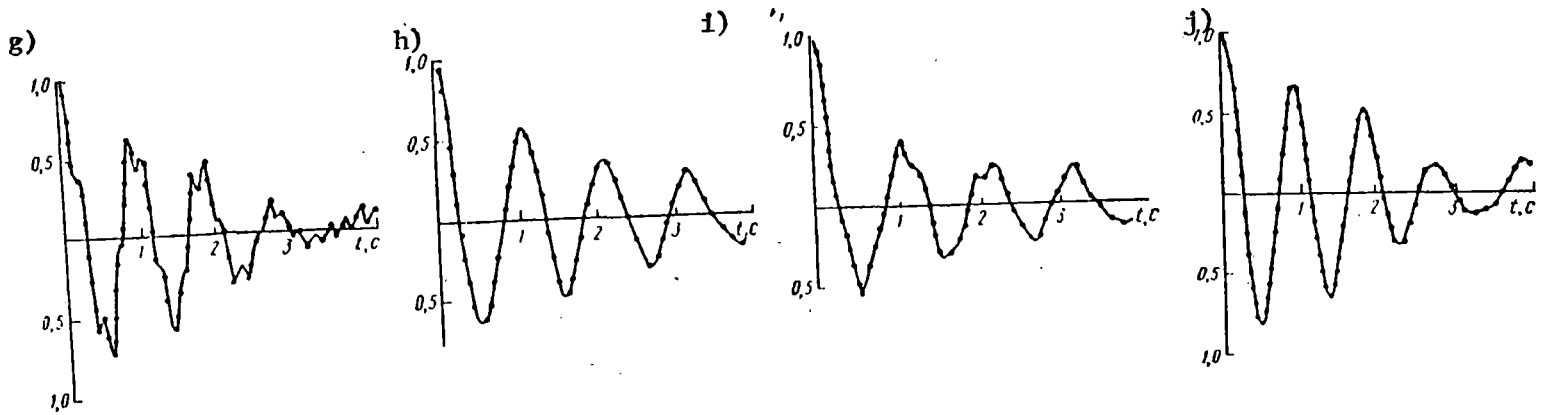

Figure 10.5. [See preceding page for first part of graph] Graph of the normalized correlation function of dynamic stresses; a--In the central foot of the body; 1--For v = 40 to 50 km/hr; 2--For v = 80 to 90 km/hr; b--In the connecting beam of the eight-axle gondola; 1--For v = 40 to 50 km/hr; 2--For v = 80 to 90 km/hr; c--In the beam above the spring of the TsNII-Kh3-0 truck of the four-axle gondola; 1--For v = 40 to 50 km/hr; 2--For v = 80 to 100 km/hr; d--In the angle of the axle-box opening of the solid frame of the eight-axle gondola; 1--For v = 40 to 50 km/hr; 2--For v = 80 to 100 km/hr; e--At the angle of axle-box opening of the solid frame of the four-axle gondola: 1--For v = 40 to 50 km/hr; 2--For v = 80 to 100 km/hr.

If $\omega_0/2\pi \gtrsim \Delta f_e$, then the loading process is called narrow band; if $\omega_0/2\pi \lesssim \Delta f_e$, the loading process is close to wide band.

The stress spectra of the beams above the spring and the connecting beam, the central slit of the body--the typically narrow-band spectra--and the corresponding random process--narrow-band. The stressed state of the lateral frames of the eight-axle cars is determined by the frequencies distributed in the range from 0.6 to 1 to 32 to 40 hertz with quite high power of the processes with respect to all frequencies. Accordingly, for the bench fatigue tests it is necessary for the unsprung parts to consider the effect of the wide band nature of spectrum on the endurance limit of the parts.

The discrete values of the normalized correlation function were calculated on the basis of the current values of the ordinates of the loading process by the formula

$$\rho(\tau)=\rho(\mu\Delta\tau)=\frac{1}{\mathbf{D}(n-\mu+1)}\sum_{i=0}^{n-\mu}[\sigma(i\Delta\tau)-m_\sigma][\sigma(i\Delta\tau+\mu\Delta\tau-m_\sigma)], \qquad (10.3)$$

where

$$m_\sigma=\frac{1}{n}\sum_{i=0}^{n-1}\sigma(i\Delta\tau)\,;\ \mathbf{D}=\frac{1}{n-1}\sum_{i=0}^{n-1}[\sigma(i\Delta\tau)-m_\sigma]^2\,;$$

$\mu = 0, 1, 2, \ldots, n$ is the number of y-axis of the correlation function;

$i = 0, 1, 2, \ldots, n-1$;

$\Delta\tau$ is the breakdown step of the realization of the random function.

In Figure 10.5 the graphs are presented for the normalized functions $\rho^1(\pi)$ of the random processes of the variation of the stresses for the elements of the body and the undercarriages of the eight-axle and four-axle freight cars for speeds of 40 to 50 and 80 to 100 km/hr.

The analysis shows that the correlation functions for the processes of dynamic stresses in the feet, the beams above the springs and the connecting beams can be approximated by the analytical expression of the type

$$\rho(\tau)=e^{-\alpha^n \tau^2}\cos\omega_0\tau, \qquad (10.4)$$

where ω_0 is the angular frequency corresponding to the maximum of the spectral density function.

For $\tau \to \infty$ $\rho(\tau) \to 0$, therefore it is possible to confirm the presence of the ergodic properties of the investigated processes.

10.2. Approximate Estimate of the Loading of the Elements of the Undercarriages of the Freight Cars by the Experimental Data

The experimental data obtained as a result of processing on the analog-digital complex permit approximate determination of the intensity of the elements of the undercarriages of freight cars, the basis for which can be the procedure discussed in the norms for the calculations of the strength of the cars.

As is demonstrated above (see Figure 10.4) for the majority of elements of undercarriages the spectra have a single-frequency nature, that is, the processes are narrow-band. For them there is a defined frequency which determines

the number of cycles of application of the load per unit time. The side frame of the truck (especially for the eight-axle car) constitutes an exception where the frequencies of application of the vertical loads are distributed in a large interval (from 0.6 to 1 to 30 to 40 hertz). However, as analysis of the oscillograms indicates, usually the high-frequency component appears in the form of a superposed frequency on the low-frequency process, and its role reduces to an increase in amplitudes of the low-frequency cycle. This increase in amplitudes is taken into account when processing the recordings on magnetic tape of the coefficients of the vertical dynamics of the side frames of the trucks with respect to the basic (low frequency) tone without the application of the low-frequency filter.

Therefore, in order to estimate the load of the lateral frame under the vertical forces in the first approximation it is possible to use the data from the indicated processing where the frequency of the application of the load corresponds to the frequency of the low-frequency component, and the amplitude must be taken considering the low-frequency additive. For the performance of the calculation, the operating indexes of the car must be known: the daily run L_c, the mean section speed on the railroad network $v_{section}$, the empty run coefficient $k_{\pi} = L_{por}/L_{gr}$ is the ratio of the run empty to the run loaded, the service life of the car N and also the data obtained in the experiment: the velocity distribution histogram of the freight trains on the railroad network, the distribution parameters or the quantile diagrams for the given load for different speeds of the car on the average frequency of application of the load f. The latter is defined as

the ratio of the total number of amplitudes in the experiment (n_0) to its duration T_0:

$$f = \frac{n_0}{T}.$$

The total operating time of the freight car during the service life is

$$t_c = \frac{365\, NL_c}{v_{уч}(1+k_n)}\ \text{ч}. \tag{10.5}$$

The total operating time of the car in each of the kth speed intervals is determined by the distribution histogram of the speeds of the trains

$$t_k = p_k\, t_c, \tag{10.6}$$

where p_k is the relative time of the trains in each speed range.

The total number of cycles of the application of a load operating in motion in the indicated speed interval will be

$$n_k = t_k\, f_k\, 3{,}6 \cdot 10^3,$$

where f_k is the mean frequency of application of the load for the given speed.

The load interval from the maximum Q_{max} to the minimum Q_{min} is broken down into i intervals:

$$\Delta = \frac{Q_{max} - Q_{min}}{i}.$$

In each of these intervals the number of cycles of the application of the load is determined by the formula

$$n_i = \sum_{k=1}^{k=n_{max}} p_{ki}\, n_k, \tag{10.7}$$

where

$$p_{ki}=u_{k(i+1)}-u_{ki};$$

$u_{k(i+1)}$ and u_{ki} are the upper and lower quantiles of the ith load interval for the kth speed interval obtained experimentally.

If the distribution laws of the loads are defined for different speeds, then the probability p_{ki}

$$p_{ki}=F_k(Q_{i+1})-F_k(Q_i),$$

where F_k is the load distribution function for the kth speed interval.

Substituting the data from formula (10.5) and (10.6) in formula (10.7), we finally obtain

$$n_i=\frac{1{,}3\cdot 10^6\cdot L_c\ N}{v_{yq}(1-k_n)}\sum_{k=1}^{k=n_{max}} p_k\ p_{ki}\ f_k\ . \qquad (10.8)$$

Performing these calculations for each of the i load intervals, we obtain the distribution histogram of the cycle amplitudes applied to the element during the service life of the car.

In order to determine the number of load cycles of one specific fiber of the wheel web by the vertical forces for each of six time intervals p_B, it is necessary to use formula (10.8), in which the wheel diameter is taken into account:

$$n_i=\frac{3{,}65\cdot L_c\ N\cdot 10^7}{\pi\ d_k(1+k_n)}\sum_{k=1}^{4} p_k\ p_{ki}\ . \qquad (10.9)$$

Analogously, the calculations can also be performed for other elements of the undercarriages of the cars.

CONCLUSION

1. As a result of the studies, a large volume of data are obtained for the first time in the form of magnetic recordings on the conditions of the dynamic loading of the undercarriages of the basic types of loads of the cars both for the existing speeds and for prospective ones.

2. The dynamic testing of the cars as part of the freight trains on the basic loaded lines encompass a significant test ground of the railroad network with respect to the plan view, the profile and the technical condition and with respect to the traffic regimes of the freight trains. The cars of the basic types of different technical condition were subjected to study. They represent more than half the entire fleet of freight cars and have an increased level of dynamic forces by comparison with the other types of cars. The results obtained must be considered representative and used for designing the cars.

3. It was established that the distribution laws of the amplitudes of the coefficients of vertical dynamic overloads for all types of cars are close to normal, except the cars on the MT-50 trucks for which the amplitudes are distributed by a logarithmically normal law; the distribution laws of the horizontal (frame) forces for all types of cars are close to normal.

4. The highest values of the dynamic forces, the probability of the appearance of which is about 0.13 percent in the vertical (k_d) and horizontal (H_p) planes depends on the speed and to a significant degree are determined by the unevennesses of the track. The effect of the technical condition of the track on the growth of the extremal dynamic forces turns out to be stronger than the increase in speed. The wear of the undercarriages of the given type of car has no great effect on the level of the dynamic forces.

5. The maximum values of the coefficients of vertical overload k_d^{max} recorded in the experiments when processing the vibrations with respect to the basic tone reached 0.55 on the four-axle cars on the TsNII-Kh-3-0 trucks, and 0.32 on the eight-axle cars. During processing, considering the high-frequency k_d^{max}, they reached 0.75 and 0.62 respectively.

6. The distribution laws of the instantaneous values of the vertical dynamic loads acting on the wheels of the four-axle (on the TsNII-Kh3-0 trucks) and eight-axle cars are close to normal. The vertical dynamic loads on the wheels of the freight cars vary within broader limits than the analogous loads on the side frames of the trucks. This is explained by the effect of the inertial loads and the effect of the frame forces.

7. The range of variation of the vertical dynamic loads on the wheels of the cars of all types measured when moving as part of the freight trains with operating speeds to 80 to 85 km/hr in different sections of track is on the average 4 to 25 tons.

8. The dynamic overloads of the axles of the four-axle cars (on the TsNII-Kh3-0 trucks) and the eight-axle freight cars are appoximately identical, and they are within the limits of the values determined by the procedure for strength calculation of the axle. The data for the axle of the eight-axle gondolas on the sections with passes on the L'vov railroad where with recovery on descents, significant overload coefficients are obtained on the cross-sections of the axle beyond the hubs exceeding the calculated values according to the norms for strength calculation of railroad cars, constitute an exception.

9. The horizontal forces acting on the wheels without running against the rail are limited to the frictional force equal to 2 to 2.5 tons. The distribution law of the lateral forces occurring when the wheels run against the rails is close to normal for all types of cars (excluding the four-axle car on the MT-50 trucks). For the four-axle cars on the MT-50 trucks, the distribution law of the lateral forces when the wheel runs against the rail differs from the normal law, especially when the speeds increase to 95 to 100 km/hr.

10. The developed procedure and the processing program permit regressive analysis of the experimental data. It has been established that for the eight-axle gondola the correlation between the coefficients of vertical dynamics and the frame force acting on the lateral frames of the two-axle trucks is relatively weak; the correlation coefficient r on the average is 0.3. Between the vertical and the lateral forces acting on the wheel running against the rail, there is a closer correlation; the correlation r for the eight-axle gondola is on the average equal to 0.6.

11. The information obtained during the tests on the stressed state of the bearing assemblies, both spring mounted and nonspring mounted parts of the freight cars, can be used when estimating the endurance limit of the basic bearing elements and when correcting the strength calculation norms.

12. The dynamic stresses in the investigated assemblies of the undercarriages andin the elements of the body are characterized in the majority of cases by a quite high level of amplitudes exceeding 200 to 300 kg-force/cm^2, which indicates the necessity for performing the calculations of such assemblies for endurance. The distribution of the peak amplitudes of the dynamic stresses is satisfactorially subject to Rayleigh's law.

13. The effective frequencies of variation of the voltage in the bearing elements of the undercarriages and the bodies of the freight cars fluctuate from 1.0 to 6.5 hertz in the operating range of speeds. The maximum stress spectra, as a rule, for the eight-axle cars, coincides with the rolling frequencies of the body at operating speeds. These frequencies fluctuate from 0.6 to 1.5 hertz. The variation in stress at higher frequencies (30 to 40 hertz) is primarily observed in the elements of the undercarriages that are not spring mounted.

14. The coefficients of dynamic overload are distributed in a wide range--from minimum values comparing with the coefficients of vertical dynamics (0.28 to 0.60), to values exceeding 3.4 to 4.0. The greatest dynamic overloads are observed in the pedestal assemblies of the truck and the body. They are determined by the lateral oscillations of the spring-loaded masses.

During strength calculations of the cars, it is necessary to consider the actual values of the dynamic overloads characterized by all types of oscillations of the car. This must be considered during routine correction of the norms.

15. All types of freight cars on the TsNII-Kh3-0 and the MT-50 trucks have a sufficient derailment coefficient $\eta \geqslant 1.7$. to ensure traffic safety under the existing conditions of operation at speeds to 80 to 85 km/hr.

16. With an increase in speed to 100 km/hr, all types of cars on the TsNII-Kh3-0 trucks had margins of stability of 1.7; for the four-axle gondolas on the MT-50 trucks on the Yar-Kirov section at v = 90 km/hr, in 99.9 percent of the cases the margins of stability were less than 1.5. In individual experiments at this speed minimum coefficients of 1.1 were observed. For vehicles 100 km/hr in individual cases the minimum values of the coefficients were less than 1.0. In order to estimate the safety in this cases it is necessary in addition to the ratio of the lateral and vertical forces, to consider the time, the angle of collision of the wheel with the rail and the other factors which were not taken into account in the present study.

17. The eight-axle freight cars have the largest margins of stability in operation at increased speeds to 100 km/hr.

18. Among the important newly developed methods of experimental investigation it is necessary to consider the use of the instruments for precise magnetic recording with the development of monitoring equipment for prolonged studies

of the dynamics and strengths of the cars on longer stretches of the railroad; measurement of the forces acting on the wheels near their contact with the rails with respect to web deformations--a procedure has been developed on the basis of this for estimating the derailment coefficient of the cars; development of a method of analyzing experimental data recorded on magnetic tape and the creation of an analog-digital complex based on using the Nairi-C type digital computer and analog computer and then Dispersiometr special-purpose computer and the M-6000 type third-generation computer; development of methods of estimating the experimental data by the statistical method with respect to the extremal values, the loading regimes, the margins of stability, overloads of the axles, and so on.

19. The most improved were the following: the procedure for determining the coefficient γ--the ratio of the lateral force to the vertical force--by the deformations of the truck frame; the procedure and equipment for centralized electrical calibration of the strain amplifier channels; the procedure for measuring the deformations of the elements of the wheel pair with the application of mercury current collectors designed by the VNITI Institute, permitting studies to be made over longer stretches of the railroad.

20. The data obtained on the force loading regimes of the undercarriages of freight cars must be considered during routine correction of the norms for strength calculations of railroad cars. The calculated formulas for determining the coefficients of vertical dynamics must be corrected considering the high-frequency components of the loads. It is expendient to introduce a section into the norms that regulates the calculation indexes of the

dynamic overload coefficients of the basic bearing assemblies of the railroad cars, the loading of which is determined by the simultaneous effect of both horizontal and vertical forces.

BIBLIOGRAPHY

1. Kudryavtsev, N. N., Melent'yev, L. G., Granovskiy, A. N., "Measurement of Vertical Forces Acting From the Wheels of Rolling Stock on the Rails," VESTNIK VSESOYUZ. NAUCH.-ISSLED. IN-TA ZH.-D. TRANSP. (Vestnik of the All-Union Scientific Research Institute of Railroad Transportation), No 6, 1973, pp 31 to 34.
2. Dolmatov, A. A., Kudryavtsev, N. N., DINAMIKA I PROCHNOST' CHETYREKHOSNYKH ZHELEZNODOROZHNYKH TSISTERN. (Dynamics and Strength of the Four-Axle Railroad Tank Cars), Moscow, Transport, 1963, 124 pp (Works of the All-Union Scientific Research Institute of Railroad Transportation, 1963).
3. Baguley, R. W. "Vehicle Testing for Higher Speeds, ENGINEERING JOURNAL, 1973, No 3, pp 13-31.
4. Molodikov, V. A., Alekseyev, G. M., "Problem of Measuring the Forces Taken by the Wheel Pair," VESTNIK VSESOYUZ. NAUCH.-ISSLED. IN-TA ZH.-D. TRANSP. (Vestnik of the All-Union Scientific Research Institute of Railroad Transportation), 1971, No 1, pp 29-32.
5. Kudryavtsev, N. N., "More Precise Definition of the Method of Measuring Frame Forces," VESTNIK VSESOYUZ. NAUCH.-ISSLED. IN-TA ZH.-D. TRANSP. (Vestnik of the All-Union Scientific Research Institute of Railroad Transportation), 1958, No 7, pp 48-50.

6. Kudryavtsev, N. N., Barteneva, L. I., Saskovets, V. M., Zaytsev, A. F., Stupichev, I. N., "Determination of the Forces Acting on the Railroad Car Wheels and their Relations," VESTNIK VSESOYUZ. NAUCH.-ISSLED. IN-TA ZH.-D TRANSP. (Vestnik of the All-Union Scientific Research Institute of Railroad Transportation), 1972, No 1, pp 23-27.

7. Kudryavtsev, N. N., ISSLEDOVANIYE DINAMIKI NEOBRESSORENYKH MASS VAGONOV (Investigation of the Dynamics of the Masses of Railroad Cars not Spring Mounted), Moscow, Transport, 1965, 168 pp (Works of the All-Union Scientific Research Institute of Railroad Transportation, No 287).

8. Bychkovskiy, A. V., Mikhnenko, Ye. F., Bespalov, I. P., "Measuring the Wheel Pressure on the Rails during Movement of Electric Locomotive," VESTNIK VSESOYUZ. NAUCH.-ISSLED. IN-TA ZH.-D. TRANSP (Vestnik of the All-Union Scientific Research Institute of Railroad Transportation), 1964, No 6, pp 13-16.

9. Shafranovskiy, A. K., NEPRERYVNAYA REGISTRATSIYA VERTIKAL'NYKH I BOKOVYKH SIL VZAIMODEYSTVIYA KOLESA I REL'SA (Continuous Recording of Vertical and Lateral Forces of Interaction of the Wheel and Rail), Moscow, Transport, 1965, 96 pages (Works of the All-Union Scientific Research Institute of Railroad Transportation, No 308).

10. Shafranovskiy, A. K., IZMERENIYE I NEPRERYVNAYA REGISTRATSIYA SIL VZAIMODEYSTVIYA KOLESNYKH NAP LOKOMOTIVOV S REL'SAMI (Measurement and Continuous Recording of the Forces of Interaction of the Wheel Pairs of Locomotives with Rails), Moscow, Transport, 1969, 120 pages (Works of the All-Union Scientific Research Institute of Railroad Transportation, No 389).

11. Konichi S., "Measurement of Loads on Wheel Set," TRANSACTIONS OF THE JAPAN SOCIETY OF MECHANICAL ENGINEERS, 1967, March, v 8, No 3, pp 26-29.

12. Nakamura, H., Tapasa S., "Lateral Forces Acting to Wheel, Wheel Load, Coefficient of Derailment and Bending Stress of Wheel-Axle of Car on the New Takaido Trunk Line, QUARTERLY REPORT RTRI, 1967, v 8, No 2, pp 103-106.

13. Andriyevskiy, S. M., Krylov, V. I., SKHOD KOLESA S REL'SA (Derailment), Moscow, Transport, 1971 (Works of the All-Union Scientific Research Institute of Railroad Transportation, No 393).

14. Kheyman, Kh., NAPRAVLENIYE ZHELEZNODOROZHNYKH EKIPAZHEY REL'SOVOY KOLEYEY (Guidance of Railroad Trains by the Railroad Track), Moscow, Transzheldorizdat, 1957, 416 pages.

15. Kudryavtsev, N. N., Saskovets, V. M., "Automatic Determination of the Derailment Coefficient with the Application of an Analog Computer," VESTNIK VSESOYUZ. NAUCHN.-ISSLED. IN-TA ZH.-D. TRANSP. (Vestnik of the All-Union Scientific Research Institute of Railroad Transportation), No 5, 1971, pp 1-4.

16. Vershinskiy, S. V., Kudryavtsev, N. N., "Procedure for Continuous Recording of the Trajectory of the Contact Point of the Wheel of Rolling Stock with the Rail," Author's Certificate No 169555 as of 4 May 1963, BYULL. IZOBR (Invention Bulletin), No 7, 1965, p 31.

17. Vershinskiy, S. V., Kudryavtsev, N. N., "Method of Continuous Recording of the Oscillation Amplitude of the Contact Point of the Wheel of Railroad Rolling Stock with the Rail," Author's Certificate No 176315 as of 31 April 1965, BYULL. IZOBR (Invention Bulletin), No 22, 1965, p 33.

18. Kudryavtsev, N. N., "Determination of the Perturbation Functions for the Study of Railroad Car Oscillations," VESTNIK VSESOYUZ. NAUCH.-ISSLED. IN-TA ZH.-D. TRANSP. (Vestnik of the All-Union Scientific Research Institute of Railroad Transportation), No 3, 1964, pp 9-13.

19. Dolmatov, A. A., Kudryavtsev, N. N., Kochnov, A. D., et al, OSOBENNOSTI DINAMIKI VAGONOV PRI VYSOKIKH SKOROSTYAKH DVIZHENIYA (Peculiarities of the Dynamics of Railroad Cars at High Speed), Moscow, Transport, 1968, 160 pages (Works of the All-Union Scientific Research Institute of Railroad Transportation, No 342).

20. Myers, E. T., "Track Analysis Car Guides C. N. Maintenance," MODERN RAILROADS, No 10, Oct 1970, pp 62-63.

21. Cherkashin, Yu. M., DINAMIKA NALIVNOGO POEZDA (Dynamics of a Tank Car Train), Moscow, Transport, 1975, 136 pages (Works of the All-Union Scientific Research Institute of Railroad Transportation, No 543).

22. Vershinskiy, S. V., Kudryavtsev, N. N., Tsvetkova, M. M., Cherkashin, Yu., M., "New Method of Strength Calculation of a Railroad Car Axle," DINAMIKA PROCHNOST' I USTOYCHIVOST' VAGONOV V TYAZHELOVESNYKH I SKOROSTNYKH POEZDAKH (Dynamics, Strength and Stability of Railroad Cars on Heavy and High-Speed Trains), Moscow, Transport, 1970, pp 121 to 145 (Works of the All-Union Scientific Research Institute of Railroad Transportation, No 425).

23. Rumshiskiy, L. Z., MATEMATICHESKAYA OBRABOTKA REZUL'TATOV EKSPERIMENTA (Mathematical Processing of Experimental Results), Moscow, Nauka, 1971, 162 pages.

24. Zolotarskiy, A. F., Vershinskiy, S. V., Yershkov, O. P., Ivashchenko, G. I., Shestakov, V. N., Chernyshev, M. A., ZHELEZNODOROZHNYY PUT' I PODVIZHNOY

SOSTAV DLYA VYSOKIKH SKOROSTEY DVIZHENIYA (High-Speed Railroad Track and Rolling Stock), Transport, 1964, 272 pages.

25. Verigo, M. F., Kogan, A. Ya., "Stability of the Movement of a Wheel over a Rail," VESTNIK VSESOYUZ. NAUCH.-ISSLED. IN-TA ZH.-D. TRANSP. (Vestnik of the All-Union Scientific Research Institute of Railroad Transportation), No 4, 1965, pp 3 to 8.

☆U.S. GOVERNMENT PRINTING OFFICE: 1979 O— 630-598/2624 REGION 3-1

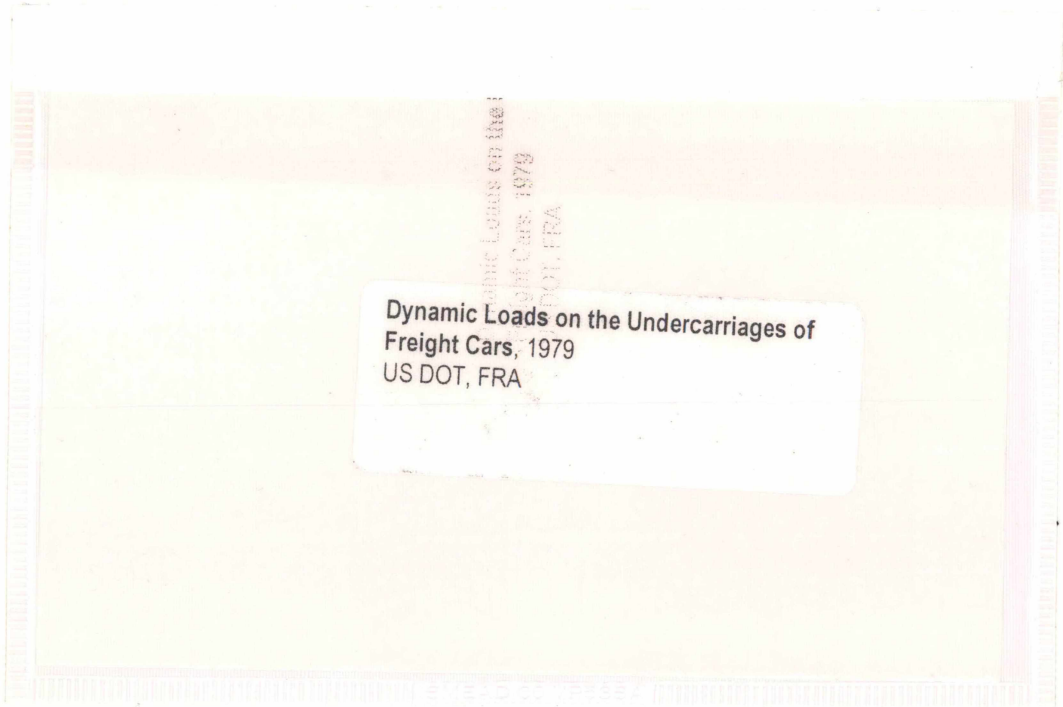
Dynamic Loads on the Undercarriages of
Freight Cars, 1979
US DOT, FRA